



POLITECNICO DI BARI

06

2023

DICATECh

D.R.R.S

Doctor of Philosophy in Environmental and Building Risk and Development

Coordinator: Prof. Michele Mossa

XXXV CYCLE
Curriculum: ICAR 10/ ICAR11

DICATECh
Department of Civil, Environmental, Building Engineering and Chemistry

Francesco Carlucci

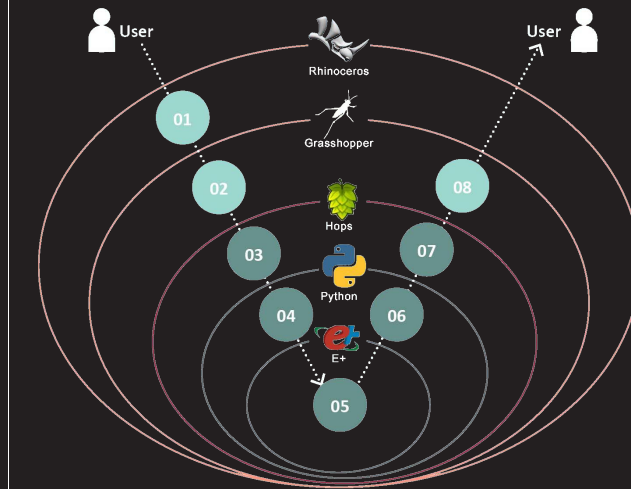
Francesco Carlucci

Responsive envelopes performance analysis in current and future climate scenarios: development of an interactive computational platform

Prof. Guido Raffaele Dell'Osso
Department of Civil, Environmental, Building Engineering and Chemistry, Polytechnic University of Bari

Prof. Francesco Fiorito
Department of Civil, Environmental, Building Engineering and Chemistry, Polytechnic University of Bari

Co-supervisors:
Prof. Roel C. G. M. Loonen, Eindhoven University of Technology
Prof. Kristoffer Negendahl, Technical University of Denmark



Cover image: Structure and plugins of the computational platform proposed

Responsive envelopes performance analysis in current and future climate scenarios: development of an interactive computational platform

06

Abstract

Considering the building envelope research field, responsive technologies are recently playing a key role thanks to their capability to react to external environmental stimuli. Despite these technologies were conceived with the aim to adapt themselves to external environmental changes on short/mid-term time scales (sub-hourly, hourly, daily, and seasonal), recent studies are evaluating their contribution on larger time scales (decades) to improve the resilience of building envelopes to climate change. Nevertheless, currently the simulation of their energy behaviour can be particularly long and complex and this issue is limiting their spread. This work aims to provide, firstly, a detailed description of the state of the art including methods and tools for energy simulation of complex responsive systems. Hence, the main output of the work consists of an interactive computational platform for the energy analysis of these systems in present and future climate scenarios. The developed platform – based on EnergyPlus, Python, and Grasshopper – allows to select different climate zones represented by 25 European cities and different responsive envelope technologies – phase change materials, shape morphing shadings, electrochromic windows – selecting the climate scenario (current, 2050, 2080) to be analysed with a simple interface, widely spread, and easily customizable. Starting from simple inputs (i.e., location, climate scenario, technology, control type) selectable from pop-up lists, the platform – via Python algorithms launched directly from Grasshopper on a local server – edits the energy model, launches the simulations, and provides directly a comparison sheet where the responsive model is compared with a traditional reference static model. Therefore, the different topics covered by the platform allow the user to easily compare the behaviour of different responsive technologies in different geographical contexts, future scenarios, or – for externally controlled systems – through different control strategies using validated and easily comparable models. The development of a simple platform capable of managing dynamic energy simulations of complex systems aims to provide the required tools to consider responsive envelopes as real alternatives to traditional technologies by evaluating their long-term contribution, considering the climate change underway.



POLITECNICO DI BARI

D.R.R.S

06

Doctor of Philosophy in Environmental and Building Risk and Development

2023

Coordinator: Prof. Michele Mossa

XXXV CYCLE
Curriculum: ICAR 10/ ICAR11

DICATECh

Department of Civil, Environmental, Building Engineering and Chemistry

Responsive envelopes performance analysis in current and future climate scenarios: development of an interactive computational platform

Prof. Guido Raffaele Dell'Osso
Department of Civil, Environmental, Building Engineering and Chemistry
Polytechnic University of Bari

Prof. Francesco Fiorito
Department of Civil, Environmental, Building Engineering and Chemistry
Polytechnic University of Bari

Co-supervisors:
Prof. Roel C. G. M. Loonen, Eindhoven University of Technology
Prof. Kristoffer Nørgaard, Technical University of Denmark

Francesco Carlucci



POLITECNICO DI BARI

D.R.R.S

06

Dottorato di Ricerca in Rischio e Sviluppo ambientale, territoriale ed edilizio

2023

Coordinatore: Prof. Michele Mossa

XXXV CICLO
Curriculum: ICAR 10/ ICAR 11

DICATECh

Dipartimento di Ingegneria Civile, Ambientale, del Territorio, Edile e di Chimica

Analisi prestazionale di involucri responsivi in scenari climatici presenti e futuri: sviluppo di una piattaforma computazionale interattiva

Prof. Guido Raffaele Dell'Osso
Dipartimento di Ingegneria Civile, Ambientale, del Territorio, Edile e di Chimica
Politecnico di Bari

Prof. Francesco Fiorito
Dipartimento di Ingegneria Civile, Ambientale, del Territorio, Edile e di Chimica
Politecnico di Bari

Co-supervisors:
Prof. Roel C. G. M. Loonen, Eindhoven University of Technology
Prof. Kristoffer Negendahl, Technical University of Denmark

Francesco Carlucci



LIBERATORIA PER L'ARCHIVIAZIONE DELLA TESI DI DOTTORATO

Al Magnifico Rettore

del Politecnico di Bari

Il sottoscritto Francesco Carlucci nato a Bari il 19/12/1989 residente a Bari in Via Latilla 16 e-mail francesco.carlucci@poliba.it iscritto al 3° anno di Corso di Dottorato di Ricerca in Rischio e Sviluppo Ambientale, Territoriale ed Edilizio ciclo XXXV ed essendo stato ammesso a sostenere l'esame finale con la prevista discussione della tesi dal titolo:

“Responsive envelopes performance analysis in current and future climate scenarios: development of an interactive computational platform”

DICHIARA

- 1) di essere consapevole che, ai sensi del D.P.R. n. 445 del 28.12.2000, le dichiarazioni mendaci, la falsità negli atti e l'uso di atti falsi sono puniti ai sensi del codice penale e delle Leggi speciali in materia, e che nel caso ricorressero dette ipotesi, decade fin dall'inizio e senza necessità di nessuna formalità dai benefici conseguenti al provvedimento emanato sulla base di tali dichiarazioni;
- 2) di essere iscritto al Corso di Dottorato di ricerca Rischio e Sviluppo Ambientale, Territoriale ed Edilizio ciclo XXXV, corso attivato ai sensi del *“Regolamento dei Corsi di Dottorato di ricerca del Politecnico di Bari”*, emanato con D.R. n.286 del 01.07.2013;
- 3) di essere pienamente a conoscenza delle disposizioni contenute nel predetto Regolamento in merito alla procedura di deposito, pubblicazione e autoarchiviazione della tesi di dottorato nell'Archivio Istituzionale ad accesso aperto alla letteratura scientifica;
- 4) di essere consapevole che attraverso l'autoarchiviazione delle tesi nell'Archivio Istituzionale ad accesso aperto alla letteratura scientifica del Politecnico di Bari (IRIS-POLIBA), l'Ateneo archiverà e renderà consultabile in rete (nel rispetto della Policy di Ateneo di cui al D.R. 642 del 13.11.2015) il testo completo della tesi di dottorato, fatta salva la possibilità di sottoscrizione di apposite licenze per le relative condizioni di utilizzo (di cui al sito <http://www.creativecommons.it/Licenze>), e fatte salve, altresì, le eventuali esigenze di “embargo”, legate a strette considerazioni sulla tutelabilità e sfruttamento industriale/commerciale dei contenuti della tesi, da rappresentarsi mediante compilazione e sottoscrizione del modulo in calce (Richiesta di embargo);
- 5) che la tesi da depositare in IRIS-POLIBA, in formato digitale (PDF/A) sarà del tutto identica a quelle **consegnate**/inviate/da inviarsi ai componenti della commissione per l'esame finale e a qualsiasi altra copia depositata presso gli Uffici del Politecnico di Bari in forma cartacea o digitale, ovvero a quella da discutere in sede di esame finale, a quella da depositare, a cura dell'Ateneo, presso le Biblioteche Nazionali Centrali di Roma e Firenze e presso tutti gli Uffici competenti per legge al momento del deposito stesso, e che di conseguenza va esclusa qualsiasi responsabilità del Politecnico di Bari per quanto riguarda eventuali errori, imprecisioni o omissioni nei contenuti della tesi;
- 6) che il contenuto e l'organizzazione della tesi è opera originale realizzata dal sottoscritto e non compromette in alcun modo i diritti di terzi, ivi compresi quelli relativi alla sicurezza dei dati personali; che pertanto il Politecnico di Bari ed i suoi funzionari sono in ogni caso esenti da responsabilità di qualsivoglia natura: civile, amministrativa e penale e saranno dal sottoscritto tenuti indenni da qualsiasi richiesta o rivendicazione da parte di terzi;
- 7) che il contenuto della tesi non infrange in alcun modo il diritto d'Autore né gli obblighi connessi alla salvaguardia di diritti morali ed economici di altri autori o di altri aventi diritto, sia per testi, immagini, foto, tabelle, o altre parti di cui la tesi è composta.

Bari, 18/04/2023

Firma



Politecnico
di Bari

Il sottoscritto, con l'autoarchiviazione della propria tesi di dottorato nell'Archivio Istituzionale ad accesso aperto del Politecnico di Bari (POLIBA-IRIS), pur mantenendo su di essa tutti i diritti d'autore, morali ed economici, ai sensi della normativa vigente (Legge 633/1941 e ss.mm.ii.),

CONCEDE

- al Politecnico di Bari il permesso di trasferire l'opera su qualsiasi supporto e di convertirla in qualsiasi formato al fine di una corretta conservazione nel tempo. Il Politecnico di Bari garantisce che non verrà effettuata alcuna modifica al contenuto e alla struttura dell'opera.
- al Politecnico di Bari la possibilità di riprodurre l'opera in più di una copia per fini di sicurezza, back-up e conservazione.

Bari, 18/04/2023

Firma

EXTENDED ABSTRACT (eng)

The growing frequency and magnitude of extreme weather events have increased the attention of scientific and international community regarding the correlation between anthropized environment and external environment. The climate change effects are now clear and, despite several recent global commitments undertaken in last years, the trend for near future will still be characterized by a significant rise in average temperatures. According to the latest report (AR6) of the Intergovernmental Panel on Climate Change (IPCC), even limiting the global warming to 1.5°C compared to pre-industrial levels in the short-term scenario (2021-2040), would limit the damage related to extreme weather events but would not avoid them. Although this topic regards all human activities, the strong incidence of building energy consumption – equal to nearly 40% of total consumption in highly developed countries – makes the building field particularly affected by mitigation actions.

Recently, the research has shifted its attention from an approach based on the maximization of the energy disconnection between internal and external environment, to an approach in which the building envelope can adapt themselves to consider the variations of the boundary conditions; the envelope is then perceived as an interface rather than a shield. The latest studies are therefore focusing on the potential of responsive envelopes or rather envelopes capable to adapt their properties – geometrical, solar, thermal, etc. - to external stimuli. Despite these technologies were conceived with the aim to adapt to external environment changes on short/mid-term time scales (sub-hourly, hourly, daily, and seasonal), recent studies are evaluating their contribution on

larger time scales (decades) to improve the resilience of building envelopes to climate change.

This work aims to provide, firstly, a detailed description of the state of the art of responsive systems and of methods and tools for energy simulation of complex responsive systems. Hence, the main output of the work consists of an interactive computational platform for the energy analysis of these systems in present and future climate scenarios. The developed platform – based on EnergyPlus, Python, and Grasshopper – allows to select different climate zones represented by 25 European cities and different responsive envelope technologies – phase change materials, shape morphing shadings, electrochromic windows – selecting the climate scenario (current, 2050, 2080) to be analysed with a simple interface, widely spread, and easily customizable. Starting from simple inputs (i.e., location, climate scenario, technology, control type) selectable from pop-up lists, the platform – via Python algorithms launched directly from Grasshopper on a local server – edits the energy model, launches the simulations, and provides directly a comparison sheet where the responsive model is compared with a traditional reference static model.

Therefore, the different topics covered by the platform allow the user to easily compare the behaviour of different responsive technologies in different geographical contexts, future scenarios, or – for externally controlled systems – through different control strategies using validated and easily comparable models. The development of a simple platform capable of managing dynamic energy simulations of complex systems aims to provide the required tools to consider responsive envelopes as real alternatives to traditional technologies by evaluating their long-term contribution, considering the climate change underway.

key words

climate change, energy efficiency, responsive envelopes, architectural engineering, sustainable design, digital innovation, computational platform

EXTENDED ABSTRACT (ita)

La crescente frequenza ed intensità di eventi climatici estremi ha aumentato l'attenzione della comunità scientifica ed internazionale verso il rapporto tra l'ambiente antropizzato e l'ambiente esterno. Gli effetti del cambiamento climatico sono ormai evidenti e, nonostante diversi recenti impegni globali intrapresi negli ultimi anni, la tendenza relativa al futuro immediato sarà comunque caratterizzata da un significativo innalzamento delle temperature medie. Secondo l'ultimo report (AR6) dell'Intergovernmental Panel on Climate Change (IPCC), anche limitando il riscaldamento globale a 1.5°C rispetto ai livelli preindustriali nello scenario a breve termine (2021-2040), limiterebbe i danni legati ad eventi climatici estremi ma non li eliminerebbe. Nonostante il tema riguardi tutte le attività antropiche, la forte incidenza dei consumi energetici relativi al patrimonio costruito – pari a circa il 40% dei consumi totali nei paesi altamente sviluppati – rende il settore edilizio particolarmente interessato dalle azioni di mitigazione.

Negli ultimi anni la ricerca ha spostato la sua attenzione da un approccio basato sulla massimizzazione della disconnessione energetica tra interno ed esterno ad un approccio in cui l'involucro edilizio possa adattarsi per accomodare le variazioni delle condizioni al contorno; l'involucro viene quindi percepito come un'interfaccia piuttosto che come una barriera. Gli studi più recenti si stanno quindi focalizzando sulle potenzialità degli involucri responsivi ovvero involucri in grado di adattare le proprie caratteristiche – geometriche, solari, termiche, ecc. – agli stimoli esterni. Sebbene queste tecnologie nascano con l'obiettivo di adattarsi a variazioni dell'ambiente esterno su scale temporali di breve/medio termine (sub orarie, orarie, giornaliere, e stagionali), studi recenti stanno valutando il loro contributo su scale temporali più ampie (decadi) per poter migliorare la resilienza degli involucri edilizi ai cambiamenti climatici.

Il presente lavoro mira a fornire, in prima analisi, una dettagliata descrizione dello stato dell'arte dei sistemi responsivi e dei metodi e strumenti per la simulazione energetica di sistemi responsivi complessi. Quindi, l'output principale del lavoro è costituito da una piattaforma computazionale interattiva per l'analisi energetica di questi sistemi in scenari climatici presenti e futuri. La piattaforma sviluppata – basata su EnergyPlus, Python, e Grasshopper – offre la possibilità di selezionare diverse zone climatiche rappresentate da un ventaglio di 25 città Europee e diverse tecnologie responsive di involucro – materiali a cambiamento di fase, schermature a geometria variabile, vetri elettrocromici – selezionando lo scenario climatico (corrente, 2050, 2080) da analizzare con un'interfaccia semplice, ampiamente diffusa, e facilmente personalizzabile. Partendo quindi da semplici input (i.e., località, scenario climatico, tecnologia, tipologia di controllo) selezionabili da menù a scomparsa, la piattaforma – tramite degli algoritmi Python lanciati direttamente da Grasshopper in un server locale – edita il modello energetico, lancia le simulazioni e fornisce direttamente un foglio comparativo in cui il modello responsivo viene confrontato con un modello statico tradizionale di riferimento.

Pertanto, i diversi temi trattati dalla piattaforma consentono all'utente di poter confrontare facilmente il comportamento di diverse tecnologie responsive in diversi contesti geografici, in diversi scenari futuri, o – per i sistemi a controllo estrinseco – attraverso diverse strategie di controllo utilizzando modelli validati e facilmente confrontabili. Lo sviluppo di una piattaforma semplice in grado di gestire simulazioni energetiche dinamiche di elementi complessi mira a fornire gli strumenti necessari per considerare gli involucri responsivi come reali alternative alle soluzioni tradizionali valutando il loro contributo anche nel lungo termine, alla luce dei cambiamenti climatici ormai in atto.

key words

cambiamento climatico, efficienza energetica, involucri responsivi, architettura tecnica, progettazione per la sostenibilità, innovazione e digitalizzazione, piattaforma computazionale

LIST OF FIGURES

Figure 1. Annual investment in energy efficiency in the buildings sector in the Net Zero Scenario. Data from [14,15].	11
Figure 2. Annual temperature anomalies in 2022 compared with 1981-2010 average. Source [18].	12
Figure 3. Main adopted nomenclatures, possible overlapping, and examples [36].	21
Figure 4. Typical structure and functioning – schematic and not to scale – of EC devices. [109].	28
Figure 5. Typical structure and functioning – schematic and not to scale – of W03 GC devices [109].	31
Figure 6. Typical structure and functioning of a window with variable thermal transmittance based on variable air convection.	33
Figure 7. Typical structures – schematic and not to scale – of a TiO ₂ PEC device. [109]	37
Figure 8. Examples of intrinsically controlled SMA screen of the Piraeus Tower. [109]	40
Figure 9. Functioning criterion of the Al Bahr Tower shading system [109]	41
Figure 10. Schematization of the Special Report Emission Scenarios.	49
Figure 11. Schematization of the AR6 scenarios.	50
Figure 12. Medium office reference model geometry.	55
Figure 13. Global heating and cooling energy demand in reference and ideal loads office model.	58
Figure 14. Dry bulb temperature (a) and global horizontal radiation (b) of the 25 selected cities.	60
Figure 15. Individuation of the sample of 25 cities used for the analyses. [37]	62
Figure 16. Lighting schedule for weekdays (above) and Saturdays (below).	64
Figure 17. Electrical equipment schedule for weekdays (above) and Saturdays (below).	65
Figure 18. Occupancy schedule for weekdays (above) and Saturdays (below).	66
Figure 19. HVAC operational schedule for weekdays (above) and Saturdays (below).	67
Figure 20. Incidence of different office types (a), construction types (b), and historical buildings (c) in the analysed office buildings.	69
Figure 21. Structure and plugins of the computational platform proposed.	73
Figure 22. Platform general interface.	74
Figure 23. General input interface.	74

Figure 24. Upload of the Python scripts on the server. 75

Figure 25. Output of the location evaluator module..... 76

Figure 26. Numerical output module. 77

Figure 27. Example of the comparison sheet..... 78

Figure 28. Differences between (a) traditional approach (combination of output) in a daylighting example and (b) proposed approach based on the combination of inputs in an energy example. Source [40]..... 80

Figure 29. Conceptualization of the final algorithm. Source [40] 82

Figure 30. Selection of the activation thresholds. 84

Figure 31. Combination algorithm flow chart. Source [40] 85

Figure 32. Screenshot from the dynamic shading module of the computational platform..... 86

Figure 33. Heat-temperature curve for the PCM-enhanced plasterboard. 88

Figure 34. Enthalpy curve modelling in the computational platform starting from the physical properties (density, specific heat, latent heat, starting melting temperature, final melting temperature) of the material. 88

Figure 35. Shading control for EC windows in EnergyPlus..... 90

Figure 36. Commercial EC windows provided as viable alternatives in the platform. 92

Figure 37. Shading control for EC windows in EnergyPlus..... 94

Figure 38. Geometrical details of the dynamic shading system considered. Adapted from [39]..... 97

Figure 39. Total energy variation by source for the EC test case study in the current weather scenario (above) and 2080 scenario (below)..... 100

Figure 40. Total energy variation by source for the PCM test case study in the current weather scenario (above) and 2080 scenario (below)..... 104

Figure 41. Total energy variation by source for the DS test case study in the current weather scenario (above) and 2080 scenario (below) compared with the reference model without any shading. 108

Figure 42. Total energy variation by source for the DS test case study in the current weather scenario (above) and 2080 scenario (below) compared with the reference model with a static ST1 shading..... 112

Figure 43. Total energy variation by source for the DS test case study in the current weather scenario (above) and 2080 scenario (below) compared with the reference model with a static ST2 shading..... 116

LIST OF TABLES

Table 1. Shading systems available in EnergyPlus v.9.4. [40]	46
Table 2. Comparison between statistical and dynamical downscaling methods.	52
Table 3. Geometric characteristics of the medium office reference model.	55
Table 4. MBE and CVRMSE values obtained comparing the ideal loads and the original model for all the locations considered.....	57
Table 5. Characteristics of the 25 European cities considered (data from epw weather file). [37]	61
Table 6. Characteristics of the envelope properties for each climatic zone.....	62
Table 7. Characteristics of PCM-enhanced plaster panel.....	87
Table 8. Available commercial EC device. Adapted from [209].....	91
Table 9. Simulations conducted during the testing phase and relative inputs considered.....	98
Table 10. Results obtained for the EC models.....	101
Table 11. Results obtained for the PCM models.	105
Table 12. Results obtained for the DS models compared with the unshaded reference model.	109
Table 13. Results obtained for the DS models compared with the static ST1 shading.	113
Table 14. Results obtained for the DS models compared with the static ST2 shading.	117

INDEX

LIST OF FIGURES.....	5
LIST OF TABLES.....	7
INDEX.....	8
1. INTRODUCTION.....	10
2. STATE OF THE ART.....	19
2.1 Responsive envelopes.....	19
2.1.1 Phase Change Material.....	23
2.1.2 Switchable glazing.....	27
2.1.3 Dynamic Shading.....	39
2.1.4 Responsive envelopes and modelling tools.....	43
2.2 Climate change and future analyses.....	48
3. METHODOLOGY.....	54
3.1. Software and definition of the reference models.....	54
3.2. Locations and envelope properties.....	59
3.3. Internal loads and operational schedules.....	64
3.4. Future weather files.....	70
4. COMPUTATIONAL PLATFORM.....	71
4.1 Users' interface development and programming.....	71
4.2 Responsive technologies modelling.....	79
4.2.1 Dynamic shading modelling.....	79
4.2.2 PCM modelling.....	87
4.2.3 Electrochromic modelling.....	90
4.3 Testing the platform: case studies.....	95
4.3.1 Electrochromic windows: results.....	99
4.3.2 Phase Change Material: results.....	103
4.3.3 Dynamic shading: results.....	107
4.4 Limitations and future developments.....	120

5. CONCLUSIONS	124
6. ACKNOWLEDGEMENTS	128
7. LIST OF ABBREVIATIONS	129
8. REFERENCES/BIBLIOGRAFIA	132
CURRICULUM.....	150

1. INTRODUCTION

The implication of the built environment in the global energy consumption is henceforth clear; therefore, its key role in the reduction of the greenhouse gas (GHG) emissions and the consequent attempt to limit the climate change is as relevant as ever. Accounting for almost 32% of the total global energy consumption, nearly 19% of the global GHG emissions can be attributed to the building sector [1]. More specifically, these figures depend on the geographical areas due to different incomes, energy prices, and climatic conditions. For example, in highly developed countries, the building sector accounts for nearly 40% of the total energy consumption [2]. The EU is in line with this average as in 2016 the total energy consumption reached 1108 Mtoe (Million tonnes of oil equivalent) of which nearly 458 Mtoe (41%) were consumed by the building sector (65% for households and 35% for services) [3,4]. Among the other highly developed Countries, in the USA the building sector accounted for nearly 40% of the total consumption in 2019 [5], with a constant increase from the 33.7% registered in 1980 [6]. Completely different values – nearly 20% – can be found in China due to a very different income-energy price ratio [7].

In light of these data, the global community in the XXI century is clearly aiming to the reduction of the GHG emissions to reduce the effects of the current climate crisis. Therefore, in the last decades, a series of commitment of the international community has led to many fundamental goals – e.g. the United Nations Sustainable Development Goals [8] (in particular this study refers to goals 11 and 13), the Paris Agreement Commitment [9] first and the Glasgow Climate Pact [10] then – to reach the net-zero GHG emissions in the next years. The EU, for example, has developed a specific regulatory framework – the Energy Performance of Buildings Directive [11,12] – which is currently under review as part of the latest “Fit for 55” Commission Work Programme which has set the ambitious goal of a full decarbonisation of the building stock by 2050 [13]. In this regard, figure 1 shows the actions of the main Countries in term of annual investment in energy efficiency in the building sector where the strong commitment of the EU can be clearly seen in recent years.

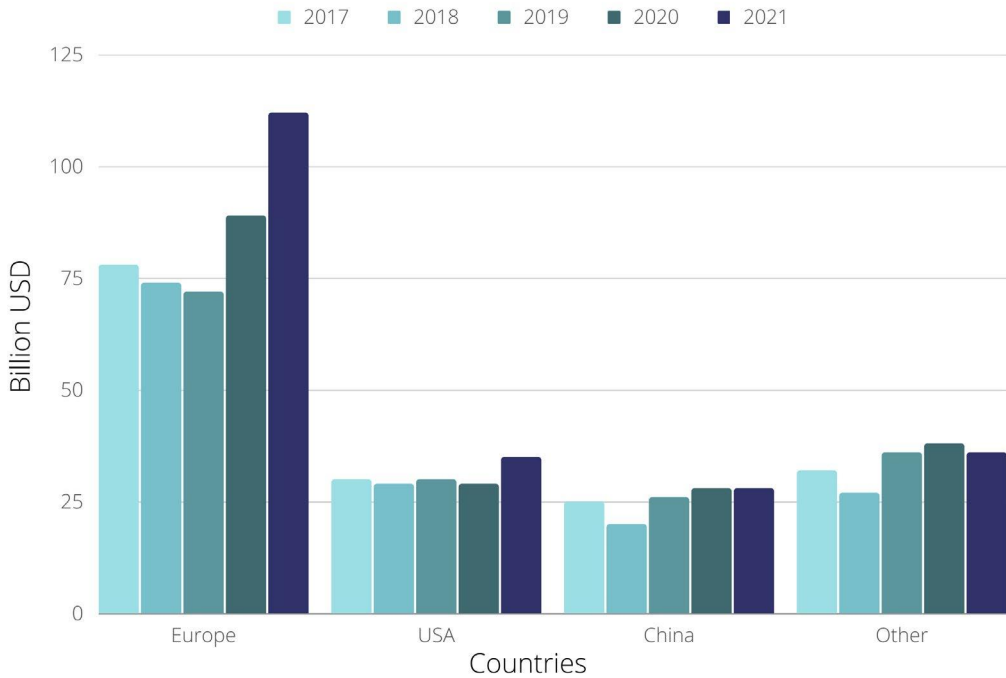


Figure 1. Annual investment in energy efficiency in the buildings sector in the Net Zero Scenario. Data from [14,15].

Many of the above-mentioned commitments and laws comes from the awareness that the human induced climate change is increasing the frequency and the magnitude of temperature anomalies and extreme adverse weather events. For example, figure 2 shows the annual temperature anomalies registered in 2022 compared with the 1981-2010 average values. Despite the effect of La Niña – a climate pattern that describes the cooling of surface-ocean waters along west coast of South America –, this figure clearly highlights that last year was characterized by an overall increase of the temperature anomalies.

The climate related hazards are strictly linked to the global warming and exceeding the set threshold of 1.5°C in the near-term scenario (2021-2040) would increase the hazard according to other socioeconomic aspects. However, even containing the global warming below 1.5°C should only reduce the damages of adverse events but cannot completely avoid them [16]. Regardless the scenario considered and the actions taken

to contain the phenomenon, the main trend in the following years – up to 2040 – is characterized by a global surface temperature increase [17]. Instead, regarding long term scenarios (2040-2100), the hazard for extreme weather events is strictly related to the mitigation actions taken during these years that could reduce the risk.

Annual Temperature Anomalies 2022

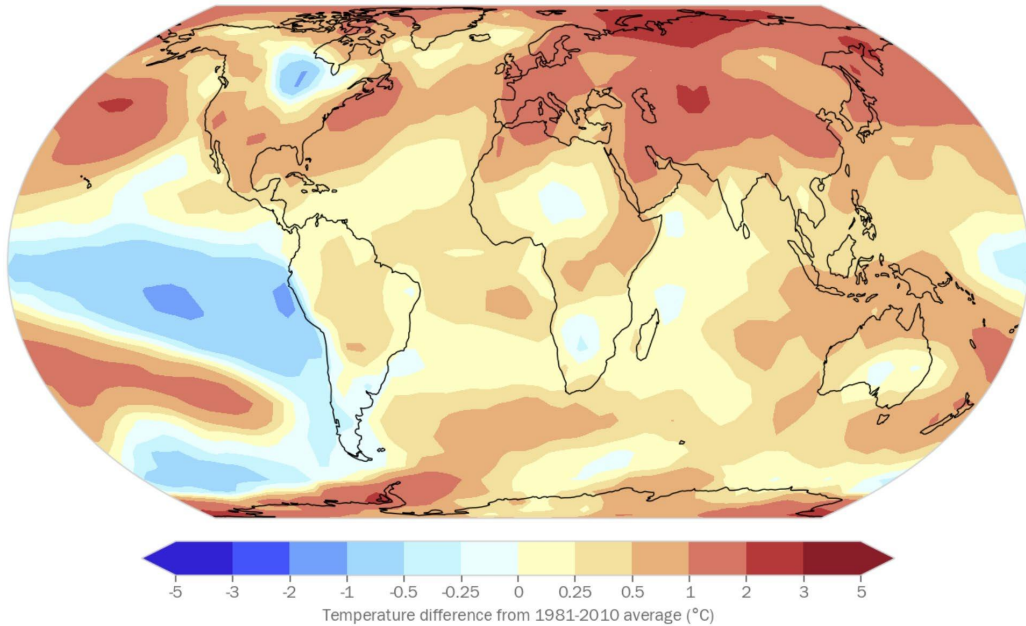


Figure 2. Annual temperature anomalies in 2022 compared with 1981-2010 average. Source [18].

This climate and building consumption framework, has attracted the attention of researchers in this field as demonstrated by the rising number of studies concerning building energy behaviour in future scenarios [19].

Despite this new awareness and regulations are well established, data on global scale, collected in the past years, sometimes seems to contradict the expected results highlighting different gaps between reality and rhetoric. This historic period makes extremely difficult the comparisons between last years, due to unpredictable and extraordinary phenomena such as the Covid-19 pandemic in 2020/2021 and the energy crisis related to the Russian war in 2022. For example, in 2020, the lockdowns required by the pandemic crisis led to a clear reduction of the coal and oil demand reducing the

energy consumption of nearly 4%. Nevertheless, this change was clearly temporary as the economic upturn has taken the consumptions back to 2019 levels. These trends are referred on a global scale but, considering more specific socioeconomic contexts, diverging trends can be found. For example, the emerging markets account for nearly 70% of the global energy demand growth while highly developed economies are going to be 3% below the 2019 figures [20]. Looking more in detail the building field, the construction sector is responsible for nearly 32% of the energy consumption and almost 15% of direct CO₂ emissions. Despite the above-mentioned regulatory frameworks, the building sector emissions have grown of nearly 1% per year in the last 10 years, until the Covid-19 pandemic. This trend seems to be opposed to the spread of renewable energy system that leads to a strong reduction of the emissions related to the power generation systems; nevertheless, this result can be explained considering the higher access to energy sources and to larger constructed floor spaces. The access to space cooling has risen in the last 10 years (2010-2020) of nearly 8% from 27% to 35% [15], moreover in the last 20 years the constructed floor space has risen of nearly 65%; it follows that the average unitary energy demand (kWh/m²) has been lowered by 25% [21].

However, despite the fluctuations due to specific events or to specific geographical areas, the building sector is not keeping up with the 2050 carbon neutrality targets and hence further efforts are required to meet the set goals [22]. The International Energy Agency (IEA) provides a detailed tracking report to monitor the evolution of the building sector from an energy point of view; in their latest release (2022) [15], the IEA registered that in 2021 only the lighting systems were on track with the set goals. All other energy related systems are not on track and require more efforts; in particular, the district heating and the envelope design are the furthest from the set goals.

To improve this trend, analysing the variation of the building consumption by energy source can help to understand the current state of the building energy efficiency to define the best course of action for the building design. Nowadays, it is widely agreed that almost half of the energy demand of industrial and residential buildings are attributable to the Heating Ventilation and Air Conditioning (HVAC) system [23] and the HVAC

consumptions are strongly related to the envelope losses [24] and the building heat gains [25]. The strong impact of the HVAC consumption explains why the energy efficiency efforts are focusing on one side on the energy transportation and generation and, on the other one, on the building envelope enhancement [23,26].

Looking more in detail the building consumption, the space heating consumption has significantly decreased in the last 10 years (2020-2010) with a reduction of nearly 20% followed by the lighting consumption (reduction of nearly 17%) and finally the cooling consumption registered a reduction of only 7% [27]. Even though these variations are the results of the combination of many elements – including the climate change –, this gap can be explained considering mainly two main trend: the spread of new highly efficient lighting technologies (LED) and the energy conservation approach that has led to a considerable increase of the building insulation. The former has clearly reduced the lighting consumptions; instead, the latter has, on the one hand, reduced the heating demand while, on the other hand, it has increased the summer overheating, especially in hot climates.

This conservative static approach – where the main goal is to minimize the thermal losses – was largely adopted in the envelope design up to the first years of the 21st century. In this design strategy, the indoor-outdoor disconnection was maximized aiming to a good energy conservation in buildings [28]. Despite this strategy minimize the thermal losses, it is completely decoupled from the dynamism of the external environment. The awareness that the environmental variables (solar radiation, dry bulb air temperature, humidity, wind, rainfalls etc.) can constantly change during the days has started to spread a new concept of dynamic envelope in the scientific community. The climatic variables can change during the day (sub hourly and hourly variations), during days (daily and weekly variations), during seasons (monthly variations), and – considering the climate changes – during decades. Moreover, if we consider that the users' behaviour is constantly changing, the boundary conditions of the buildings energy phenomena can be defined as extremely dynamic. This awareness has slowly lead to consider the envelope as a multifunctional interface element rather than a single behaviour static boundary [29] improving the importance of considering all the interactions

between environment and buildings. This paradigm shift has led also to increase the importance of the Indoor Environmental Quality (IEQ) because the traditional static approach can lead to disadvantages such as the summer overheating [30] or visual discomfort [31] that cannot be addressed by static envelopes. Thanks to this new approach, many other fundamental aspects of the building physics – such as natural ventilation [32], thermal, and visual comfort [33,34] – were considered in addition to the energy consumption as demonstrated by the growing number of studies on IEQ in the last years [35]. Hence, the latest efforts in the envelope design research fields are focused on the design of responsive technologies; these systems can change their properties – solar, thermal, optical, etc. as better described in following sections – to reduce the energy demand and improve the users' comfort. Clearly, the dynamism of the envelope increases the complexity of the analyses adding a further degree of freedom to the phenomenon. For example, in the dynamic energy analyses, not only the external weather but also the envelope properties can change over time according to specific activation strategies – in the extrinsically controlled systems – or to the external environment, in the intrinsically controlled system. Moreover, a further layer of complexity is provided by the uniqueness of each technology that can work on different aspects such as the control of the solar radiation – kinetic shading, chromogenic glazing, etc. –, on the thermal mass – Phase Change Materials (PCM) –, on the thermal transmittance – variable transmittance envelopes –, or on a combination of the previous such as the PCM windows.

Despite the potential of these technologies, they are still not widespread in the building field. One of the reasons of this slow spread is the lack of easy and proper tools to predict their behaviour. Currently, the energy modelling software include only few default, simple, and easily accessible responsive technologies – e.g. the dynamic curtains – while more sophisticated systems require specific programming knowledge and/or workarounds and are significantly more time consuming and less accessible. Hence, while many studies are conducting technological analyses on these devices, their energy analysis is getting behind and is still less diffuse.

Moreover, the energy results are strictly connected to the climate, settings, and model considered; this feature adds further clutter to a topic still under development. It follows that the available energy studies on the same technology are few and hardly comparable. All these elements slow down the spread of responsive systems; this could be a missed opportunity to innovate the building envelope field with devices that allow to accommodate the environmental changes rather than simply providing a disconnection between internal and external environments.

Furthermore, although these systems were conceived considering short and mid-term changes (sub hourly, hourly, daily, seasonal), their responsiveness could be helpful on larger time scales (decades) to address the above-mentioned effects of climate change that could occur during the whole envelope lifespan. Hence, evaluating and optimizing these systems in both current and future weather scenarios could drive the spread of these technologies improving the energy efficiency and the users' comfort on a wider perspective.

Therefore, the main research gaps found can be summed up in the following list:

- Lack of proper simulation tools to easily analyse complex responsive envelopes in a single environment;
- Current studies on responsive envelopes are strictly related to specific model, settings, and climates, therefore it is extremely difficult to conduct comparisons to study in deep the behaviour of each technology;
- Few studies consider the benefits of responsive envelopes in both current and future climate scenarios.

The aim of this work is to fill in these gaps providing all the required tools to allow easy, reliable, comparable, and future-projected energy analyses for complex responsive systems.

To that end, after a preliminary detailed analysis of the most diffuse and promising responsive technologies, this study provides as main output the development of an interactive tool that allows to model these complex energy phenomena easily and reliably. Considering that the intrinsic nature of these technologies is strictly dependant on

climate, the proposed platform allows to choose among 25 different European locations to compare and/or optimize the responsive systems in different climatic zones.

Furthermore, in order to study, test, and compare different technologies in different contexts, the platform provides a reference model that allows to run comparable analyses. Therefore, the behaviour and the main strengths and weaknesses of the analysed technologies can be studied in different contexts and can be easily compared.

Moreover, in the light of the above introduction, specific modules regarding the future climate projections were included for two main reasons. Firstly, nowadays the energy assessment on buildings should not ignore the future climate projections to be considered truly up to dated; secondly, the dynamic nature of responsive systems can significantly help the buildings to adapt to long term variations.

To sum up, the research questions that this work tries to analyse can be listed as follows:

- a) Which is the current state of the art in the responsive envelope design and energy analysis field?
- b) How can we study the features of a specific responsive technology in different geographical and climatic contexts running reliable comparisons?
- c) How can we simulate complex responsive technologies easily, rapidly, and in a single simulation environment without any programming workarounds?
- d) Can we provide the users with a fast and easy-to-use single tool that can address all the previous points?

The research activities conducted to address these questions were developed splitting the research questions in different coherent topics and working on different macro themes which are reflected in the structure of this work. In particular, after this brief introduction to the general context, the problem statement, and the main aims of the research, section 2 provides the state of the art of the main topics interested by this work to answer to the first research question (a). Going more in detail, section 2.1 describes the state of the art of the responsive envelopes with a specific focus, on the one hand, on the nomenclature and classification and, on the other hand, on the technological functioning (subsections 2.1.1, 2.1.2, 2.1.3). Moreover, subsection 2.1.4

provides a review of the main tools and workarounds available for the energy modelling of responsive envelopes. The state of the art of the second main topic of this work is provided in section 2.2 where climate change and future weather projections are described from both a theoretical and a modelling point of view. To answer to the second research question (b), a specific methodological approach was adopted in this study; in particular, in section 3 all the propaedeutic models, weather files, and tools are presented, analysed, and adapted to this specific application.

The main result of this research – that addresses the last two research questions (c, d) – is described in section 4 where a detailed presentation of the platform is provided. In particular, the first subsection (4.1) is focused on: structure of the platform, tools and libraries adopted, management of the general inputs, and output presentation. On the contrary, the second subsection (4.2) describes the required inputs and the simulation approach adopted for each specific responsive technology. Then, the third subsection (4.3) tests the platform considering a case study application where the platform has been tested to better define the limitations of this tool. According to the results obtained, the third subsection (4.3) highlights the main limitations found and the possible future developments of this research. Finally, the last section (5) sums up the study conducted and the results obtained; afterwards, three sections including respectively acknowledgments, references and a brief Curriculum Vitae are provided.

2. STATE OF THE ART

The complexity of the themes mentioned in the previous section, highlights the need of a thorough analysis of the current state of the art to define the main strengths and gaps of the research on these topics.

The aim of this chapter is to define the current context of each of the subtopics that defines the research questions. Each following subsection addresses a specific topic which has been studied in deep and published in dedicated journal papers by the writer. In particular [36] was considered as main state of the art reference paper, [37] for the PCM subsection, [36,38] for the switchable gazing subsection, [36,38,39] for the dynamic shading state of the art, [40] for the modelling tools state of the art, and [41] for the climate change assessments.

2.1 Responsive envelopes

The framework described in the introductory section explains the increasing awareness among policymakers regarding the need to improve the energy efficiency in buildings. Researchers are supporting this new awareness – and the subsequent changes – focusing their attention on new technologies. In particular, among the different innovative solutions, this work is focused on responsive envelopes, namely those systems that aim to improve the energy efficiency and the users' need through reversible changes of the device properties to adapt them to changing boundary conditions [42]. Depending on the specific technology, these systems can act on the control of the solar radiation – both solar loads and daylighting –, on thermal storage and insulation, and on ventilation to adapt the envelope to different external stimuli [43]. Firstly, an in-depth description of the available nomenclature and classification systems is provided to allow a clear understanding of the proposed concepts.

The fast spread of these concepts in recent years has led to a confusing use of many similar terms – e.g., adaptive, responsive, kinetic, etc. – even though the first theorizations of these concepts are older. One of the first conceptualization of responsiveness was provided by Negroponte [44] who defined architecture – in particular housings –

as “unresponsive”. This first architectural theorization was then declined in 1981, from a more technical point of view, in the paper “A wall for all seasons” [45]; in this article the author conceived a single layer transparent envelope to satisfy different performance requirements. Notwithstanding these first theorizations, the real spread of these concepts started in the 21st Century thanks to the increasing development of new technologies and materials. In this renovated context, responsive [46], adaptive [47], kinetic [48], dynamic [49], intelligent [50], smart [51], and switchable [52] are the most common adjectives associated to envelopes with time-varying properties. Despite all these terms seem interchangeable, each one focuses on specific features which were theorised in a previous study [36] and are visualized in figure 3.

In the author’s opinion, the widest definition is given by the term “responsive” proposed in the Annex 44 of the IEA - Energy Conservation in Buildings and Community Systems Programme (IEA-ECBCS) [53]. According to this source, the Responsive Building Elements (RBEs) were defined as component that can react in a predefined way in response to external stimuli or to users’ interaction to control the transfer and storage of heat, light, air, and water [54].

A slightly different definition can be adopted for adaptiveness; Loonen considers Climate Adaptive Building Shells (CABS) those envelopes that can change their properties repeatedly and reversibly according to a variation of the boundary conditions to improve the IEQ and reduce the energy demand [28]. In the writer’s opinion, this definition includes few technologies which are not literally “adaptive” (e.g. electrochromic glazing); on the contrary, the adaptive systems should include only self-triggering devices with autonomous sensing and actuating systems.

While the previous definitions are usually considered extremely similar, the term kinetic is usually characterized by a slightly different meaning. The Acclimated Kinetic Envelopes (AKEs) were defined by Wang et al. as envelopes that react to external stimuli with visible physical changes [55]; therefore, this definition is mainly focused on macroscopic – usually the movement of building components – rather than microscopic variations. The term dynamic is usually adopted as synonym of kinetic even though dynamic is sometime used also in different contexts such as dynamic glazing.

Instead, the main feature of intelligent devices is their organization in specific components for perception, cognition, and action to whom correspond sensors, controllers, and actuators [56]. Hence, thanks to this structure, these devices can change their properties through automated adjustments [57].

Another extremely diffuse term is “smart” which is usually associated to both materials and technologies; it is apparently very similar to “intelligent” but includes further shades of meaning. Smart materials can be classified in property exchanging or energy exchanging [58]; the former can change their thermal, mechanical, magnetic, optical, or electrical properties (e.g. photochromic films) while the latter can convert energy (e.g. photovoltaic). Although, the term smart can also be applied to larger contexts such as buildings, grids, or cities when the term smart is referred mainly to advanced control systems for interconnected operability [59]. This brief description highlights a wide possible use of the term smart which can be used to describe both intelligent and adaptive systems [60].

Finally, the last term considered in this brief review is “switchable”. This adjective is usually adopted in the windows and glazing field. The switchable glazing can modulate or switch its properties according to external stimuli; depending on its functioning it can be classified as actively (electrochromic) or passively (photochromic) controlled [52].

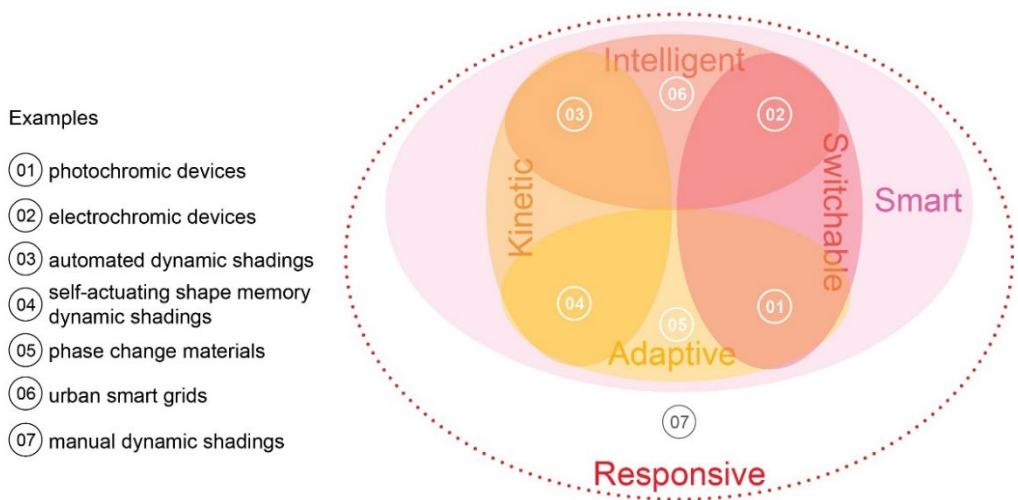


Figure 3. Main adopted nomenclatures, possible overlapping, and examples [36].

This brief list of the nomenclature adopted in this research field hints the complexity of the topic and the broad number of different contributions and studies conducted in the last years. The spread of these studies and the large availability of disparate technologies were supported by the creation of different classification systems based on different criteria. For example, one of the most recent systems [61] is based mainly on the opinions of the main stakeholders. Indeed, after interviewing architects, engineers, manufacturers, contractors, and operators, the authors defined four main families – dynamic shadings, chromogenic façade, solar active façade, and active ventilative façade – composed by 11 technologies overall. A further level of description is provided to each technology which could be classified based on its application-purpose (privacy, insulation, etc.), control type (manual, automated, etc.), building type (residential, etc.), and technology-material (wood, suspended particles, etc.).

A different approach was considered by Loonen et al. who provided two different classification systems. The first one [42] considers the physics of the system (thermal, optical, air flow, and electrical) and then identifies its time scale (seconds, minutes, hours, seasons), its scale of adaptation (micro or macro), its control type (intrinsic or extrinsic) and its typology (built, subsystems, full scale, or reduced scale prototype). The second one [62] is a review of the first one and starts from the purpose-goal of the system (thermal comfort, indoor air quality, visual performance, acoustic quality, energy generation, personal control), then considers the responsive function (e.g. modulate solar gains), the operation (intrinsic or extrinsic), the technologies-materials adopted (e.g. PCM, switchable glazing), the response time, the spatial scale (building material, façade element, wall, fenestration, roof, whole building), the visibility (no, low, high) and finally the degree of adaptability (on/off or gradual). This last classification system is considered extremely complete and, therefore, was considered in this study as main reference.

Referring to AKEs, the classification proposed by Wang et al. [63] could be considered as a possible approach. Firstly, the authors identify the relation between climate source and façade (solar responsive, air flow responsive, others). The following classification level considers the parameters that control the devices: solar heat, daylight, solar

electricity for the solar responsive systems, natural ventilation, or wind electricity for the air flow responsive, and precipitation or air temperature are included in the “others” class.

While these systems can describe the largest number of responsive technologies, other classification systems can be considered specifically for certain devices. For example, with regards to kinetic systems, another classification system [64] takes into account four main classification levels: kinematic (limited, medium, major, variable), control technique (direct-responsive, internal or direct, responsive indirect), system configuration (embedded, dynamic), control limit (minor, medium, significant, variable), and cost (small, medium, big, huge). Combining these four criteria, different categories (skin unit systems, retractable systems, revolving buildings, and biomechanical buildings) can be identified to describe the considered system.

Instead, a different approach was adopted by Ochoa and Capeluto [65] who consider three main categories (input elements, control processing elements, actuating elements) to classify the devices. Starting from these main classes, the authors reach more than 40 possible combinations branching each class in different subclasses (category, design variable, sub-variable, common values).

In the following subparagraphs the most promising technologies are described and classified in accordance with the nomenclature system proposed by Loonen et al. [62].

2.1.1 Phase Change Material

This brief introduction foreshadows the wide range of technologies available; among these, the PCMs are undoubtedly one of the most developed thanks to a broad experimentation conducted in past years [66,67] in different research fields including the buildings energy efficiency [68], waste heat recovery devices [69], the electronic field [70] and the aerospace field [71]. The main advantage of these materials lies in their capability to store and release naturally available heat in low-volume elements, improving their energy storage density [72]. Focusing the attention on the building design domain, the PCMs can mainly bring benefits to two macro topics investigated: the reduction of thermal consumptions and the reduction of thermal discomfort. Previous

studies [73] outlined the contribution of PCMs to the reduction of HVAC energy demand which could be decreased by up to 30% when applied as retrofit solutions for residential buildings in cold climates. Furthermore, these materials can also significantly reduce the thermal discomfort by stabilizing the indoor radiant temperature [74].

These advantages are strictly related to the physical behaviour of the materials and to the different products available; hence, it is fundamental to understand their nature and functioning to properly design a PCM-integrated building element. Every material can store and release heat through three different approaches: sensible heat storage (SHS), latent heat storage (LHS), and thermochemical heat storage. The latter is usually not applied to the building field while SHS and LHS strongly contribute to the thermal behaviour of the building [72]. Considering the SHS, the heat absorbed or released is related to the increase/decrease of temperature in relation to the mass of the body (m), the specific heat (c), and the variation of temperature (dT), as described in Equation (1).

$$Q_S = \int_{T_1}^{T_2} m c dT \quad (1)$$

On the contrary, during the LHS, the temperature of the material does not change as the heat absorbed/released triggers the change of phase as it happens, for example, in the melting from solid to liquid. In the LHS phase, the heat stored depends on the mass, the fraction melted (f_m), and the variation of enthalpy of fusion per unit mass (Δh_m) (Equation (2)).

$$Q_L = m f_m \Delta h_m \quad (2)$$

Usually, both SHS and LHS can take part to thermal phenomena; for example, considering a gypsum-PCM board, the exchanged heat corresponds to the enthalpy variation of each material embedded in the board (gypsum and PCM in this case) according to equations (3), (4), and (5) [75]:

$$\Delta H_{tot} = m \cdot [(1 - f) \cdot \Delta h_{gypsum} + f \cdot \Delta h_{PCM}] \quad (3)$$

where, considering the complete melting of the PCM ($f_m = 1$), the partial enthalpies are:

$$\Delta h_{gypsum} = \int_{T_1}^{T_2} m c_S dT \quad (4)$$

$$\Delta h_{PCM} = \left(\int_{T_1}^{T_m} c_S dT + \Delta h_m + \int_{T_m}^{T_2} c_L dT \right) \quad (5)$$

Where f is the mass fraction of the PCMs in gypsum, c_S and c_L are, respectively, the specific heat of the solid and liquid states, and T_m is the melting temperature of the PCM.

It follows that, in the building field, to take advantage from the LHS, the melting temperature of the PCMs should be within the human comfort range (20 °C–30 °C) [76]. In these cases, these materials can store a good amount of heat in low-volume elements without increasing their temperature affecting the users' thermal comfort. From a theoretical point of view, PCMs can store or release heat in different phase transitions: solid–solid, solid–liquid, gas–liquid, gas–solid [77]; nevertheless, usually, the solid–liquid transitions take place in the building field.

Depending on their composition, PCMs can be classified in three main classes: organic, inorganic, and eutectic. The first ones are composed of paraffins, fatty acids, fatty-acid esters, and sugar alcohols and, in general, can be classified as paraffin or non-paraffin. The main strength of organic PCMs is that they are not affected by phase segregation during repeated melting-freezing cycles and that they are slightly affected by super-cooling. On the contrary, as paraffinic PCMs are derived from oil refining, their main weakness is the low ignition resistance that makes difficult the use of these materials for envelope applications. Considering the melting temperature, organic PCMs ranges from -57°C to +187°C with a melting latent heat that varies between 85 and 300 J/g [78–80]; it follows that the choice of the right PCM is fundamental to optimize their functioning.

Inorganic PCMs can be classified as salt-hydrates or metallic and the main difference with the organic PCMs is that they have higher density that allows to reach higher melting latent heat per unit volume, notwithstanding the similar enthalpy per mass.

Compared with organic PCMs, inorganic ones are characterized by higher ignition resistance, higher conductivity, and higher melting points. The main disadvantages of these materials are related to the risk of supercooling, phase segregation, and corrosion. Finally, the eutectic PCMs combine the main properties of different kind of PCMs with the same melting points; depending on the materials adopted to create the eutectic PCMs, they can be classified as organic–organic, inorganic–inorganic, and organic–inorganic.

From a technological point of view, to avoid damaging interactions between PCMs and environment or other materials, they are usually encapsulated. This process can also help to reduce the risk of corrosion and phase segregation improving, besides, their handling and the heat exchange surface [81,82]. These capsules can be made of different materials - aluminium, plastic, polyolefin, rubber, polymers, etc. – and different shapes (balls, tubes, plates, and boxes) [82]. According to the size of the adopted capsules, the encapsulation process can be classified as macroencapsulation ($d > 1$ mm), microencapsulation ($1 \mu\text{m} < d < 1$ mm), or nanoencapsulation ($d < 1 \mu\text{m}$). From a technological point of view, the application of PCMs in the building field was largely studied and most of the solutions developed can be classified into two main categories: active and passive storage systems. The formers work using heat exchangers and forced convection and are classified into direct and indirect systems. In indirect systems the transfer medium (the fluid) and the storage element are distinguished; on the contrary in direct systems the heat transfer fluid performs both functions [83]. Many applications were developed for active systems [84] applied to different building elements such as suspended ceilings [85,86], ventilation systems [87,88], double-skin envelopes [89], solar collectors [90,91], heat storage water tanks [92,93], integrated photovoltaics [94,95], and building cores enhanced with PCMs activated through the use of pipes [96].

On the contrary, no forced convection can be used in passive systems; hence, these systems are simply classified depending on the placement of the PCMs in the building element, thus: inside the material, as a new layer, and in windows or as sun protection [97]. When encapsulated, PCMs can be easily embedded in other construction

materials (concrete [98], plaster [99], cellulose, or glass fibres [100]) increasing the overall thermal inertia of the building component. Another way to increase the thermal inertia – usually with reference to lightweight constructions – is to create a new layer with PCMs embedded boards; in particular, PCMs-enhanced gypsum plasterboards or PCM sandwich panels [101] are often used as additional layers to improve the envelope overall performance. The use of PCMs as additional layers is quite widespread thanks to the different commercial products already available. For example, among the micro-encapsulated PCMs-enhanced gypsum plasterboards Rigips-Saint Gobain markets the Alba Balance board, while Delta-Cool24 (Dorken) or the Energain (Dupont) are other commercial products that uses macroencapsulated PCMs in plates or bags.

Another completely different use of PCMs in building components regards the solar protection. Different studies evaluate the use of these materials in internal blinds [102] or inside the windows adding, for example, additional gaps behind the inner glazing [103].

As already mentioned, the broad variability of the PCMs melting point requires a dedicated study to select the proper material for each application. In accordance with previous studies [77,104–106] the optimal melting point for cooling applications is up to 21°C, while for heating applications the optimal melting point is 22°C or 2 °C above the heating setpoint. Regarding other applications of PCMs in the building field, the optimal melting temperature for thermal comfort ranges between 22 and 28°C while hot water applications require higher temperatures usually between 29 and 60°C. Instead, very high melting points are required for waste heat recovery applications.

For this study, a PCM new layer was implemented as inner layer of external walls, as better described in the following sections.

2.1.2 Switchable glazing

Thanks to the spread of glazed envelopes and to their high suitability for retrofitting interventions, new devices that are recently catching the attention of both researchers and manufacturers are based on switchable glazing. Due to the high number of technologies available, they are usually classified depending on their control type. Extrinsic

or active devices are controlled and triggered by a sensor-processor-actuator system that allows a flexible control of the window. On the contrary, intrinsic or passive devices can self-adjust their properties according to environmental stimuli – such as solar radiation, temperature, humidity etc. – that trigger the envelope response. Each of the following subsections describes in detail the most diffuse and promising technologies adopted in the building field domain excluding all those devices (e.g., Liquid Crystal and Suspended Particle Devices) adopted only for aesthetic or privacy applications or in other application fields [107].

2.1.2.1 Extrinsicly controlled glazing

Electrochromic, plasmonic electrochromic, and nanocrystal in-glass composites

One of the most evolved active switchable systems is, undoubtedly, the Electrochromic (EC) technology thanks to its capability to switch – according to customizable settings – its transmittance properties. The switch between bleached and coloured state is allowed thanks to a reversible oxidation or reduction reaction that occurs as a response to an electrical stimulus in a 5-layers coating applied to the glazed panes. The coating outer layers are two external transparent conductive layers respectively followed by EC films deposited on each conductor and an intermediate electrolyte layer [108,109] as shown in figure 4.

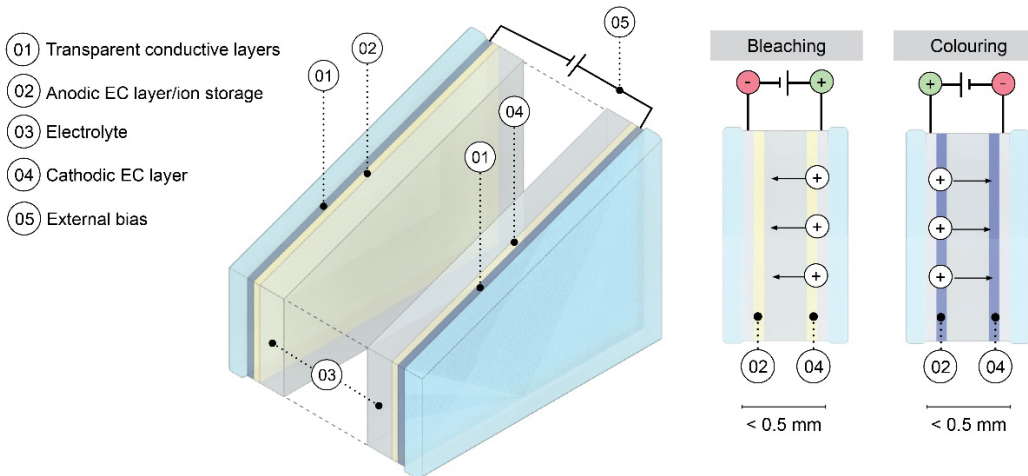


Figure 4. Typical structure and functioning – schematic and not to scale – of EC devices. [110].

When an external low voltage is applied to the transparent conductive layers, the cations – usually H^+ or Li^+ – embedded in the electrolyte are displaced from the cathodic to the anodic or ion-storage coating. Hence, due to this lack of electrical balance, electrons move from the conductors to the coatings, or vice versa, changing the transmittance properties of the window. EC devices can be classified as Conventional ElectroChromic (CEC), Near Infrared Radiation switching EC (NEC) and Dual-Band ElectroChromic (DBEC) according to the specific EC film adopted which can act on specific solar radiation wavelengths. While CECs can change their transmittance properties contemporaneously on Near Infrared Radiation (NIR) and on Visible Light (VL) spectra, NECs act only on the NIR spectrum changing the thermal behaviour without affecting the day-lighting. A more flexible behaviour is offered by the DBECs which can assume three different states: transparent in both NIR and VL spectra, dark in the NIR spectrum and transparent in the VL spectrum, and dark in both NIR and VL spectra [111].

In the NECs the use of doped semiconducting nanocrystals allows the modulation of the surface plasmon [112] that increases the spectral shift. For example, using the tin doped indium oxide (ITO) – which is characterized by a localized surface plasmon resonance (LSPR) in the NIR spectrum – allows to reach a larger spectral shift thanks to the electrochemical doping effect [113]. The DBECs are based on a similar functioning but their different structure results, sometimes, in a different definition (nanocrystal in-glass composites); despite this, as the functioning criterion is exactly the same of the CEC, they can be considered simply a different EC application. This technology uses the ITO nanocrystals embedded in a niobium oxide (NbO_x) glassy matrix [114]; this specific structure allows to change the optical properties in different ways according to the applied voltage as the nanocrystals and the glassy matrix perform differently. When the highest voltage is applied (4 V) both materials are in their clear configuration, when the voltage is decreased (2.3 V) only the nanocrystals – which act on the NIR spectrum – turn dark and, finally, with the lowest voltage (1.5 V) the device acts on both NIR and VL spectra as both materials are in their dark states [114].

To sum up, among the main advantages of EC technology, we can consider [38,115,116]:

- possible users' extrinsic control,
- possible complex sensing and control algorithms to improve energy efficiency and IEQ,
- low switching voltage (1-5 V),
- good open circuit or optical memory,
- power absorption only during the switching phase (depending on the optical memory),
- minimal polarization with a subsequent reduction of birefringence and distortion,
- the possibility to apply to large areas,
- a good building integration and retrofitting suitability,
- low maintenance costs.

On the other hand, the high investment cost and the aesthetical issues related to their chromatic change could slow down their spread [38].

Colour-temperature-tunable window

As just mentioned, one of the limits of the EC devices is the aesthetical issue related to their changing colour. The colour-temperature-tunable windows try to overcome this issue thanks to an additional feature that allows the control of the light colour temperature and not only the modulation of the quantity of light transmitted (used for shading purposes). This property is obtained through the use of an electrophoretic dispersion of dual-particles of 2 biprimary complementary colours controlled by three properly located electrodes that move the coloured particles in the electrophoretic dispersion. This displacement leads to different states of the window from the neutral clear state to the neutral dark one [117].

Gasochromic glazing

The gasochromic glazing (GC) is an active technology based on the use of a thin gasochromic layer deposited on the glass pane. This GC layer reacts with certain

chemicals, such as H_2 and O_2 , that trigger a reversible coloration of the layer changing the overall transmittance properties of the window [118]. Unlike the EC systems, the GC devices are less complex and expensive as they are based on a single GC porous layer (figure 5) instead of a 5 layers EC system. From a chemical point of view, the GC layer is made of a tungsten oxide (WO_3) film with different textures, morphologies, and compositions even though recent studies [119] are also considering the molybdenum oxide (MoO_3), which is usually adopted as photochromic film, as GC film. In order to trigger the chemical reactions, the window cavity is filled with H_2 or O_2 to switch, respectively, from bleached to dark state or from dark to bleached state [120]. The window cavity – which is usually filled with Argon to stabilize H_2 and reduce the thermal transmittance – is connected to a piping and pumping system that can fill the cavity with these gases according to the required state. The switch from clear to dark state is due to a chemical reaction on the GC layer – which is covered by a thin (4 - 5 nm) platinum or palladium catalyst – triggered by the H_2 pumped in the cavity. When the cavity is filled with O_2 , the chemical bond between H_2 and O_2 (that produces H_2O) allows to return to the clear configuration as shown in figure 5.

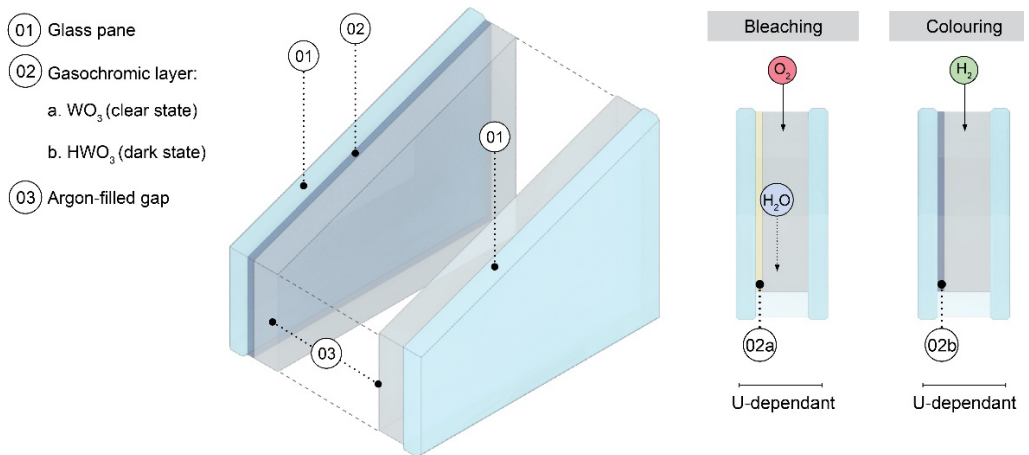


Figure 5. Typical structure and functioning – schematic and not to scale – of WO_3 GC devices [110].

Deformation Tunable Device

While EC and GC windows can be considered similar from a technological point of view, the so-called Deformation Tunable Devices are based on a completely different functioning. In particular, rather than considering a chemical reaction, the Deformation Tunable Devices change their properties through a microscale deformation of the device itself. The windows opacity can be changed wrinkling the window surface through reversible microscopic geometric deformations that change the light scattering. Compared with chromogenic materials, the main advantage of this technology relies in its colour neutrality in all the configurations. Controlling the surface topography is a developing technique which is going to increase its spread thanks to the wide experimentations conducted in different fields such as dry adhesives or micro-lens arrays [121]. These devices are composed by silver nanowires embedded in a soft dielectric elastomer; when a specific voltage is applied to the nanowires, the elastomer changes its geometry from a microscopic point of view. It follows that this new irregular surface changes the light refraction with a resulting lower transmittance at all the wavelengths [122].

Considering the same functioning criterion, the deformation of the surface can be also obtained triggering the wrinkling or flattening of the surface directly applying the strain to specific devices such as those composed by silica particles embedded in a polydimethylsiloxane (PDMS) film [123]. Considering these specific systems, the activating input is the mechanical stretching or release input rather than the electrical voltage variation. Nevertheless, despite the potential of these systems, currently no specific studies applied to the energy behaviour of buildings are available.

Windows with variable thermal transmittance

The concept behind these devices is based on the need to reduce the overheating risk during summer in highly insulated envelopes. Indeed, despite the benefits of highly insulated envelopes is clear during winter and during summer air conditioning period, reducing the thermal transmittance can reduce the benefits related, for example, to the summer night heat flows. Hence, these devices try to find a balance between these

behaviours minimizing the thermal transmittance when required (i.e., during winter or during summer when the systems are on) and increasing the heat flows when required (i.e., during summer when the systems are off and the outdoor temperature is lower than the indoor temperature). The most straightforward way to reach this goal, is changing the U-values of opaque or transparent systems according to specific inputs. From a typological point of view, the variable U-values can be obtained in different ways and the variable U systems can be classified as: variable air convection, variable liquid convection, variable gas pressure, variable surface interaction, and movable insulation [124]. Specifically, considering the variable U windows, the most developed devices are based on the principles of the variable convection and movable insulation mechanisms. Usually, the air convection of the cavity is modified moving an insulating pane, installed within the cavity, from the top to the middle of the cavity and vice versa. Clearly, to ensure the functionality and the transparency of the window, the intermediate insulating pane should be a translucent material – such as open pore melamine foam ($\lambda = 0.035 \text{ W/mK}$) or aerogel materials ($\lambda = 0.013 \text{ W/mK}$) – which can provide both low conductivity and a certain amount of incoming light. When the panel is in its top position, the air convection around the panel is not allowed; on the contrary, moving the panel in its middle position, a large-scale convection phenomenon is triggered by the temperature differences as represented in figure 6 [125].

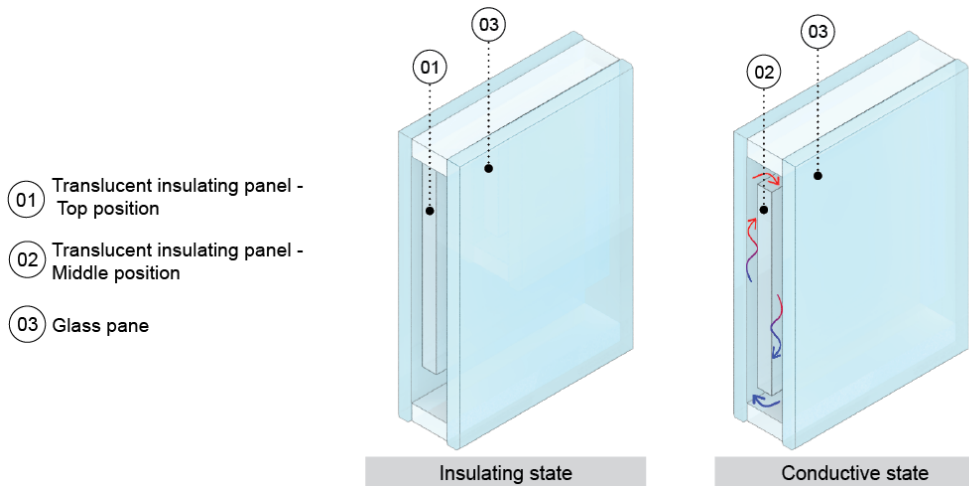


Figure 6. Typical structure and functioning of a window with variable thermal transmittance based on variable air convection.

Another way to change the thermal transmittance is to adopt movable insulation technologies which can be implemented in both opaque and transparent envelopes. For example, the number of the envelope air cavities can be increased or decreased using a series of rollable films that modifies the configuration of the air cavity changing, as consequence, the overall thermal transmittance [126]. In particular, rolling out the films, the heat flow through the envelope is reduced thanks to a series of thin air cavities; on the contrary, rolling up the films allows to increase the heat flow thanks to a single larger air cavity.

The main advantages of the two above-described variable U devices are [38]:

- possible users' extrinsic control,
- possible complex sensing and control algorithms to improve energy efficiency and IEQ,
- low triggering energy.

With reference to the main weaknesses, following drawbacks can be identified [38]:

- difficult maintenance,
- low visible transmittance for glazed devices,
- partial reduction of the external view.

2.1.2.2 *Intrinsically controlled glazing*

Thermochromic windows

Moving towards intrinsically controlled systems, Thermochromic (TC) windows are one of the most developed systems thanks to their passive behaviour driven by the temperature variation. TC materials can dynamically change their properties in accordance with their temperature triggering a self-adapting behaviour as response to the external environmental variations. Each TC material is characterized by a certain critical transition temperature. Below this threshold the material is in its monoclinic state and acts as a semiconductor, less reflective in the NIR spectrum. On the contrary, exceeding the transition temperature, the TC material changes its internal configuration

changing from monoclinic to rutile state; in the rutile state the material behaves like a semi-metal increasing, hence, the NIR reflections [127].

It follows that these systems do not require any sensors, controllers, or actuators simplifying significantly the overall complexity of these devices. Among the TC materials, the most adopted for windows applications are the vanadium dioxide (VO_2) [128], hydrogels, liquid crystals, ionic liquids [129], and perovskite [130]. Two macro behaviour can be identified in these systems; in particular, during the crystal transition VO_2 nanocrystals, ionic liquids, and perovskite TC materials can directly change the absorbance intensity or the absorbance peak. A slightly different behaviour characterizes the hydrogels and liquid crystals which vary their scattering and reflecting properties acting on the phase separation and on the orientation of the crystals rather than on the spectral absorbance [131]. The most considered TC material for windows application is the VO_2 which is characterized by a transition temperature of 68°C that triggers phase transition of the crystals. As previously mentioned, the transition in these materials improves the absorbance in the NIR spectrum without affecting the VL and UV wavelengths. Clearly, for building applications, this behaviour may need some improvements for example to reduce the transition temperature or to act also on the VL spectrum. To that end, specific dopants such as Tungsten and Magnesium can be added respectively to reduce the transition temperature and to change the VL absorbance. These devices can be coupled with other technologies – such as electrochromic, electrothermal, or photochromic materials – to develop highly performance multifunctional TC windows [131].

Photochromic glazing

The Photochromic (PC) systems are based on the chromogenic properties of certain PC materials that change their colour in a reversible manner when exposed to specific solar wavelengths. In the building field, the PC materials are usually embedded in a transparent matrix to create a PC film to be applied on a transparent substrate – usually glass – to add a dynamic behaviour to the windows. This dynamic behaviour can be obtained with different PC materials which are classified as organic or inorganic. The former, are characterized by a transition between two chemical isomers triggered by solar radiation; this transition leads to a change in the absorbance spectra that provides

the required dynamism of the solar properties. Organic PC molecules can, in turn, be classified as thermal reversible – or thermally stable – and thermal irreversible – or thermally unstable – depending on their bleaching mode. The thermally stable molecules return in their clear state when exposed to visible light; on the contrary, the thermally unstable molecules turn back to their original colour when heated or irradiated with light [131]. Molecules such as diarylethene [132], spiropyran, and spirooxazine [133] are included in the organic class; among these, spirooxazine molecules are the most used in the building field for aesthetical reasons as they turn from transparent to a blue state rather than to the red/purple colour typical in other materials.

Instead, the inorganic molecules – such as the transition metal oxides WO_3 , TiO_2 , MoO_3 etc. – behave in a different way. For example, the WO_3 – which is particularly suitable for building applications for its transparent/blue colours – can change colour thanks to a redox reaction triggered by photons [134]. Hence, when the PC film is irradiated, pairs of electrons and holes are formed and the reactions between WO_3 , hydrogen ions, and electrons form the H_xWO_3 compound that changes the colour of the film. When the solar radiation goes below a certain threshold, the PC film returns reversibly in its clear state. The modulation range of these devices is lower than other chromogenic technologies and this feature leads to lower energy savings in the building field, even though only few studies consider the energy benefits of these devices [109].

Photoelectrochromic and Photovoltachromic glazing

The PhotoElectroChromic (PEC) devices can be considered the passive adaptation of the EC systems thanks to the use of renewable energy sources to trigger the EC redox reaction. To achieve this goal, the EC films are usually coupled with photovoltaic (PV) materials – such as dye sensitized TiO_2 – to self-produce the energy required for modulating the transmittance properties. It follows that these systems can be used both as intrinsically and extrinsically controlled depending on the management of the device. PECs are usually classified with regards to materials, layers' structure, and state of aggregation [135]. Considering the structure of the systems, the EC and PV materials can be located on the same substrate – in the so-called combined devices – or can be

placed on different electrodes in the separated devices [136] as shown in figure 7. A further evolution of these systems was proposed by Wu et al. [137] who developed a PhotoVoltaChromic (PVC) device to increase the amount of energy produced exceeding the threshold required for the EC films activation. After the complete transition of the EC films to the dark state, the exceeding energy produced can be used in any other electrical applications within the electrical grid. Thanks to this feature, the PVC devices can produce energy, reduce the energy demand (from -6% to -32% [138]), and reduce the glare discomfort.

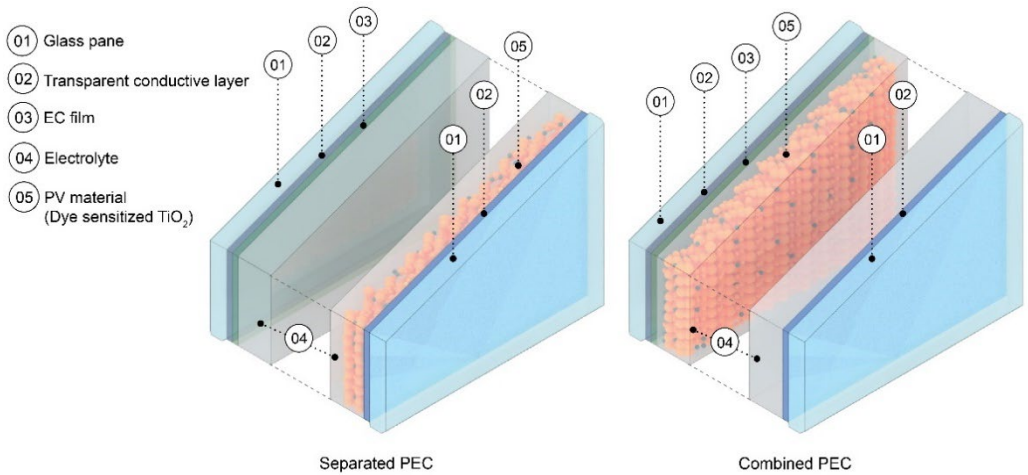


Figure 7. Typical structures – schematic and not to scale – of a TiO₂ PEC device. [110]

Shading fluid windows

Among the intrinsically controlled devices, a very simple and cheap system was developed by Fazel et al. [139] thanks to the shading effect of a thin coloured fluid layer. Depending on the temperature, this coloured fluid moves within a small cavity, changing the shading effect of the device. With reference to the structure of the device, the shading fluid windows can be classified as gas-liquid or liquid-liquid devices. In the former the expansion of a transparent gas pushes the shading fluid in a small cavity; on the contrary, in the liquid-liquid devices, a transparent liquid or a coloured liquid – characterized by different thermal expansion coefficients – are pushed alternatively according to the temperature variation.

PCM windows

Thanks to the spread of glazed façade in the last years, the performances of transparent envelopes were improved from different point of views. While the thermal, solar, and visible properties were significantly improved, the low thermal inertia of windows is still an open topic, especially in hot climates. The PCM window is an innovative responsive technology that tries to increase the thermal inertia of glazed envelopes through the use of translucent PCMs within the windows' cavity. These systems are usually based on paraffin PCMs which are translucent in their solid state and fully transparent in the liquid state. An example of paraffine wax PCM windows was proposed by Goia et al. [140] who studied a 8-15-6 mm Double Glazing Unit (DGU) with a cavity filled with a Rubitherm commercial grade paraffine wax (melting temperature of 35° C and a heat store capacity of 170 J/g). The experimental results highlighted that the increased thermal inertia led to an improved energy performance during summer in a temperate climate. Another study [141] evaluated the effect of the use of PCM windows from a daylighting point of view; in particular, in this study, the PCM windows showed a better visual comfort (intended as useful illuminance and Daylight Glare Probability) only when sky luminance is low. The main issue of PCM windows is that the melting and solidification act simultaneously on different physical domains reducing the control of the system. While, on the one hand, certain behaviours such as the heat storage during the melting phase are improved, on the other hand, the summer solar properties are worsened in the liquid phase, hence, predicting their behaviour could be more complex. Despite this, the benefits on the thermal inertia can be fundamental to improve the overall windows performance, therefore it could be worth considering this technology. To sum up, following main strengths can be identified [38,142]:

- improved time shift of the heat loads during summer,
- increase of the thermal mass and of the heat storage phenomenon,
- reduction of surface temperature and subsequent improvement of the thermal comfort,
- low maintenance cost,
- low glare risk in the solid phase configuration thanks to a good scattering effect.

On the other hand, following weaknesses can slow down the spread of these devices [38,142]:

- low fire safety related to the paraffine flammability,
- chemical incompatibility with sealants,
- reduction of daylight and external view in the solid phase configuration,
- high solar transmission in the liquid phase configuration,
- aesthetic inhomogeneity during the melting/solidification phase,
- no external controls allowed,
- improvement in the summer period corresponds to worsening during winter,
- strictly climate-dependant.

2.1.3 *Dynamic Shading*

Fixed shading systems were largely adopted in the vernacular architecture in hot climates using different materials – ranging from clay to wood [143] – to control the direct solar radiation. The spread of modern architecture led to a gradual dismissal of these systems up to 1973 when the energy crisis pushed the designers to reconsider passive strategies to reduce the energy demand. Hence, starting from the static systems, recent studies have developed a wide set of solutions to adapt this concept to the new awareness that the external environment is highly dynamic.

The first expressions of this new awareness have spread in the first half of the 20th century with examples such as the “Girasole villa” designed by Angelo Invernizzi in 1930. In this project, the author – inspired by the sunflowers’ movement – considers the dynamism in the building design through the rotation of the whole building around a vertical axis to improve the solar access of the inner glazed courtyard [34]. This project is also one of the first examples of a biomimetic concept, a new approach that emulates the natural principles to solve engineering problems [144]. These new concepts supported by strong technical and technological improvements, have led to a fruitful experimentation period in the envelope design field, whose outputs are a wide set of dynamic shading systems with disparate shapes, functioning strategies, and activation criteria. Despite their high variability, all these kinetic shadings can always be

considered comprised of components for perception, cognition, and action [56] and one of the main classifications for these systems is based on the integration degree of these three components. In particular, in autonomous (or adaptive) systems the perception, cognition, and action are embedded in the shading structure – hence they can be classified as intrinsically controlled – while in non-autonomous (or automated) systems these components are outsourced to sensors, controllers, and actuators. For example, all those shadings that consider solar-activated Shape Memory Alloy (SMA) wires embedded in the shading fibres [145,146] can be classified as autonomous systems. In the solar-activated SMAs shadings the system is triggered by a thermal stimulus (dependant on incident solar radiation and air temperature) that “naturally” changes the shape of the SMAs wires and, accordingly, the whole shading. Hence, when directly activated by the outdoor temperature and solar radiation, these systems are autonomous as perception, cognition, and action are all handled by the SMA wire. Nevertheless, the same system can be classified as automated – hence extrinsically controlled – when the SMAs wires are activated through electrically-induced heat [147,148]. In this case, the perception is handled by one or more sensors (daylighting, solar radiation, indoor/outdoor temperature sensor, etc.), the cognition is handled by a controller (or by the user), while the action is handled by the activation system. The Piraeus Tower [145] and the Tent, Curtain and Blind prototypes [147] can be considered two examples of the different use of the SMAs in dynamic systems; the former is directly triggered by the solar radiation (figure 8) while in the latter the activating heat is produced through electrical current.

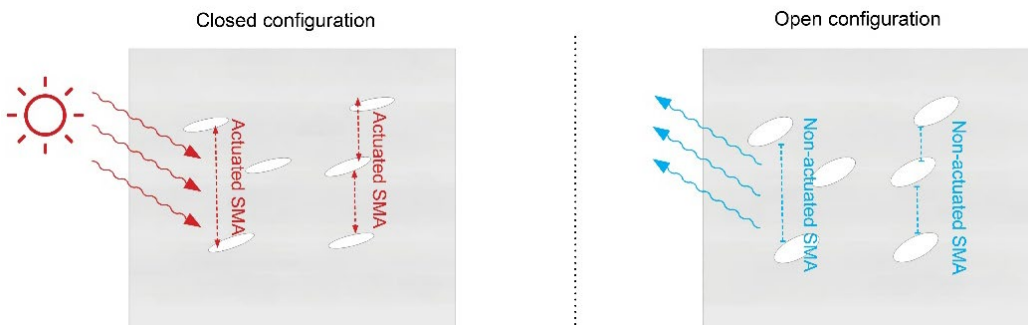


Figure 8. Examples of intrinsically controlled SMA screen of the Piraeus Tower. [110]

In general, the automated systems can be considered more flexible and can be customized according to specific needs simply changing the activation threshold or the sensors. It follows that the automated systems are more developed and includes very heterogeneous systems ranging from SMA systems to mechanical [149] and hydraulic [150] systems. The automated mechanically activated systems are already well developed and there are different built examples ranging from very simple devices such as venetian blinds to complex three-dimensional shading patterns. The application of external mechanical stimuli triggers three different kinds of movements of the shading elements: translation, rotation (swivel, revolving, swing), or their combination (folding, expanding, and contracting) [151]. Built applications of complex automated shadings have spread since the end of last century. For example, the well-known Arab World Institute realized in Paris in 1988 by Jean Nouvel is characterized by a dynamic façade constituted by 240 main shutters that increase or reduce the amount of incoming light thanks to 30000 light sensitive diaphragms (sensors), a central computer (controller), and a mechanical system (actuator)[152]. Another recent and different example of an automated dynamic shading is the one realized by Aedas and Arup in 2013 for the Al Bahr Towers in Dubai where the designers merged the concept of the Islamic “Mashrabiya” screens with three-dimensional mechanically activated origami umbrellas [153]. This shading system is composed by 1049 triangular origami elements that cover the glazed curtain wall of two 150 m tall circular towers on the southern, eastern, and western exposures [154].

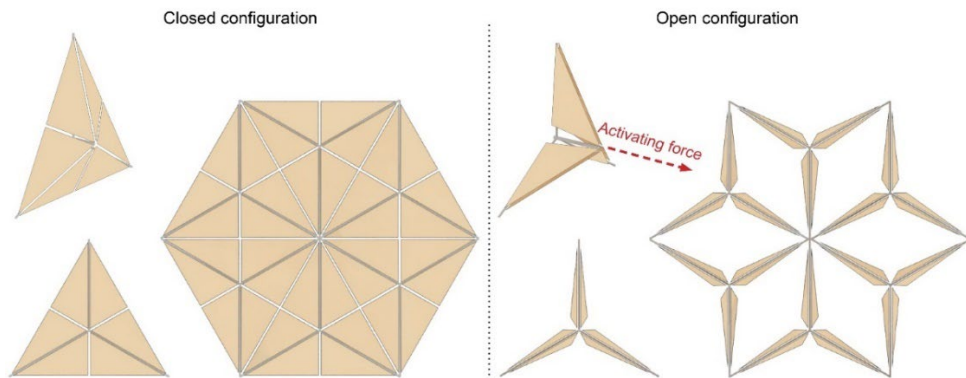


Figure 9. Functioning criterion of the Al Bahr Tower shading system [110]

Each element of the shading system can fold or unfold according to the sun position thanks to a barycentric pushing piston that can move the middle point of the shading element up to 1m, folding the panels and providing up to 85% of unshaded area (Fig. 9) [155].

To improve the durability and the overall performances, the shading elements are made of Polytetrafluoroethylene (PTFE) coated glass fibre mesh and the system was largely tested before the realization. In particular, more than 30000 opening-closing cycles were conducted in a climatic chamber to evaluate the behaviour under different boundary conditions such as different temperatures, presence of sand and salt water on the joints, etc.

A further boost to the development of these systems was provided by the spread of biomimetics and phytomimetics concepts [156]. Indeed, starting from nature-inspired solutions and supported by new technological advancements, a new class of shading systems based on specific fibres anisotropy was developed by researchers to improve the buildings' performance. Similarly to what happens in nastic structures, adopting specific distribution and orientation of the material's fibres allows the movement of the shading systems. This movement can be triggered directly by environmental stimuli (e.g., solar activated SMAs) in the autonomous systems or by external energy source in the automated systems. For example, Flectofin® [149] is an automated flapping shading system inspired by the *Strelizia reginae* plant based on the anisotropy of Glass Fibre-Reinforced Polymer. In this device, the external compression or bending force causes the buckling of the shading element that rotates around the vertical axis reducing the incoming solar radiation.

As already mentioned, coupling these concepts to smart materials – e.g., Shape Memory Alloys (SMAs), Shape Memory Polymers (SMPs), and Shape Memory Hybrids (SMHs) – allows to design new technologies embedding the actuators (automated system) or sensors and actuators (autonomous system) within the shading element itself. This brief introduction to the main different available dynamic systems shows an extremely faceted scenario and, according to the device and activation criterion considered, dynamic shadings can reduce energy demand up to 20% - 34% [157].

Considering the great heterogeneity of these devices, specific pros and cons could be identified for each technology. However, on the whole, considering automated or extrinsically controlled systems, following main advantages can be identified [38]:

- possible users' extrinsic control,
- possible complex sensing and control algorithms to improve energy efficiency and IEQ,
- wide range of possible solutions.

On the other hand, the main weaknesses of these systems are [38]:

- high maintenance costs of the mechanical systems,
- high architectural integration needed,
- partial reduction of the external view (strictly dependant on the system adopted).

On the contrary, considering the autonomous or intrinsically controlled dynamic systems, the specific strengths and weaknesses are strictly related to the specific device adopted.

2.1.4 Responsive envelopes and modelling tools

The previous subsections have highlighted a broad number of technologies with a wide range of functioning. Not every responsive system can be simulated in an energy simulation software and the main aim of this subsection is to highlight the main approaches that can be adopted to analyse innovative responsive technologies from an energy point of view. Currently, a large number of simulation software is available to model energy phenomena; among these the most used are IDA ICE, TRNSYS, EnergyPlus, IES-VE, and ESP-r [51]. ESP-r is an open-source simulation tool based on a finite volume approach; it allows to describe the building from an energy, heat, and moisture point of view. IES-VE is a commercial software largely used in the design field thanks to its easy-to-use interface and to its high integration with sustainability rating systems. TRNSYS is a commercial software based on a graphical environment used to simulate the behaviour of transient systems where users can easily modify existing components or

create new ones, extending the capabilities of the environment [158]. IDA Indoor Climate and Energy (ICE) [159] is a commercial software that can model buildings, systems, and its controllers to analyse energy consumption and users' comfort.

A deeper insight is provided for EnergyPlus which is the reference tool for the developed platform and it is one of the most robust and widely-used energy analysis tools [160]; moreover, this software includes a set of functions that allows to model different responsive technologies which are the main focus of this work. The modelling approaches for responsive envelopes in EnergyPlus can be divided in two main classes; the first one – the easiest – is based on default computational modules while the second one is based on the internal programming module called Energy Management System (EMS). The first approach can be used for technologies such as PCM [161], thermochromic [162], electrochromic glazing [163], and some shading systems as better explained later. Instead, considering the second approach, the users can freely include additional algorithms in the simulation writing in the EMS module the right strings of code. The EMS sensors can transform the variables and parameters used during the EnergyPlus simulation (e.g., the indoor temperature) in inputs for the additional code created in the EMS. Hence, starting from these inputs, the users – after a certain number of operations described in the EMS program – can change schedules, properties, etc. using the EMS actuators that can change the EnergyPlus simulation inputs. This second approach is clearly more complex than the previous one but allows, theoretically, many other applications such as for example photochromic windows [164] or opaque thermochromic materials [165].

Looking in detail the first approach, PCMs can be modelled as a standard material and the latent heat storage can be applied through the specific “MaterialProperty:PhaseChange” module where the user can describe the enthalpy curve of the material through the input of temperatures and relative enthalpies. To improve the accuracy of the results, the simulation algorithm should be changed in “Conduction Finite Difference” and the simulation timesteps should be more than 20.

To model thermochromic window, the users should consider a specific window object called “WindowMaterial:GlazingGroup:Thermochromic”. This component allows to

associate different glazing materials to specific temperatures; hence, during the simulation, depending on the glazing temperature, the software considers the properties associated to that specific temperature.

The EC windows can be modelled as switchable windows providing both the clear and the dark state as separate traditional constructions. The shading effect of the EC film can be simulated using the “WindowShadingControl” module that allows to choose among different shading type including the switchable glazing. Hence, selecting switchable glazing, the software switches between the two provided constructions according to the activation criterion selected. As the EC window is modelled substantially as a shading system, further details of the possible activation criteria and controls are provided below in the paragraph concerning the solar shading.

Regarding solar shading systems, EnergyPlus offers different possible choices to model and control these systems even though with certain limitations. The shading systems are classified in EnergyPlus as external obstacle to the solar radiation (called attached/detached shading surfaces) or as an additional window layer (i.e., window material). Trees, other buildings, overhang, fins, etc. can be included in the first class while additional window layers can be used to model blinds, screens, drapes or pull-down shades [166]. Nevertheless, only few of these can be modelled as dynamic systems, in particular blinds (which can be interior, exterior, or between glass), shades (which can be interior, exterior, or between glass), and screens (which can be only exterior) are the only shading types that can be controlled by specific strategy. From a modelling point of view, the user can select from the “WindowShadingControl” module the desired shading system similarly to what already described for EC windows. Table 1 provides an overview of all the possible solar shading systems and their control strategies (where available). The same control system can be considered for EC windows as they are treated as windows shading systems as already mentioned.

As clearly described in the table, the dynamic control strategies can be applied only to windows' additional layer, hence no dynamic external surfaces can be considered in the default EnergyPlus modules. Another important limitation of these default module regards the possible states of the shading systems which can switch its configurations

only between two states: retracted or activated. Therefore, no intermediate states can be easily modelled; for example, a partly shaded window can be simulated only splitting the window in two or more parts. With regards to dynamic systems, splitting the windows in parts could be more difficult to adopt as different part of the same window would be controlled separately and for a proper and advanced control the users should probably consider additional scripts in EMS.

It is worth highlighting that, currently, the change of shape of external shadings cannot be obtained by simply modifying the shading vertex coordinates in EnergyPlus through the EMS because the shadowing analysis is run at the beginning of the simulation and, therefore, following changes in the shading shapes are not taken into account and do not affect the simulation.

Considering this heterogeneous simulation context, one of the aims of this research is to provide a single tool that allows to simulate different responsive technologies in the same environment and in a comparable way making these themes more accessible also to non-expert users.

Table 1. Shading systems available in EnergyPlus v.9.4. [40]

Category	Shading types	Possible control systems
At- tached- Detached Shading Surfaces	Shading: Site Shading: Building Shading: Site:Detailed Shading:Overhang Shading:Over- hang:Projection Shading:Fin Shading:Fin:Projection Shading:Zone:Detailed	None (Static shadings)

<p>Additional Window material</p>	<p>blinds (interior, exterior, or between glass)</p> <p>shades (interior, exterior, or between glass)</p> <p>screens (exterior)</p>	<ul style="list-style-type: none"> • On if schedule allows • On if high solar on window • On if high horizontal solar • On if high outdoor air temperature • On if high zone temperature • On if high zone cooling • On if high glare • Meet daylight illuminance setpoint • On night if low outdoor temperature and off day • On night if low indoor temperature and off day • On night if heating and off day • On night if low outdoor temperature and on day if cooling • On night if heating and on day if cooling • Off night and on day if cooling and high solar on window • On night and on day if cooling and high solar on window • On if high outdoor air temperature and high solar on window • On if high outdoor air temperature and high horizontal solar • On if high zone air temperature and high solar on window • On if high zone air temperature and high horizontal solar
--	---	---

2.2 Climate change and future analyses

After studying in detail the state of the art of responsive technologies, the research was focused on the future weather files analysis to understand the best way to model and select the proper climate scenarios.

Currently, the building energy analyses are conducted using weather files composed by a sequence of the most typical weather parameters – one for each month and one for each weather parameter – selected from recorded weather data. Hence the resulting weather file is a fictitious representative typical year called Typical Meteorological Year (TMY) weather file which was introduced in 1978 [167] and updated in 1995 (TMY2) [168] and 2008 (TMY3) [169].

Today, considering only historical weather data could be considered anachronistic as the effects of the climate change makes the historical weather data less reliable than in the past. Clearly, future weather files are based on projections which are strictly dependant on our behaviour. Therefore, the future projections are related to different possible anthropogenic emission scenarios. The first IPCC emission scenarios (IS92) were released in 1992 with the supplementary report [170]. After this first contribution, new sets were released in 1996 adopted in the Third Assessment Report (TAR) in 2001 [171] and then refined in the Fourth assessment report (AR4) released in 2007 [172]. The AR4 report – which is still largely used in the research field – proposes four qualitative storylines (A1, A2, B1, B2) for the emissions driving forces (demographic, social, economic, technological, and environmental forces). Each family includes one or more different scenarios (for example the A1 family includes A1F1 for the fossil fuel intensive scenario, A1T predominantly non-fossil fuel scenario, A1B balanced scenario) as better described in figure 10. Depending on the assumptions made on global population, gross world product, and final energy, each group of scenarios can be divided in Harmonized Scenarios (HS) and Overshoot Scenarios (OS); the former share harmonized assumptions while the latter include uncertainties in the driving forces [173].

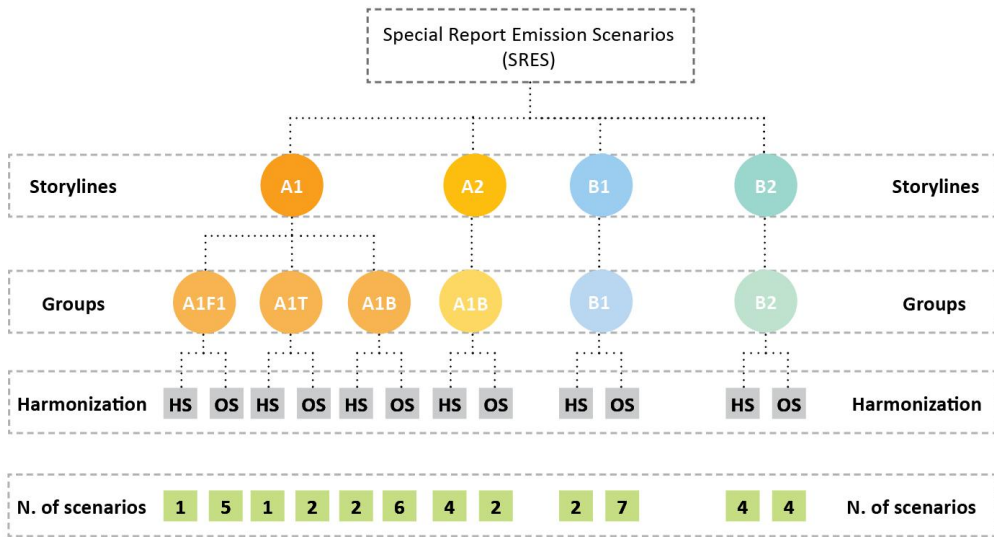


Figure 10. Schematization of the Special Report Emission Scenarios [41].

A different approach was considered in the fifth assessment report (AR5) released in 2014 [174]. In this report the authors described the Representative Concentration Pathways (RCPs) which are different scenarios that include different sets of emissions and concentration of GHGs up to 2100. The RCPs are based on the definition of radiative forcing which is according to the definition of the IPCC Annex II [175] “*the change in the net, downward minus upward, radiative flux at the tropopause or top of atmosphere due to a change in an external driver of climate change, such as, for example, a change in the concentration of carbon dioxide (CO₂) or the output of the Sun*”. The word representative used in the acronym RCP describe that it provides only one of the possible scenarios that lead to a certain radiative forcing (which is described by the RCP number). According to these definitions, the report defines four pathways from a stringent mitigation (RCP2.6) up to a high emission scenario (RCP8.5). The most optimistic scenario (RCP2.6) considers a peak of the radiative forcing at nearly 3 W/m² which declines to 2.6 W/m² in 2100. The intermediate RCP4.5 and RCP6 consider a radiative forcing of respectively 4.5 and 6 W/m² in 2100 while the worst scenario (RCP8.5) consider a radiative forcing of 8.5 W/m² in 2100 with higher values in the following years. A numerical quantification of the practical effects of these scenarios,

can be provided by the temperature increase which is increase below 2°C over the preindustrial temperatures in 2100 in the RCP2.6 and nearly 3-4 times higher in the RCP8.5 with an average global temperature of nearly 4°C.

A further description of possible future scenarios is provided in the latest assessment (AR6) released in 2022 [176]. This report introduces the Shared Socio-Economic Pathways (SSPs) which are based on the following five narratives regarding socio economic developments: the sustainable development (SSP1), the regional rivalry (SSP3), the inequality (SSP4), the fossil fueled development (SSP5), and an intermediate scenario (SP2) [177].

These narratives do not exclude the RCPs defined in the previous assessments, but they are coupled in more exhaustive framework described in figure 11.

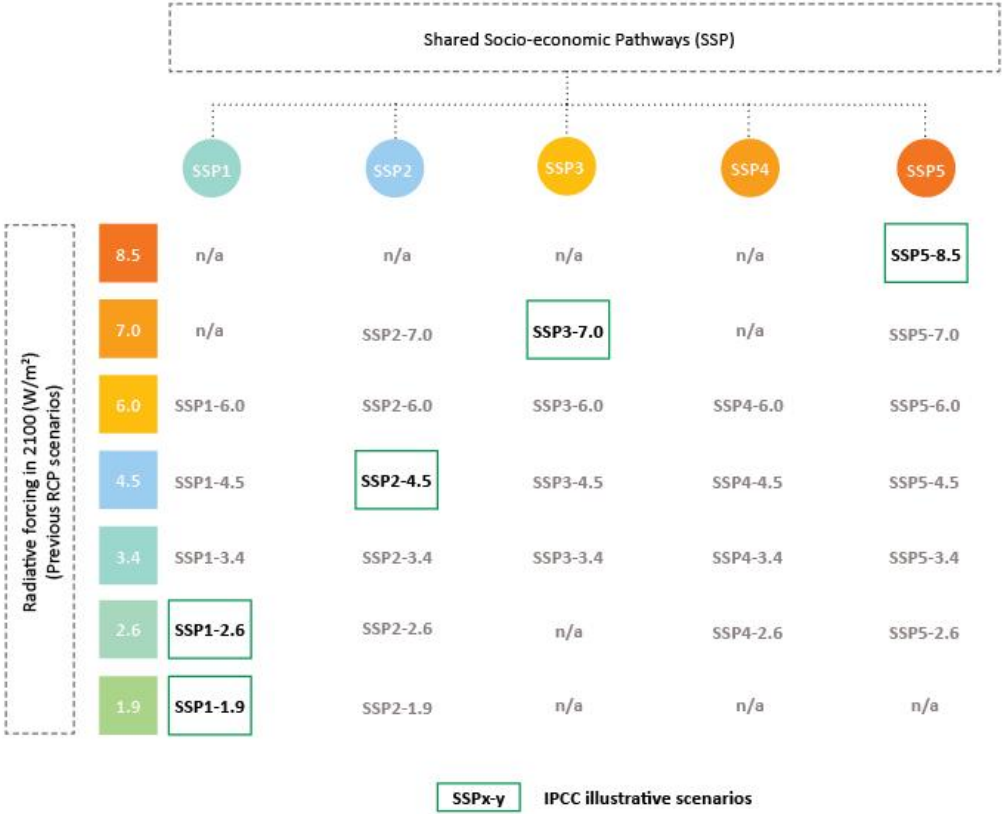


Figure 11. Schematization of the AR6 scenarios [41].

Hence, the scenarios of the AR6 are defined as SSPx-y where x refers to the Socio-Economic Pathways while y refers to the level of radiative forcing in 2100 (e.g., SSP5-8.5, SSP2-4.5, SSP 1-1.9 etc.). The AR6 report evaluates the climate response with reference to five possible future developments (SSPx-y) named illustrative scenarios [16].

The emissions scenarios are fundamental for future projections as they are used to force numerical models validated against past climate observations – called Global Climate Models (GCMs) [178] – to obtain future forecasts. The GCMs are not suitable for building energy analyses as their resolution is quite coarse from both spatial ($>100 \text{ km}^2$) and temporal point of view (monthly scale). Therefore, the weather files used in the energy analyses are usually temporally and spatially downscaled using three main methods: statistical, dynamical, and hybrid methods [179]. Statistical downscaling is based on the empirical relationships between historical large-scale data and local weather data; these relationships are combined with the future predictions of the GCMs large-scale predictions [180]. More in detail, statistical methods can be based on different techniques such as the extrapolating statistical, the imposed offset, and the stochastic method. The imposed offset method is most used among the statistical methods in the building field [181]; this method is based on the morphing technique [182] which is based on three transformation algorithms – shifting, stretching, and their combination – applied to the baseline climate parameters to obtain future projections.

A completely different approach is used in the dynamical downscaled weather files. These method uses the Regional Climate Models (RCMs) which are similar to the GCMs but are characterized by a higher spatial resolution (from 2.5 to 50 km^2) that allows to represent local landscape and atmosphere. Using local data and specific equations, the dynamical downscaling processes the atmospheric fields of the GCMs to generate local weather data [180]. The main differences between statistical and dynamical downscaling are summed up in Table 2.

Table 2. Comparison between statistical and dynamical downscaling methods [41].

	Statistical downscaling	Dynamical downscaling
Advantages	<ul style="list-style-type: none"> • Low computational resources required • The same method can be applied everywhere improving the comparability of the studies • Downscaling based on easy-to-use open-source tools • Refers to specific weather stations and are based on observed weather data 	<ul style="list-style-type: none"> • Based on physical assumptions • More accurate • All variables are internally consistent in time and space • Provides information of sites without observational data
Disadvantages	<ul style="list-style-type: none"> • Assumes that the large/local scale relationships will be the same in the future • Less accurate 	<ul style="list-style-type: none"> • Computationally expensive • Limited number of RCMs • Larger resolution scale, may require further downscaling

An intermediate solution between statistical and dynamical is offered by hybrid methods that tries to reduce the computational time of the dynamical approaches using statistical considerations.

Despite the higher reliability of the dynamical methods, statistical approaches are still the most used approach in the building energy field. This trend can be explained

considering the large availability of commercial and open-source tools such as CCWorldWeatherGenerator, WeatherShift, Meteonorm and their higher easiness of use and speed. Moreover, despite the higher accuracy of dynamical methods, considering the main weather parameters – such as the outdoor temperature – the final consumptions obtained with statistical and dynamical methods can be considered comparable [183].

3. METHODOLOGY

From a methodological point of view, before developing the computational platform, preliminary analyses and refinements were conducted on all those topics involved in the definition of the tool. Firstly, a detailed analysis of the software adopted and of the reference model considered for the study was conducted to improve the reliability of the platform. The selected reference model was then calibrated and modified to properly consider the same model in different locations and to describe the dynamic systems considering both heating, cooling, and lighting demands. Hence, 25 European locations were selected to describe different climate zones, subsequently, proper envelope properties were defined according to these climate zones. Then, a further refinement regarding internal loads and operational schedules was conducted to update the reference model with the newest technologies and building typologies. Finally, the future weather files were created using proper tools to investigate the dynamic systems' behaviour future scenarios.

Following subchapters describe in detail the above-mentioned topics. In particular, section 3.1 describes the main properties of the software and reference models, section 3.2 shows the locations and envelope properties adopted, section 3.3 investigates the internal loads and operational schedules, while section 3.4 describes the future weather files considered in the computational platform for a better understanding of the developed tool.

3.1. Software and definition of the reference models

The computational platform developed is based mainly on EnergyPlus v.9.6 [184] as, thanks to its multi-domain integration, it can be used for thermal, visual, mass-flow, and building services integration [185]. Choosing EnergyPlus gives another important advantage thanks to the availability of 16 validated reference buildings energy models very useful for energy efficiency oriented research [186]. The Department of Energy (DOE) has developed these reference models considering typical building operations starting from the Commercial Buildings Energy Consumption Survey (CBECS), ASHRAE Standards 90.1 and other scientific sources [187].

In particular, this computational platform was developed considering the medium office model – whose characteristics are reported in table 3 and figure 12 – as reference model.

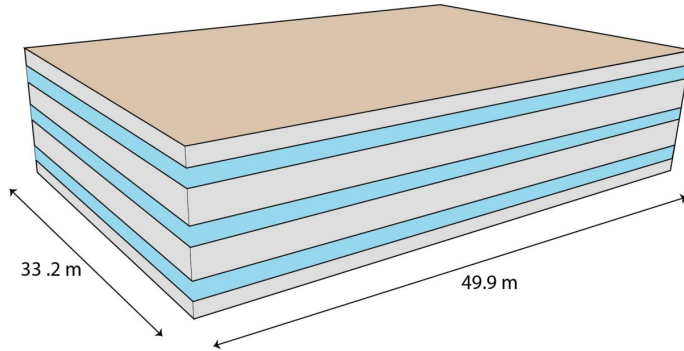


Figure 12. Medium office reference model geometry.

Table 3. Geometric characteristics of the medium office reference model.

Building type	Number of floors	Gross floor area	Floor-to-floor height	Floor-to-ceiling height	Window-to-Wall Ratio	Number of thermal zones
	[-]	[m ²]	[m]	[m]	[%]	[-]
Medium office	3	4982	3.96	2.74	33%	6 per floor (5 zones + 1 plenum)

As better explained in the following sections, the concept behind the platform is to allow the users to analyse and compare responsive technologies in different locations and climate scenarios. To that end, particular attention was paid to the definition of the software settings and of the reference model. In particular, to avoid the dependency of the consumption results on the HVAC systems, the default auto-sizing HVAC systems were substituted with properly calibrated ideal loads air systems. The ideal loads systems are included among the EnergyPlus systems and occupy the same hierarchical

place of the auto-sized HVAC units. Nevertheless, these systems are not connected to any real generation and distribution network, but each one can directly supply heating or cooling to satisfy the zones setpoints [188]. Considering that these ideal systems do not include the heating/cooling generation process, they directly provide the heating/cooling demand rather than the consumption. To obtain the energy consumption, the platform considers an ideal Energy Efficiency Ratio (EER) equal to 3 in cooling mode and a Coefficient of Performance (COP) equal to 3 in heating mode. Hence, the energy consumptions are obtained dividing the ideal loads demands by these coefficients, which can be considered average values for packaged direct expansion air systems.

The original HVAC systems include different control routines such as the multi zones control and the night-cycle availability manager which are not included by default in the ideal loads HVAC systems. To reduce the differences between the real and the ideal HVAC systems, the model has been improved including an EMS program that can modify the systems availability schedule in order to obtain results closer to the original DOE model. The only difference concerning the HVAC systems regards the minimum flow fraction because – according to the EnergyPlus developers, consulted during this validation phase – there is no way for ideal loads to match what a Variable Air Volume (VAV) system with reheat does. The VAV system has a minimum flow fraction on the terminal units – 0.3 in most of them – which results in cooling provided to the space under low load conditions until the zone reaches the heating setpoint and then reheat comes on to keep the zone from getting too cold, but during such times, the system will likely be providing cooling. Ideal loads system has no such mini-flow fraction so when the space cooling load goes to zero, it simply shuts off or if it is providing outdoor air, it will temper that air to meet the cooling setpoint.

The differences related to this discrepancy are limited and do not change significantly the energy behaviour of the model on the whole; to that end a comparative energy analysis was run on the original and modified DOE reference models. For sake of simplicity, the analyses were run on a small office model because this model and the medium office share the same zones geometry and thermal properties. The only difference

relies in the height of the buildings – three floors in the medium office and one in the small office – and in the multizone control available in the medium office. The reliability of the ideal models were verified conducting energy analyses on each thermal zone of different reference models. In particular, three different locations and climates (Miami – ASHRAE Zone 1A, Chicago – ASHRAE Zone 5A, Fairbanks – ASHRAE Zone 8) were selected among the official DOE office reference models and were equipped with the ideal loads systems. Hence, the original and the ideal loads heating and cooling consumptions were compared on hourly basis to understand the reliability of the ideal loads model as shown in figure 12.

The energy consumptions are very similar on hourly basis and the main differences mainly regard the low consumption hours; therefore, the incidence of these variations on the global energy consumption is very low.

To further confirm the model reliability, the original validated model and the ideal loads model were compared running a Mean Bias Error (MBE) and a Cumulative Variation of Root Mean Squared Error (CVRMSE) based on the hourly heating and cooling consumptions. The analyses were conducted on all the thermal zones and for all the three locations selected and the average results obtained are reported in the table below (Tab.4).

Table 4. MBE and CVRMSE values obtained comparing the ideal loads and the original model for all the locations considered.

Heating		Cooling	
Average MBE [%]	Average CVRMSE [%]	Average MBE [%]	Average CVRMSE [%]
1.2%	20.7%	4.5%	44.9% ¹

¹ Without considering Fairbanks cooling consumptions (unrepresentative), cooling average CVRMSE is 19.6%.

The results shown includes all the thermal zones for the three locations considered excluding only the zones where the HVAC system is off for at least 95% of the total hours as the thermal behaviour as the energy behaviour of these zones is not considered relevant to the whole building balance.

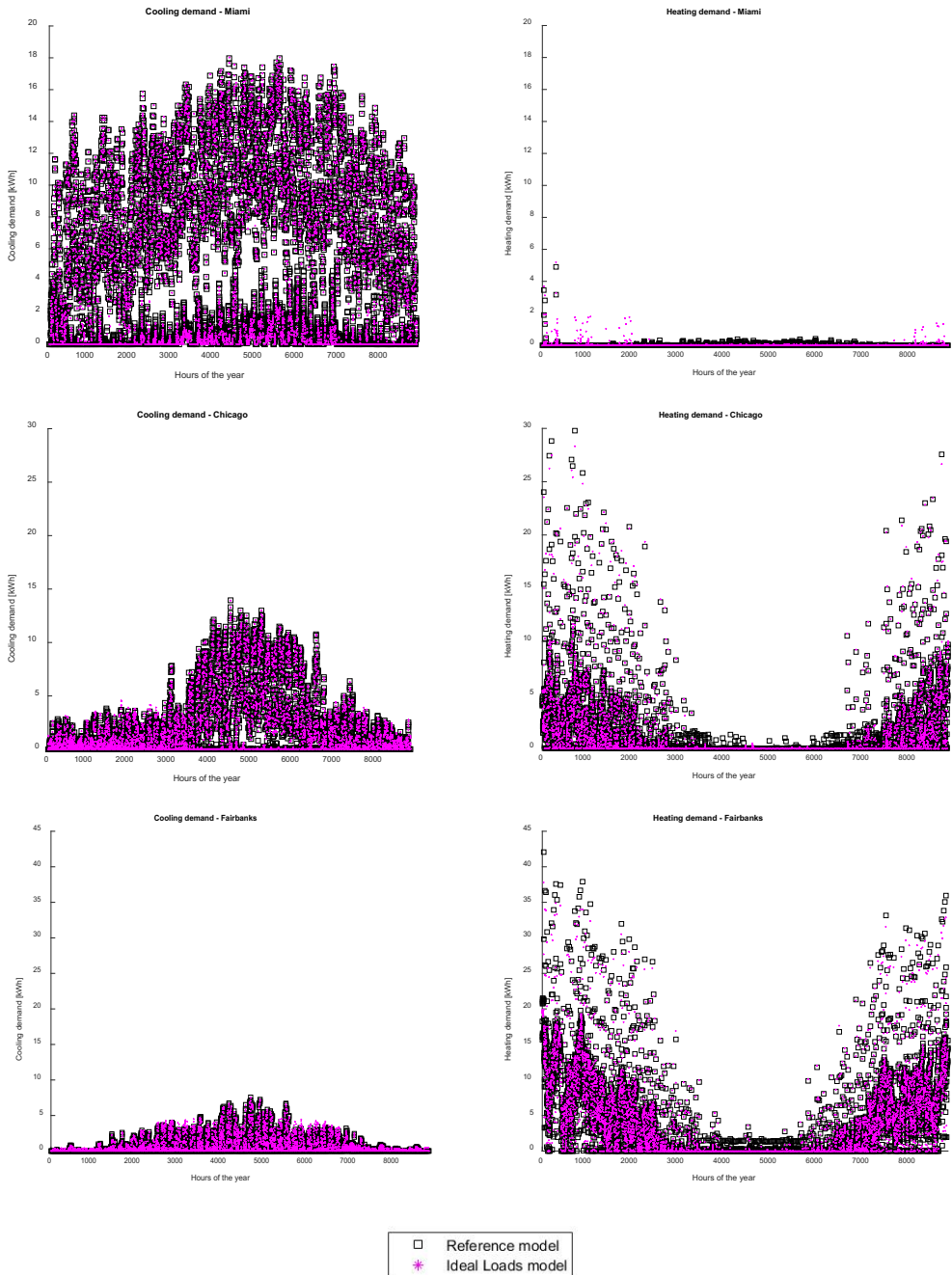


Figure 13. Global heating and cooling energy demand in reference and ideal loads office model.

As no regulations consider the validation of an ideal loads model, the values considered as reference are referred to the ASHRAE guideline 14 [189,190], which gives hourly calibration criteria for real building modelling. The results obtained confirmed that the ASHRAE hourly calibration criteria ($|MBE| \leq 10\%$ and a $CVRMSE \leq 30\%$) are satisfied except for the cooling CVRMSE which is slightly over the threshold. However, in this case the results are strongly influenced by the cooling consumption in very cold climates (Fairbanks); indeed, excluding this case would drop the CVRMSE to 19.6%. The Fairbanks results can be considered not representative as they are referred to a very short functioning period (19% of the total functioning hours) and are associated with very low magnitude consumptions. As further confirmation, if we compare the global yearly energy consumption in Fairbanks for the ideal and original models, the differences are extremely low (1.1%). For these reasons – considering that the ASHRAE thresholds are not mandatory in this case as they are referred to real measurements and are adopted only as reference – the model can be considered reliable and can be used as reference for the computational platform.

Regarding other settings, a dimmable lighting system connected to a daylighting sensor – placed in the middle of each thermal zone – with an illuminance setpoint of 500 lux was implemented to take into account the shading effect of certain technologies also on the lighting consumption. Moreover, the schedules and the original setpoints were not changed (21°C for the heating setpoint and 24°C for the cooling setpoint) while the internal loads were changed with more up to dated values as better explained in following sections.

3.2.Locations and envelope properties

One of the main features of the platform is the capability to assess the energy performance of responsive technologies in different locations. Hence, 25 European cities were considered to allow the users to explore the potentials of the responsive devices in different climatic zones. To provide a broad and non-redundant description of the European climates, different weather files were analysed to guarantee a good variability in the selected locations. The results of these preliminary analyses are reported in figure 13, 14, and table 5.

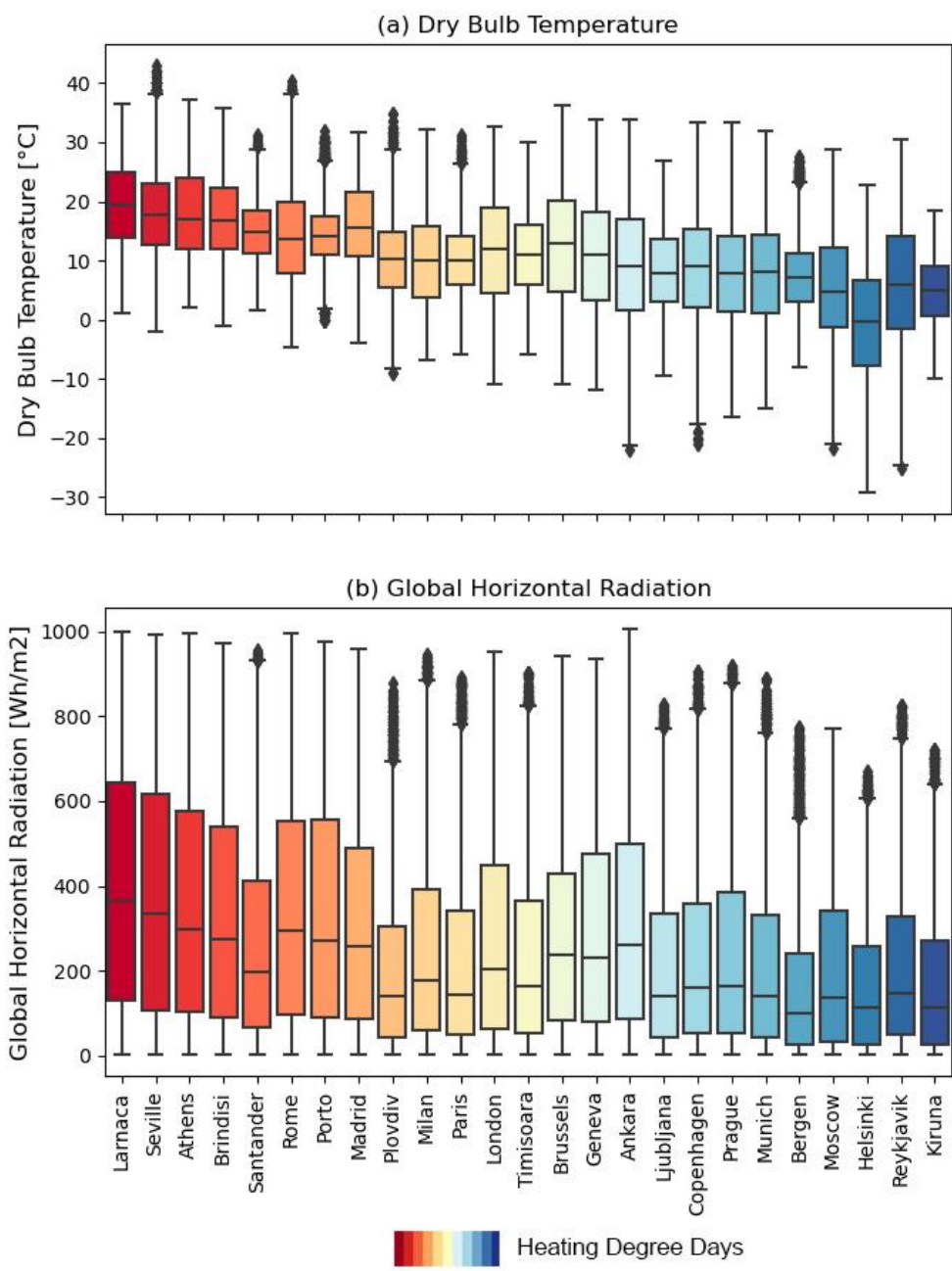


Figure 14. Dry bulb temperature (a) and global horizontal radiation (b) of the 25 selected cities.

Table 5. Characteristics of the 25 European cities considered (data from epw weather file). [37]

City	Country	Köppen–Geiger Classification	CDD_{18°}	HDD_{18°}
Larnaca	Cyprus	BSh	1259	759
Seville	Spain	Csa	1063	916
Athens	Greece	Csa	1076	1112
Brindisi	Italy	Csa	834	1151
Santander	Spain	Cfb	209	1369
Rome	Italy	Csa	649	1444
Porto	Portugal	Csb	146	1491
Madrid	Spain	Csa	628	1965
Plovdiv	Bulgaria	Cfa	543	2471
Milan	Italy	Cfa	380	2639
Paris	France	Cfb	142	2644
London	England	Cfb	32	2866
Timisoara	Romania	Dfa	365	2896
Brussels	Belgium	Cfb	96	2912
Geneva	Switzerland	Dfb	193	2965
Ankara	Turkey	BSk	253	3307
Ljubljana	Slovenia	Dfc	168	3383
Copenhagen	Denmark	Dfb	29	3563
Prague	Czech Republic	Dfb	84	3703
Munich	Germany	Dfb	79	3738
Bergen	Norway	Cfb	21	3996
Moscow	Russia	Dfb	99	4655
Helsinki	Finland	Dfb	33	4712
Reykjavik	Iceland	Dfc	0	4917
Kiruna	Sweden	Dfc	0	6967



Figure 15. Individuation of the sample of 25 cities used for the analyses. [37]

Starting from the same reference model, a specific model for each location was created in order to adapt original model to the European climates and regulations. Hence, all the thermal properties of the models were adjusted to meet the specific energy requirements [191–195]. The 25 selected locations were then grouped in six climatic zones – B,C,D,E,F,G – according to the specific location Heating Degree Days (HDDs). The envelope thermal properties were adjusted according to these climatic zones as described in the table below (Tab.6).

Table 6. Characteristics of the envelope properties for each climatic zone.

Climatic Zone	City	Köppen–Geiger Classification	Envelope Component	Thermal Transmittance [W/m ² K]	Solar Heat Gain Coefficient [-]
B	Larnaca	BSh	External wall	0.43	-
	Seville	Csa	Slab	0.44	-

			Roof	0.35	-
			Window	2.2	0.35
C	Athens	Csa	External wall	0.34	-
	Brindisi	Csa	Slab	0.38	-
	Santander	Cfb	Roof	0.33	-
			Window	2.2	0.35
D	Rome	Csa	External wall	0.29	-
	Porto	Csb	Slab	0.29	-
	Madrid	Csa	Roof	0.26	-
			Window	1.8	0.35
E	Plovdiv	Cfa	External wall	0.26	-
	Milan	Cfa	Slab	0.26	-
	Paris	Cfb	Roof	0.22	-
	London	Cfb			
	Timisoara	Dfa			
	Brussels	Cfb	Window	1.4	0.35
Geneva	Dfb				
F	Ankara	BSk	External wall	0.24	-
	Ljubljana	Dfc	Slab	0.20	-
	Copenhagen	Dfb	Roof	0.21	-
			Window	1.1	0.35
	Munich	Dfb			
G	Bergen	Cfb	External wall	0.17	-
	Moscow	Dfb	Slab	0.10	-
	Helsinki	Dfb	Roof	0.09	-
	Reykjavik	Dfc			
	Kiruna	Dfc	Window	0.8	0.35

3.3. Internal loads and operational schedules

Regarding the internal loads, all the operational schedules of the original DOE model were confirmed in the models adopted in the computational platform. Following images describe the daily trend of the main schedules that can mainly influence the internal loads and hence the energy consumption of the building.

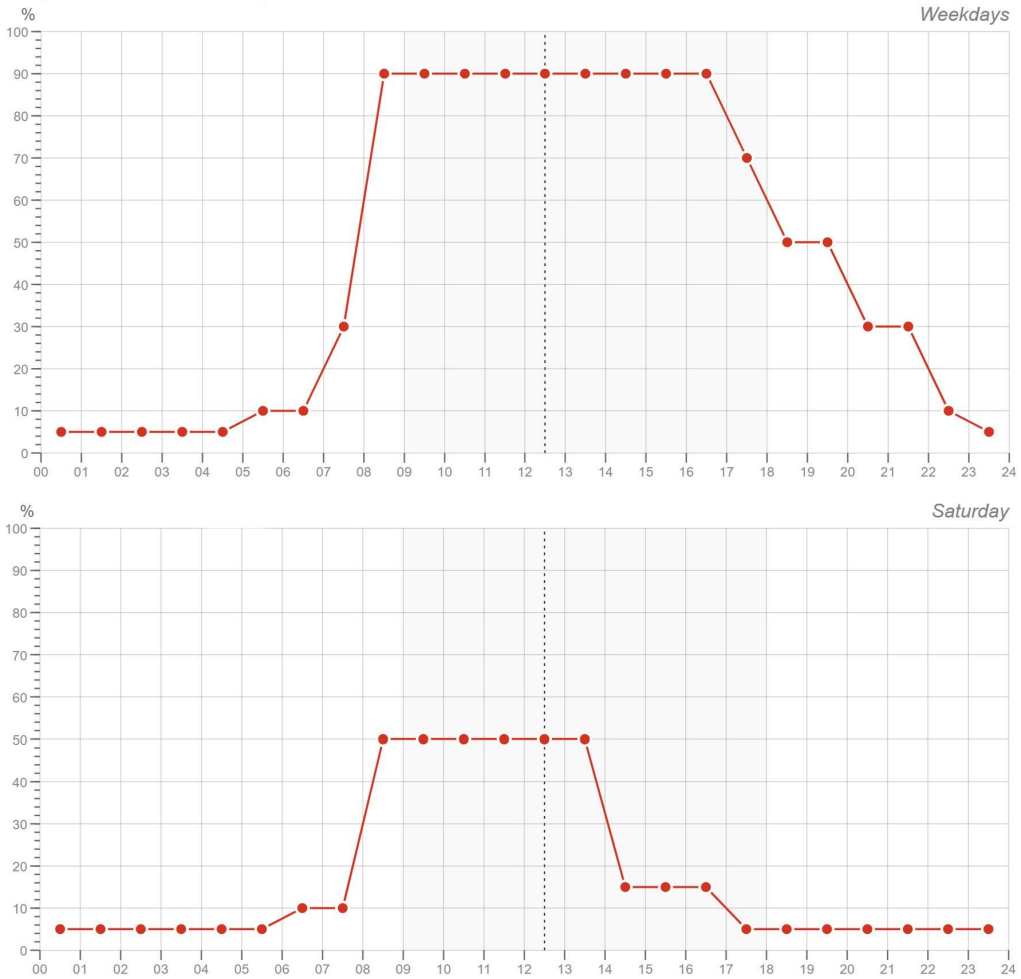


Figure 16. Lighting schedule for weekdays (above) and Saturdays (below).

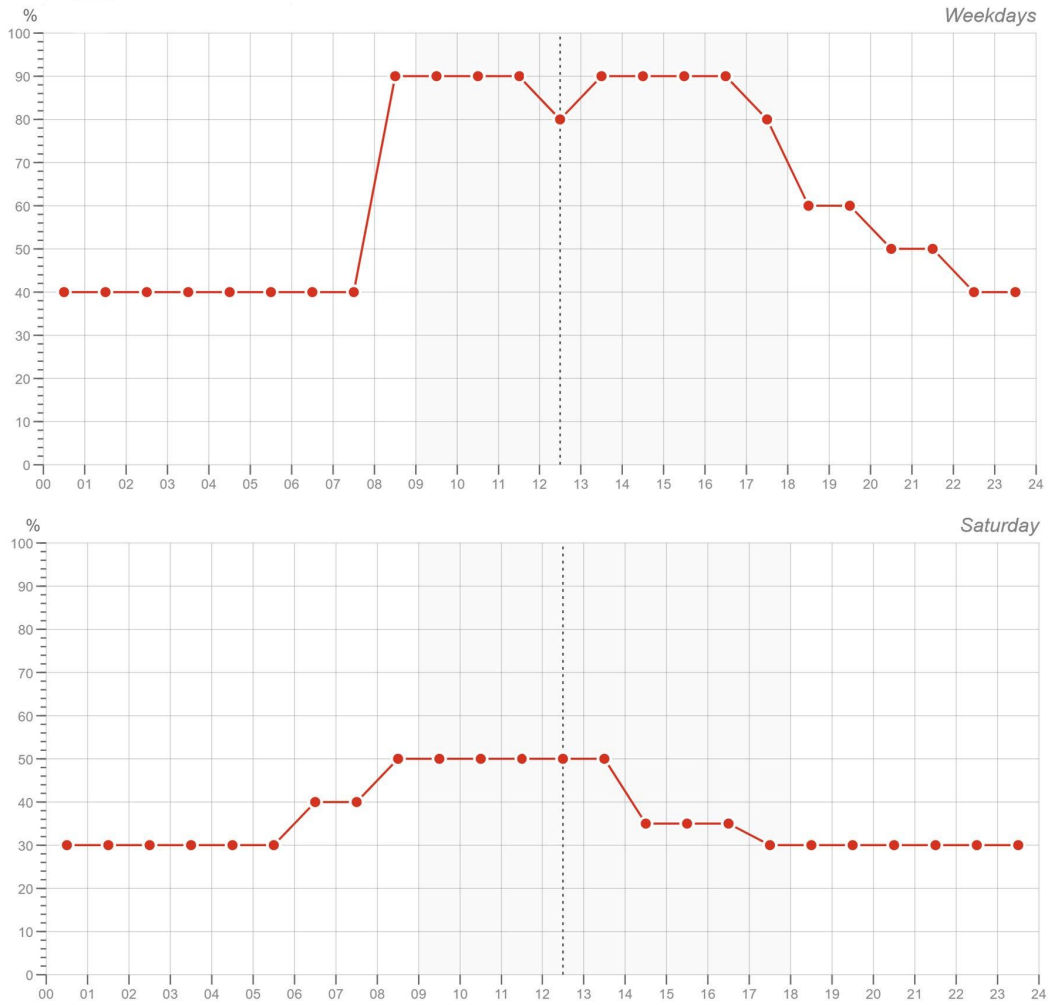


Figure 17. Electrical equipment schedule for weekdays (above) and Saturdays (below).

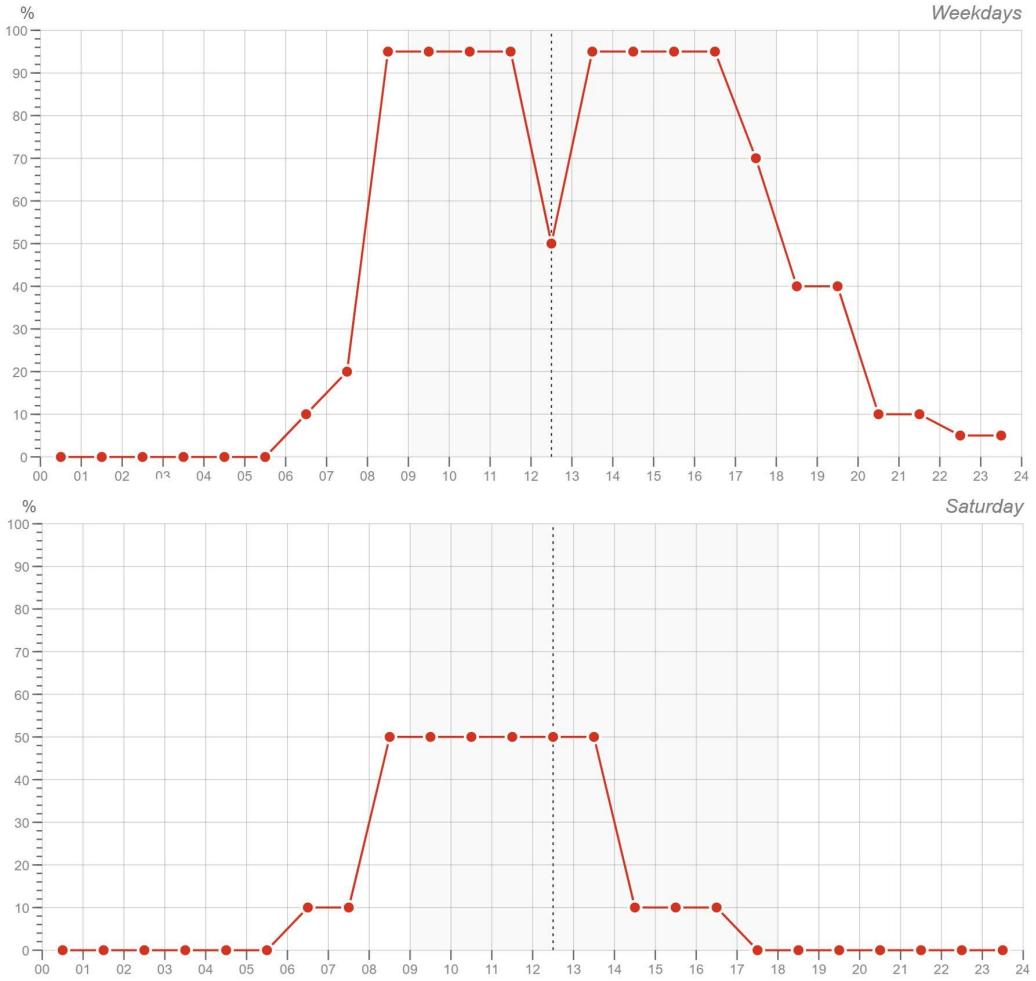


Figure 18. Occupancy schedule for weekdays (above) and Saturdays (below).

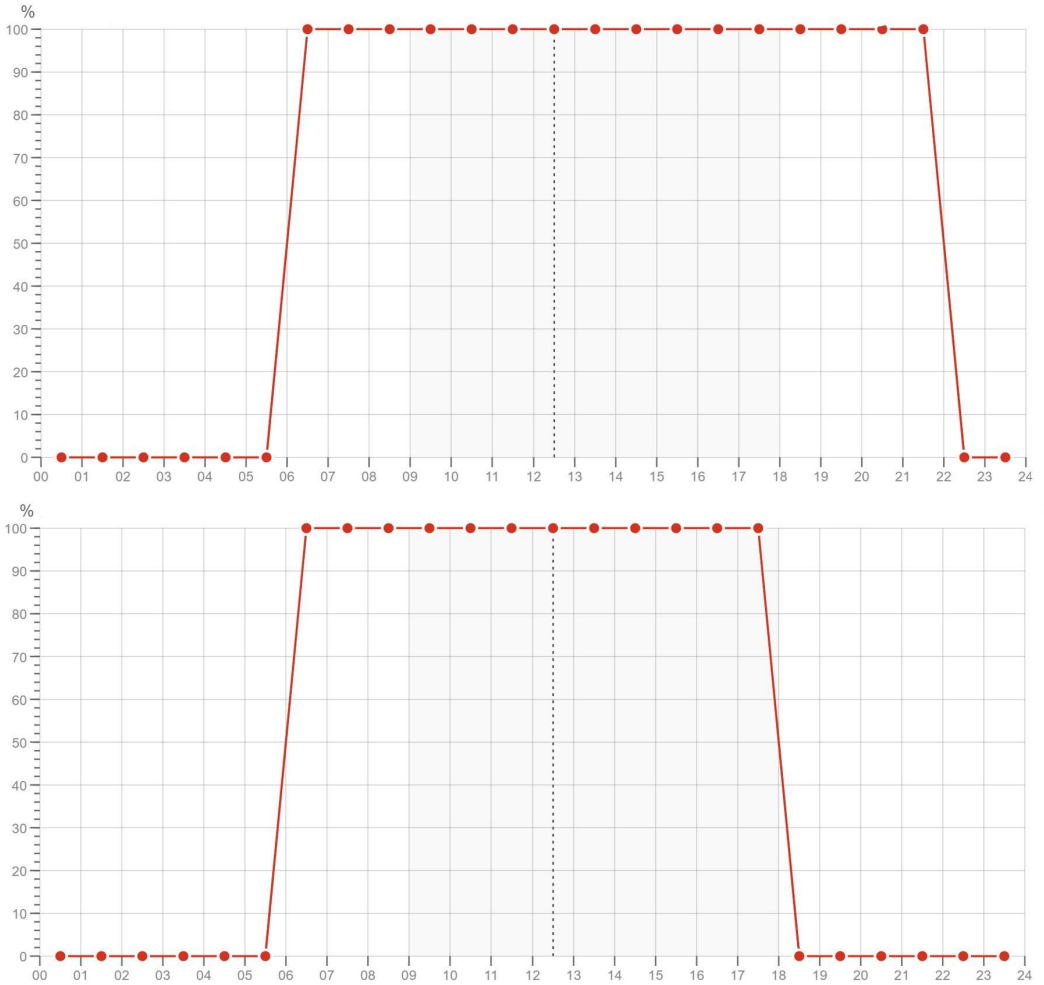


Figure 19. HVAC operational schedule for weekdays (above) and Saturdays (below).

While the daily profiles were confirmed, the unit value of the lighting, equipment, and people were updated to consider the latest technological innovation as the DOE reference model internal loads are still updated to September 2012. In particular, the lighting efficiency has significantly increased in the last years thanks to the spread of LED technologies while the increasing attention to the sustainability has significantly improved the efficiency of the electrical equipment; hence, currently, the original DOE reference model overestimates these internal loads. A study conducted by Kim et al. [196]

analysed the internal gains in office buildings for nearly 30 years defining recent trends in the lighting and electrical equipment consumptions. According to the results of this study, the power consumption related to notebooks, monitors, and computers is on a decreasing trend from 2000-2005 on; similarly, the lighting power absorption has been halved thanks to the spread of LED lamps. Clearly, considering that this change in the internal loads can have significant impacts on the whole energy balance of the building [197], the lighting and electrical equipment of the DOE models were changed according to these more updated studies [196] and technical guides [198,199]. Therefore, with reference to the lighting consumption, the original value of 10.76 W/m^2 was changed with the more reliable and up to dated value of 6.5 W/m^2 . Similarly, considering the increased efficiency of the electrical equipment, the unit value was changed from 10.76 W/m^2 to 5.52 W/m^2 .

Another important change that we can consider comparing the current design strategies and the original DOE reference models, regards the occupancy and the spread of open plan offices. In particular, the market spread after the 2008 recession, leads to a significant grow of the open-plan workspaces as a way to save on operational cost at the expense of an increased occupancy density [200].

To consider this new trend, a study on recent office buildings was conducted in order to account for a more updated occupancy density in the reference model. To that end, the plans of recent built offices (designed or built in the last five years) were analysed to consider a more reliable occupancy and results are reported in figure 19. Starting from the results obtained in this analysis, the average incidence of the office spaces and the reference technical law [201] were considered to define the new occupancy for the energy model. Hence, to account for the recent spread of open space offices, the people density was updated from $18.58 \text{ m}^2/\text{person}$ to $13.9 \text{ m}^2/\text{person}$. It is worth highlighting that each building and each energy model has its own features that depend on a series of design constraints that cannot be presumed a priori. Therefore, the aim of this analysis is simply to provide more updated and reliable values for the internal gains – rather than provide values acceptable in all the contexts – in order to work with values more contextualized with the current state of the art.

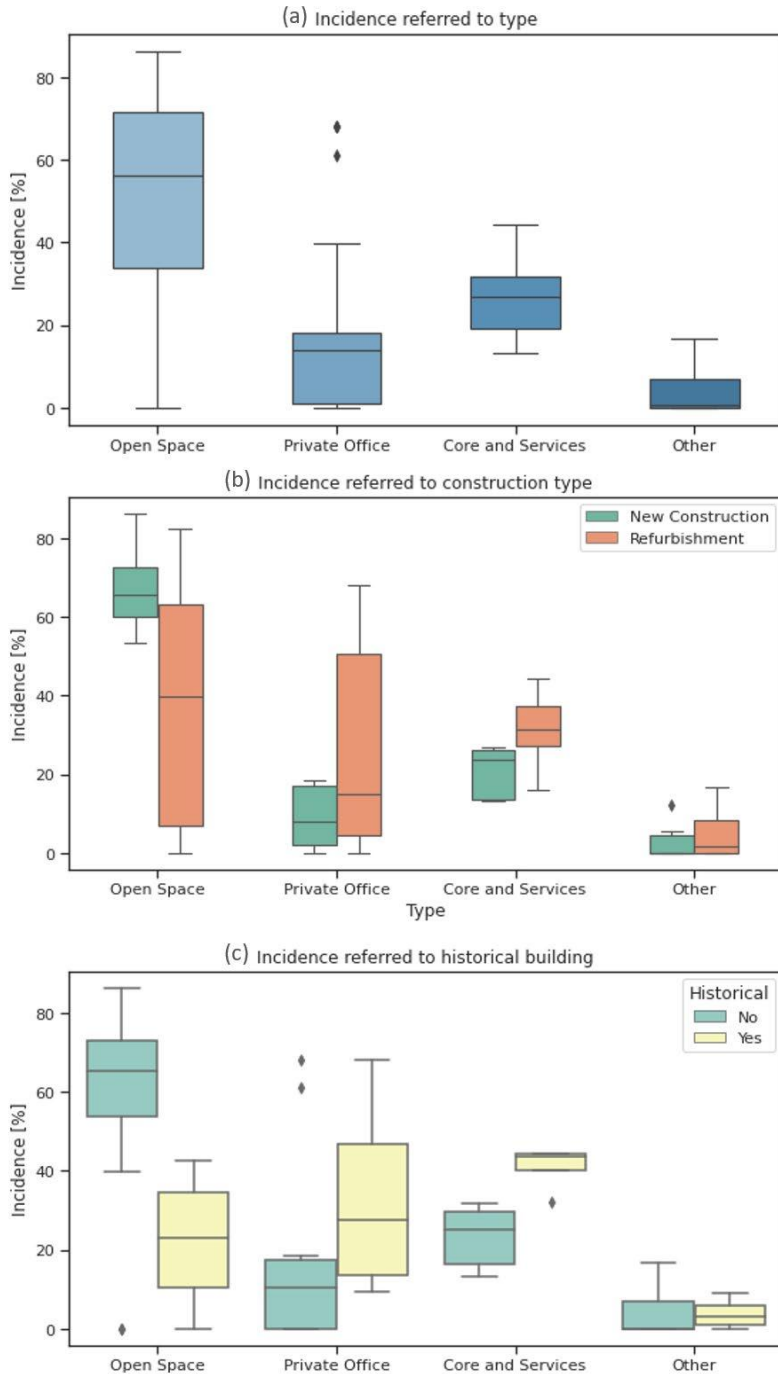


Figure 20. Incidence of different office types (a), construction types (b), and historical buildings (c) in the analysed office buildings.

To sum up, the original DOE model was firstly updated considering the ideal loads system, then the thermal properties were updated according to the European regulations creating a specific model for each location, and – finally – the internal loads were changed with more reliable and updated values. Hence, this group of 25 energy model was considered as the basis of the computational platform described in the following sections.

3.4. Future weather files

Another fundamental element of the platform is the future weather database. According to the research conducted in the state-of-the-art section, the future climate files were generated using the tool CCWorldWeatherGenerator, developed by Jentsch et al. [202]. Starting from the Hadley Centre Coupled Model version 3 outputs (HadCM3) forced with IPCC A2 emission scenario, this tool applies the morphing method to generate future weather predictions. In particular, changes referred to the period 1961-1990 are considered to modify the original EPW files; the weather variables are hence updated through the shifting and stretching algorithms to obtain the future projection as better explained in the state-of-the-art section. Thanks to these transforming algorithms, the tool generates three different future projections referred to the periods 2011-2040, 2041-2070, and 2071-2100 respectively called ‘2020s’, ‘2050s’, and ‘2080s’. Clearly, the adoption of a single GCM output and the use of an outdated emission scenario could be considered a limitation for this study; nevertheless, this tool is still the most used in the building research field [203] and the differences with other more sophisticated or up to dated software are still negligible [204].

The use of a statistical downscaling tool helps to speed up the generation of the weather files ensuring a good reliability of the results as already discussed in the previous sections. Moreover, using an open source, widespread and easy to use tool allows, on the one hand, a good comparability with other studies and, on the other hand, allows the users to generate their own future weather files starting from specific measured data that can be easily added to the platform. Indeed, additional weather data can be easily implemented in the EPW folder of the computational platform to consider these specific weather files rather than the default ones.

4. COMPUTATIONAL PLATFORM

One of the main focuses of this research is the development of a computational platform with the aim of providing a useful tool for researchers and designers to explore the potential of innovative responsive technologies. After the methodological framework described in the previous chapter, this section describes, on the one hand, the modelling technique adopted for each technology considered and, on the other hand, the programming framework considered to achieve the set goals.

As the main aim of this tool is providing an easy-to-use tool for both practitioners and researchers, the tool is based on widely used software and libraries as better described below.

4.1 Users' interface development and programming

Previous sections highlight how each technology requires specific modelling approach and settings, starting from easiest approach up to more complex workflows such as the shape morphing external shadings. The main goal of the platform is to allow non-skilled users to easily model and study these technologies. Hence, the provision of this computational platform could help the spread of responsive technologies which are still rarely selected as viable alternatives due to their intrinsic complexity and to a lack of proper simple tools.

The choice of the users' interface was considered a fundamental step to improve the spread of this platform. Despite Python was used to effectively model the responsive technologies and manage the EnergyPlus Input Data File (IDF) and outputs, the direct use of a programming language could significantly reduce the usability of the tool. Therefore, the tool was split in two main modules: i) the setting and simulation module, and ii) the interface module. The setting and simulation module was realized in Python v.3.8.11 and is used to read the users' input, set the IDF accordingly with the selected input, run the simulation, read the outputs, drawing up the comparisons, and save the results. This first module is the core of the computational platform and includes all the approaches described in the previous sections. The implementation of a second module was dictated by the need of removing the direct use of Python from the workflow as it requires a specific expertise which is uncommon among practitioners and

relatively widespread among researchers. The solution was found in Grasshopper [205] – a Rhinoceros plug-in for algorithmic design – thanks to its visual programming language nature. Grasshopper is largely used thanks to its easiness and its spread in the generative architecture field. This choice allows, on the one hand, to widen the catchment area reaching also non-expert users and, on the other hand, to significantly speed up the customization of the models for both expert and non-expert users. Moreover, Grasshopper allows the use of existing and widespread components, both native and external, that add important extra features such as, for example, the genetic optimizations through Galapagos and Octopus or the brute force solver.

Despite Grasshopper includes a native Python interpreter component (GhPython), this component is based on IronPython which is limited to Python version 2.7. This old version of Python does not support a series of useful and necessary libraries such as Eppy, Numpy, Seaborn etc. Moreover, GhPython is a very basic interpreter and can be used mainly for short and easy scripts rather than for developing a new complete platform. This limitation will be probably partly overcome in the next version of Rhinoceros (v.8 which is currently in progress) which should include a modern code editor with linting and autocomplete, Python 3.9 and the PIP (Pip Installs Packages) package manager. Nevertheless, as the release date for Rhinoceros v.8 is still unknown, the platform was developed on the latest official released version, Rhinoceros v.7.

In order to bypass the use of the old GhPython interpreter, a new component called Hops [206] was used to connect Grasshopper to a local server where the platform runs in Python 3.8 the scripts related to the responsive behaviour of the envelope. Moreover, Hops allows to solve external documents in parallel, speeding up large projects, and to run asynchronously long calculations. Hops defines a third module which is the bridge between the interface and the core modules.

Figure 20 sums up the structure and the components of the platform developed where three different main domains can be easily identified. The first one represents the interface module and is based mainly on Rhinoceros and Grasshopper, the second one is the bridge constituted by Hops, and finally the inner modules define the core modules based on Python and EnergyPlus. Hence, the platform allows to connect the users with

innermost modules – which are the less user friendly –; hence the users interact only with Rhinoceros and Grasshopper without working directly on EnergyPlus and Python.

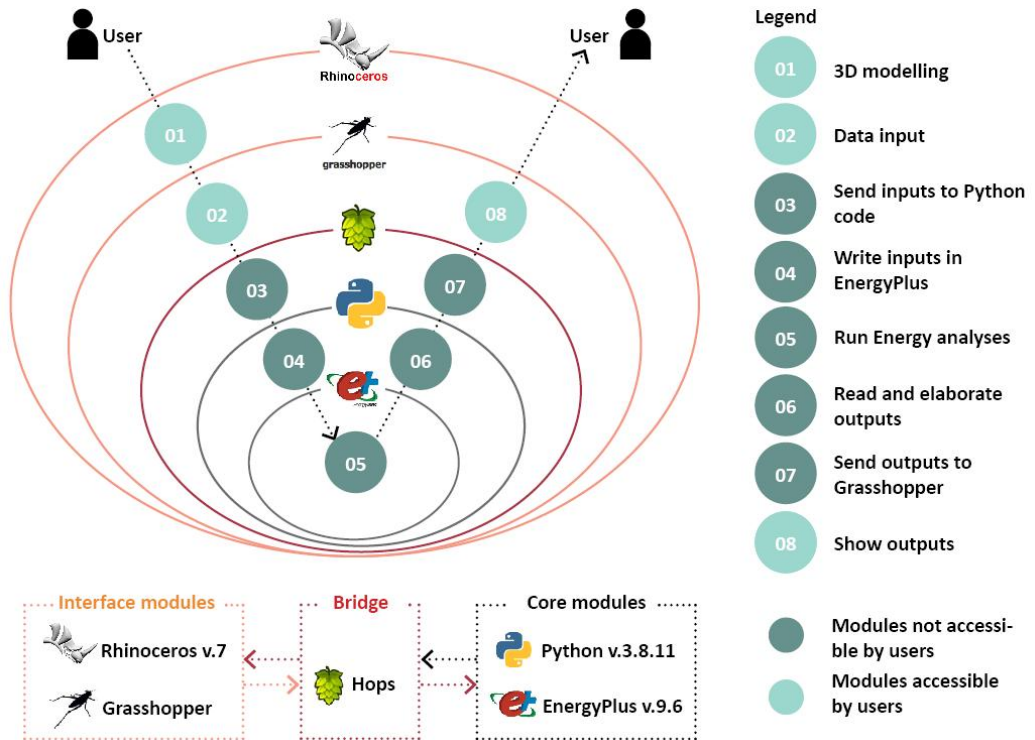


Figure 21. Structure and plugins of the computational platform proposed.

This structure does not limit the application of responsive systems because all the needed input can be managed in Grasshopper as will be better explained in following paragraphs. Instead, avoiding the access to EnergyPlus allows to avoid modelling mistakes which can be common for particularly complex systems and non-expert users. Despite this, expert users can however access externally to the Python codes for further customizations.

To use the platform, the users should firstly download the folder with all the required files and then install all the required software and libraries. To launch the platform, the user simply drags the main script in the Grasshopper canvas and a general interface will be shown on the canvas (fig. 21).

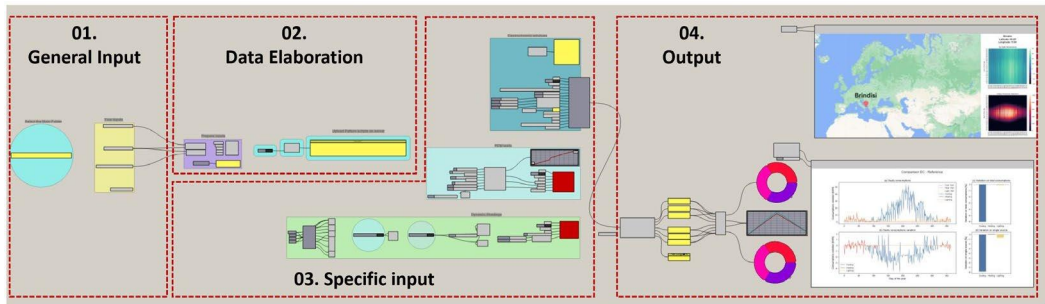


Figure 22. Platform general interface.

Firstly, the user should copy and paste the working directory – i.e., the folder path of the computational platform – in the first panel of the script (highlighted by a cyan circle in the previous figure) to properly set all the dependencies of the algorithms. Then the general input section is completed with four dropdown lists that allows the users to select: the climate scenarios, the location, the responsive technologies, and the exposure as shown in figure 22.

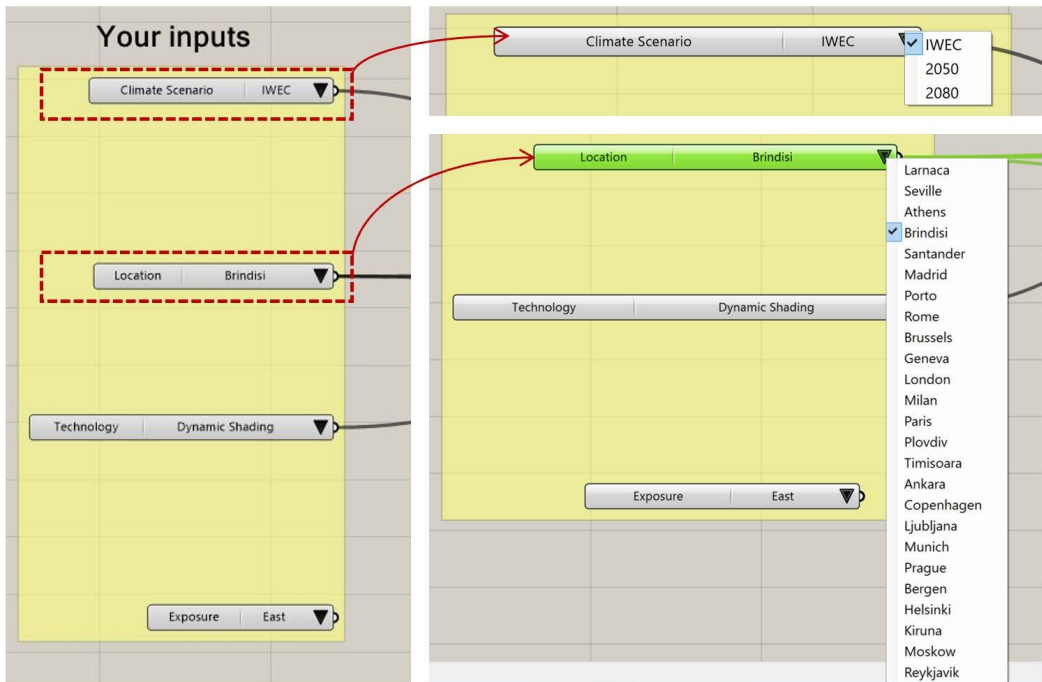


Figure 23. General input interface.

Once all the general input are provided, the script creates in the data elaboration section the command string for the windows terminal used to upload the Python script on the local server. To meet the needs of less expert users, two pop-up messages guide the users in the steps as shown in figure 23.

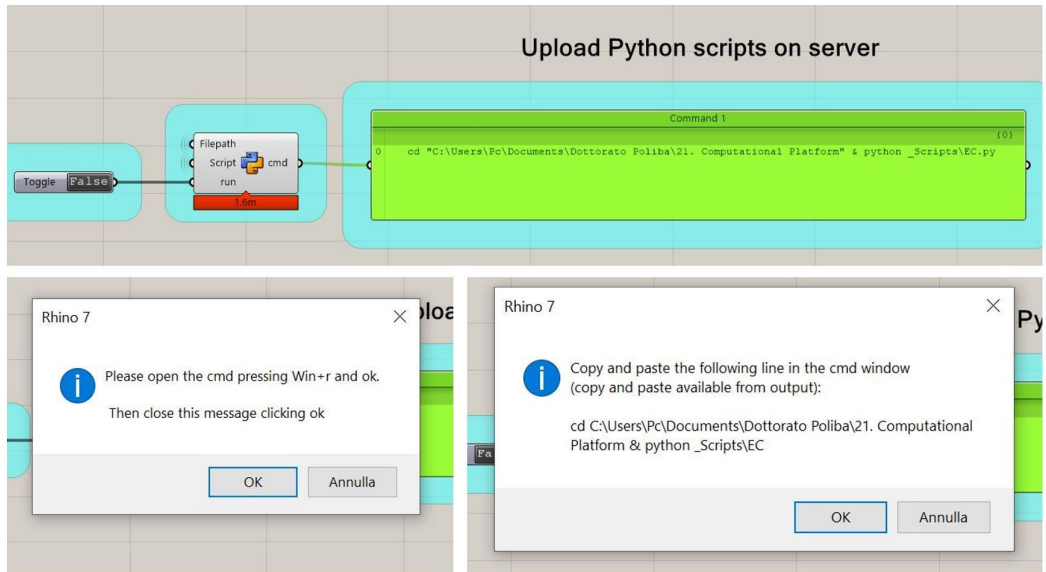


Figure 24. Upload of the Python scripts on the server.

Hence, the following step is to fill all the specific input – e.g., activation threshold, thermal properties, etc. – for the technology selected. Further details are provided in the following subsections where all the available modules are explained in detail. Finally, after all inputs are provided and all the calculations have been run, the output section will show all the results. The platform offers a complete description of the analyses conducted describing the behaviour of both the responsive and the reference model and offers also directly their comparison. The output section is composed by three main elements, the first one which describes the location selected, the second one that provides all the numerical data obtained by the simulation, and a final comparison sheet. The location evaluator is available simply filling out the general input section; it shows the selected city on the map including latitude, longitude and

provides a brief description of the weather through two heatmaps for the hourly dry bulb temperature and the hourly global horizontal radiation as shown in figure 24.

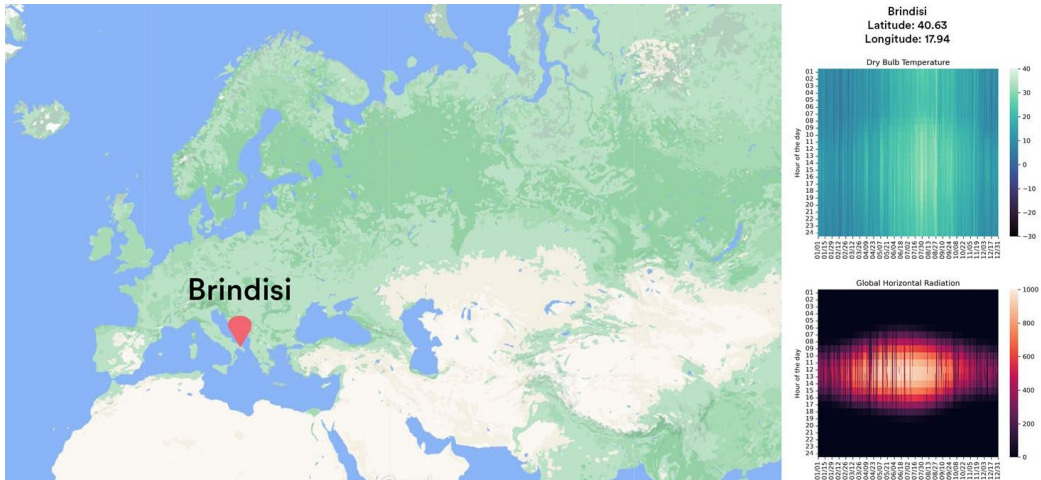


Figure 25. Output of the location evaluator module.

The other outputs derive from the simulation results and are partially rearranged according to the following equations:

$$Total\ energy\ variation = \frac{(Total\ energy)_{Dynamic} - (Total\ energy)_{Static}}{(Total\ energy)_{Static}} \quad (6)$$

$$Total\ energy\ variation\ by\ source = \frac{(Energy\ source)_{Dynamic} - (Energy\ source)_{Static}}{(Total\ energy)_{Static}} \quad (7)$$

$$Single\ source\ variation = \frac{(Energy\ source)_{Dynamic} - (Energy\ source)_{Static}}{(Energy\ source)_{Static}} \quad (8)$$

The numerical output is composed by the heating, cooling, lighting consumptions – directly obtained from EnergyPlus – for both the reference and responsive models and the total energy percentage variation calculated according to equation 6 as shown in

figure 25. This kind of output can be useful to store the results or to conduct further analyses in Grasshopper (e.g. compare different technologies, etc.).

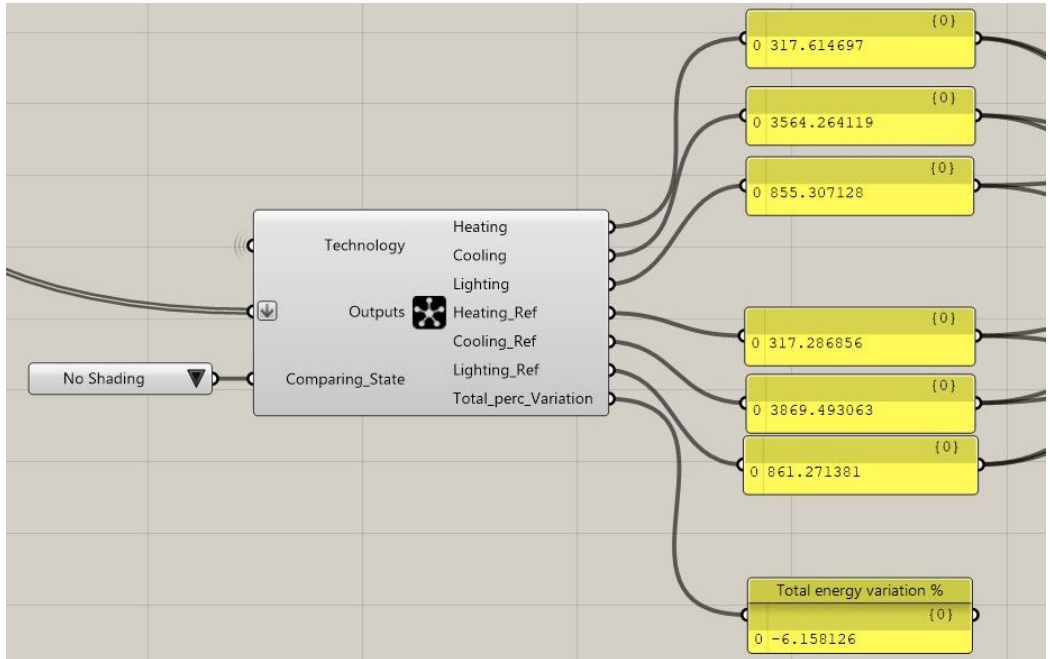


Figure 26. Numerical output module.

Finally, the comparison sheet (figure 26) allows to read the daily trend of the reference and responsive models (graph a), the daily differences (graph b), the percentage variation of each energy source referred to the total consumption – equation 7 – (graph c), and referred to each energy source – equation 8 – (graph d). The combined use of these different graphs facilitates the identification of great variations of a specific source in models where its impact on the total consumptions is limited such as for example the heating consumption in a hot climate. This allows to suggest a specific technology for other climates rather than underestimate its potential. Moreover, all the output generated in EnergyPlus are available in the results folder of the computational platform working directory in csv format according to the selected frequency output. Thanks to these files, all the results for each analysis timestep can be used for further considerations.

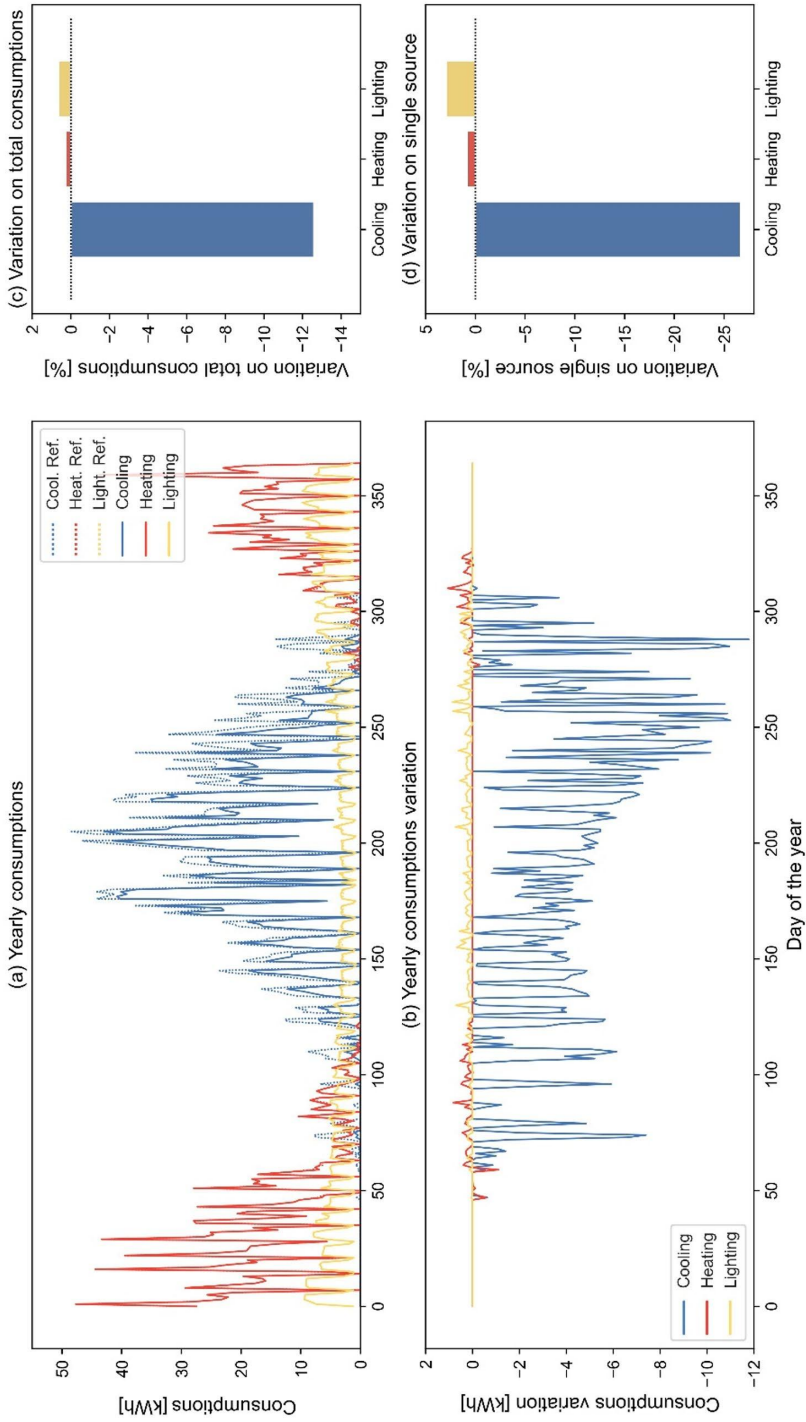


Figure 27. Example of the comparison sheet.

4.2 Responsive technologies modelling

Following paragraphs describe, on the one hand, the simulation settings and methodologies and, on the other hand, the input selection and the management of the simulations for each responsive technology included in the platform. These parameters allow the users to define the properties of the selected technology and to create their own energy models.

4.2.1 Dynamic shading modelling

According to a previous dedicated validation study [40], a specific algorithm was developed to properly model the dynamic shading systems in EnergyPlus. The main innovation of this study, compared to the traditional ones, is that it can properly accounts for the continuous and transient nature of the thermal and energy phenomena. The traditional approaches usually run a simulation for each configuration of the static shading system and then select and combine the output obtained by these different simulations according to a specific activation criterion (Fig. 27a). While these traditional approaches can be considered reliable for other physical parameters that change instantaneously – i.e., illuminance, glare, etc. – thermal and energy parameters need a single continuous simulation to properly describe their transient nature.

Rather than working on combined outputs, this innovative algorithm combines the inputs – in particular the sunlit fractions calculated for each shading state – and forces the shading calculation with this externally combined shading file. This approach assures that the energy behaviour of the system is calculated as the output of a single run – rather than as combination of different simulations – where the shape variations of the shading system lead to gradual and continuous variations in the thermal state of the building elements as outlined in figure 27b.

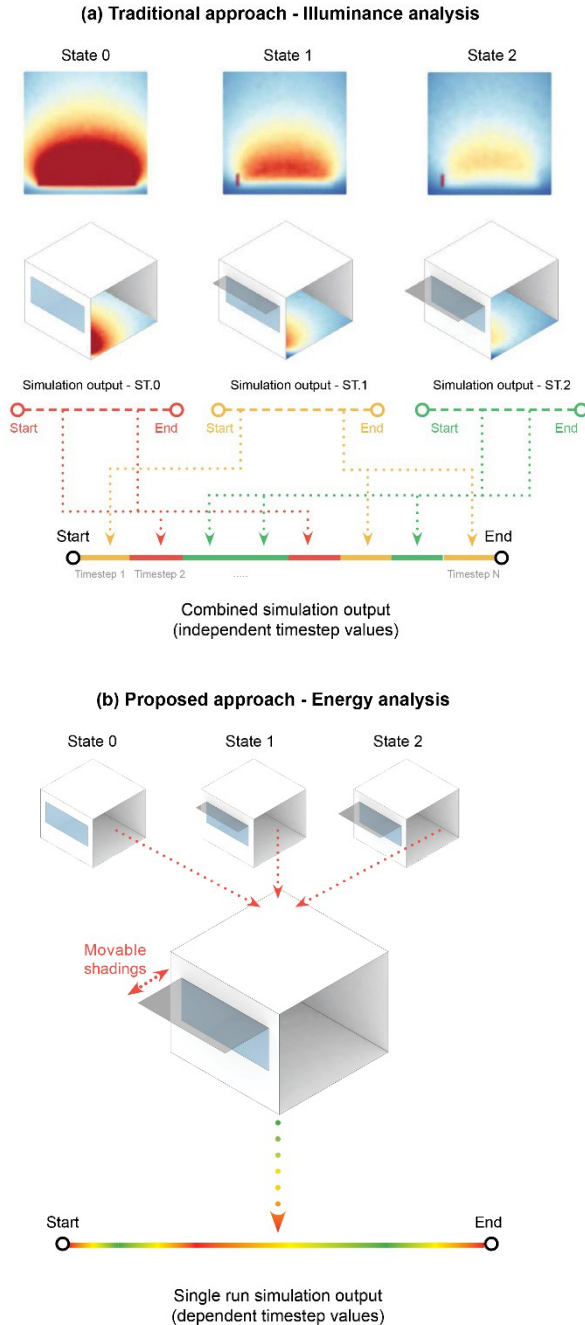


Figure 28. Differences between (a) traditional approach (combination of output) in a daylighting example and (b) proposed approach based on the combination of inputs in an energy example. Source [40].

From a practical point of view, the energy behaviour of the model is described starting from two different model types:

- A Static Shading Model (SSM) for each configuration of the shading system: in these static models the shading systems are fixed and cannot change during the simulation. These models are used to calculate the shading effect – i.e., the shading fractions – of each of the shading configuration on the model surfaces; hence these shading fractions files are combined in a Dynamic Shading File (DSF) according to the activation criterion and used in the equivalent model.
- An Equivalent Dynamic Shading Model (EDSM) for the final simulation: in this file no real shadings are provided as the shading calculation is forced with the external DSF to simulate the change of shape of the shading system.

In its complete version, the main inputs of the algorithm are simply the shading surfaces modelled directly in a 3D modelling environment (Rhinoceros) and the selected activation thresholds (Fig.28 step0). The platform can accept up to three different geometrical configurations for the states of the shading system, each one modelled in a dedicated pre-set layer. Then, the algorithm automatically creates and exports an interchange Excel file for each shading state, that contains all the vertex coordinates of the shading system. Hence, the algorithm read this file and writes the vertex coordinates directly in the EnergyPlus idf to create the SSMs (Fig.28 step1) used to obtain the sunlit fraction files called Static Shading Files (SSF) (Fig.28 step2). After creating the intermediate Equivalent Static Shading Models (ESSM) (Fig.28 step3) the SSF are combined according to the input thresholds (Fig.28 step4) to obtain the DSF and the EDSM (Fig.28 step5). Hence, the algorithm runs the analyses through EnergyPlus generating the output (Fig.28 step6) and comparing them with the ESSM (Fig.28 step8). To improve the reliability of the results, few adjustments regarding the lighting consumptions are made to consider the variation in the shading shapes (Fig.28 step7). This brief description simply aims to introduce the approach adopted, while further details of the structure and of the validation of the algorithm are available in the original validation study [40].

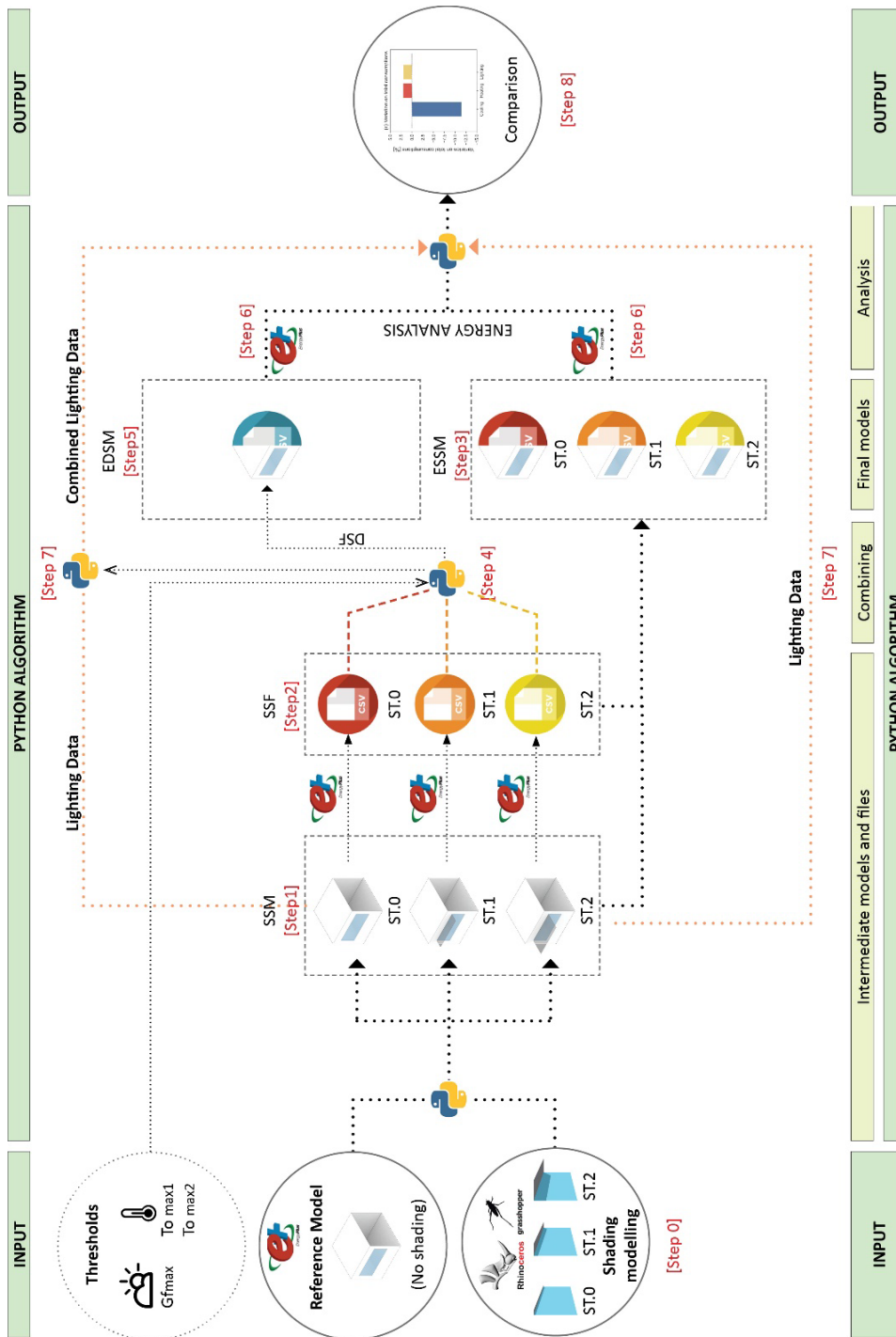


Figure 29.. Conceptualization of the final algorithm. Source [40]

The core concept of this approach is the use of equivalent models based on external shading files instead of real models. The above-mentioned study validated this approach evaluating (on eastern, western, and southern façade) the differences between real (SSMs) and equivalent (ESSMs) shading models on eight different shading systems characterized by different shapes and dimensions ranging from 3D or 2D shading patterns to fins and overhangs. The results obtained highlighted a slight difference in consumption – lower in the ESSMs – on all the analysed models. As the ESSMs always showed consumptions lower than the SSMs, the comparison between different shading types or different exposures can be considered reliable.

These evaluations were conducted on all the shading systems on eastern, western, and southern façades and the resulting average difference of the total consumption between SSMs and ESSMs was nearly 4.5% with a maximum deviation of nearly 7%. However, it is worth highlighting that, to properly validate this approach, the models considered included also very complex shading systems constituted by more than 700 small shading elements. In these models, the differences are clearly amplified by the high number of shadings indeed the highest differences in consumption correspond to the most complex models. Such complex systems are rarely considered in real studies and can be considered only a way to push the algorithm to its limits to test its reliability. Hence, considering the results obtained and more common shading systems, the differences obtained are significantly lower (3.8% on average).

After the validation of the workflow, the study developed a simple algorithm to control the shading state – hence to combine the different SSF in a single DSF – according to external environmental parameters. The combination of the static shading files aims to improve the energy behaviour in both summer and winter period; therefore, the algorithm shifts from less (ST.0) to more shading states (ST.1, ST.2) depending on the combination of the outdoor temperature (T_o) and the incident façade irradiance (G_f). The users provide a radiation threshold ($G_{f,max}$) and two different temperature thresholds ($T_{o,max1}$, $T_{o,max2}$) to maximize the benefits of the systems as described in figures 29 and

30 where the relationship between the outdoor temperature, the incident solar radiation, the heating/cooling modes, and the shading states is shown.

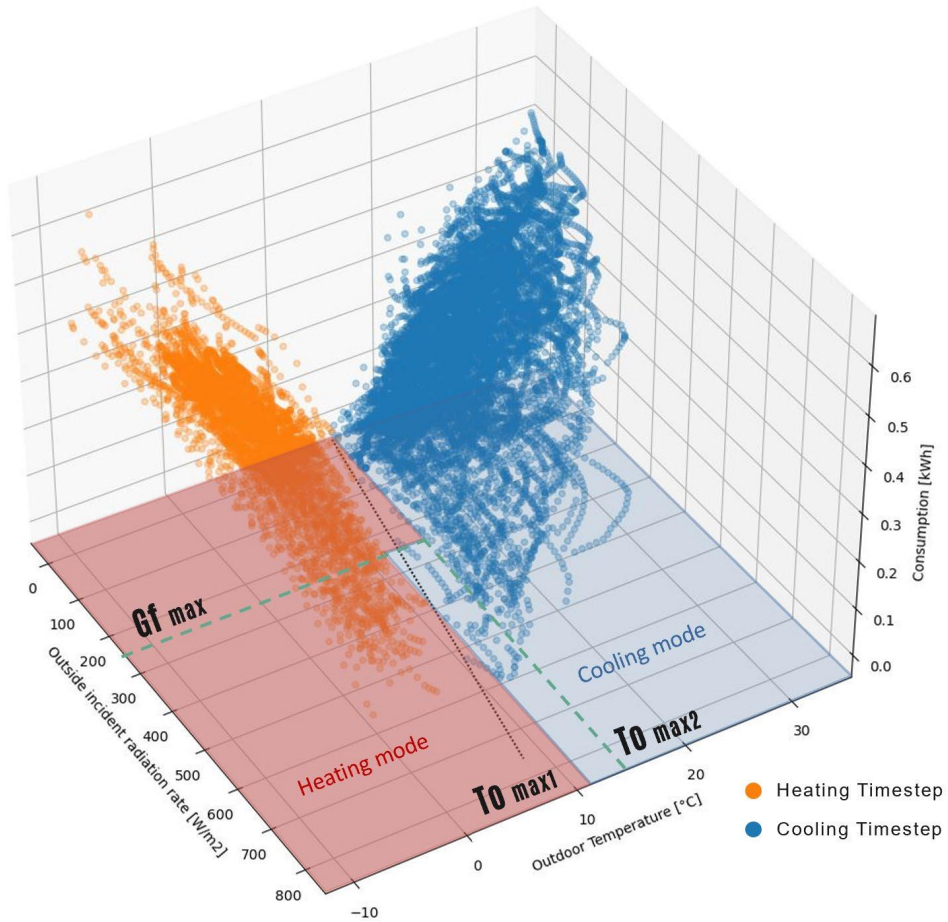


Figure 30. Selection of the activation thresholds.

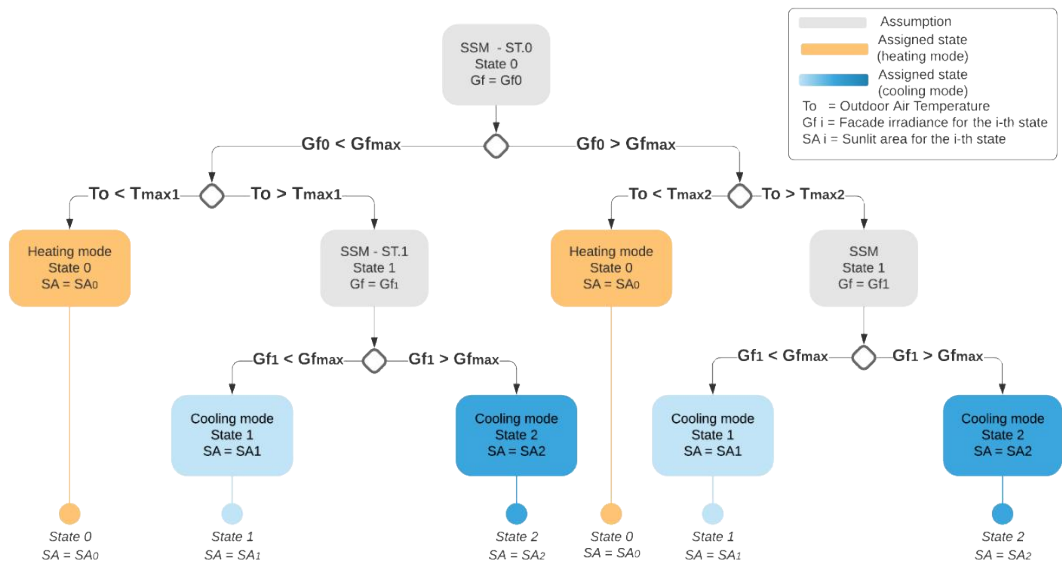


Figure 31. Combination algorithm flow chart. Source [40]

This criterion is the most flexible, but users can simply switch to a single variable control strategy choosing properly the activation thresholds. For example, to switch this control strategy in a temperature-based control, the solar radiation threshold should be set to 0; similarly, to use only a radiation control strategy, the To_{max1} should be set to a very high temperature (e.g. 100°C) while the To_{max2} should be set to a very low temperature (e.g. -100°C).

This specific algorithm can work – at least in its current form – only using activation thresholds independent from thermal parameters of the thermal zones (such as indoor temperature, cooling/heating state, etc.) because the combination of the shading files is realized before the final simulation.

Looking at the dynamic shading module of the computational platform, the user should take three simple steps to complete the dynamic shading modelling and obtain the energy consumption of the model as shown in figure 31. Firstly, selecting the button “Create 3D geometry on Rhino” the script creates in the Rhinoceros file all the surfaces and layers needed for the shading system modelling. Then, after completing in Rhinoceros the model with the geometries of the three different shading states, the user can

create the interchange files just clicking on the second button “Create coordinate files”. Finally, the last inputs needed are the solar radiation and outdoor temperature thresholds for the control strategy. Once all the inputs are provided, setting the last Boolean toggle to true will start the dynamic shading algorithm that will do all the above-described workarounds to provide the user with the final comparison sheets.

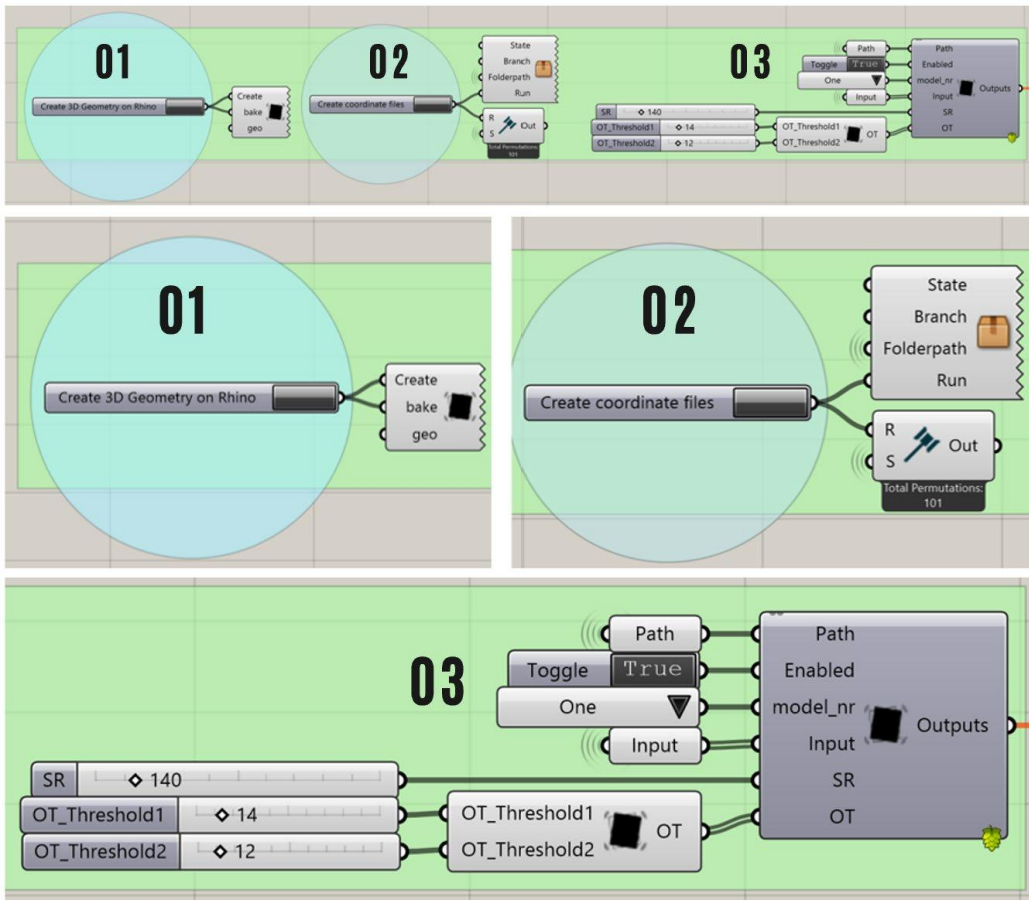


Figure 32. Screenshot from the dynamic shading module of the computational platform.

Only for this specific module, the user can select the term of comparison in the output management component between “No shading”, “Static State 1”, “Static State 2”, and “Static State 3”. Depending on the selection, the script will provide the user with the

comparison sheet showing the differences between the dynamic model and the selected term of comparison.

4.2.2 *PCM modelling*

Another responsive technology included in the platform is the PCM in order to include also a technology that can change the thermal inertia of the building envelope. The platform include by default a PCM-enhanced plaster panel commercial product - the Alba Balance by Saint-Gobain Rigips – whose producer-declared technical data are reported in table 7. The use of PCM in the plasterboard allows to store a certain amount of latent heat (figure 32) that helps to reduce the surface temperature and to shift the peak load.

Table 7. Characteristics of PCM-enhanced plaster panel.

Technical Data		
Density	ρ	1000 kg/m ³
Areal density	ρ_A	25 kg/m ²
Latent heat	dH	300 kJ/m ² (Tm 23°C) 330 kJ/m ² (Tm 26°C)
Total storage capacity (10–30 °C)	-	866 kJ/m ²
Specific heat	c	28.3 kJ/m ² K
Thermal conductivity	λ	0.27 W/mK
Transition temperature	Tm	23°C / 26°C

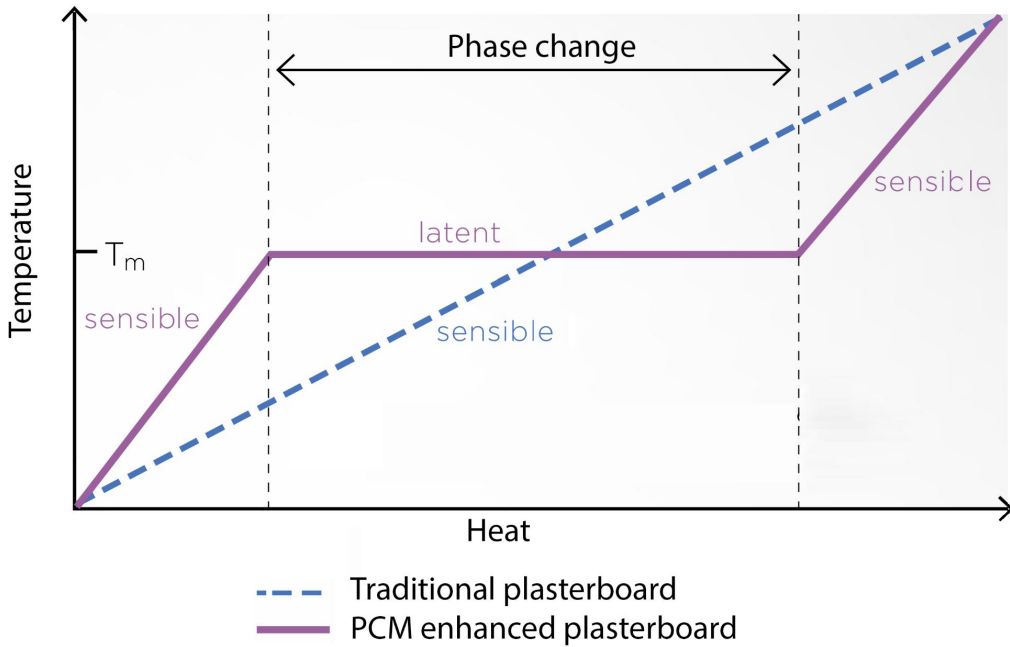


Figure 33. Heat-temperature curve for the PCM-enhanced plasterboard.

However, to ensure the maximum flexibility of the platform, the users can freely change the PCM layer simply recreating the enthalpy curve directly in Grasshopper starting from the physical properties and the thickness of the selected material (figure 33).

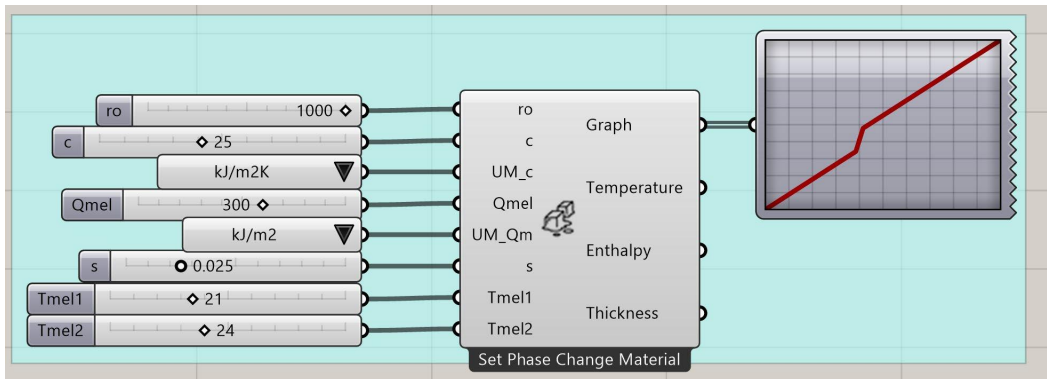


Figure 34. Enthalpy curve modelling in the computational platform starting from the physical properties (density, specific heat, latent heat, starting melting temperature, final melting temperature) of the material.

The enthalpy curve – and the enthalpy table used as input in EnergyPlus – is created by the Grasshopper component considering a sensible heat linear increase (Equation 9) before the starting melting temperature and after the final melting temperature.

$$H = mc \Delta T \quad (9)$$

During the melting phase – i.e. temperatures between the starting and the final melting temperature – the latent heat storage (300kJ/m² in the default example) is equally distributed as an enthalpy increase in the melting temperature range. Redistributing this latent heat in the melting temperature range is translated in a sudden increase in the material enthalpy which is the typical enthalpy jump which is clearly represented in the graph shown in the platform.

The following Grasshopper component inputs the enthalpy table calculated in the EnergyPlus file and – to properly model the PCM behaviour – changes the heat balance algorithm from the Conduction Transfer Function (CTF) to the Conduction Finite Difference (ConFD) algorithm, increasing the timesteps from 6 to 20 [207]. Despite these settings increase the running time, PCMs – or in general variable thermal conductivity materials – need to discretize the surfaces depending on thermal diffusivity and timestep to be properly modelled [188]. The choice of these settings is based on scientific literature, as many studies [188,207] have already verified the good adherence of the numerical model with measured data using these settings. Increasing the number of timestep would lead to a slight increase in the accuracy of the results errors of about 1% – instead of a just-few-times-higher error [208] which can be acceptable on an annual energy simulation – at the expense of larger simulation time.

The PCM layer is located by default on the inner layer of the wall because it can stabilize the radiant temperature [74] despite a study by Zwanzig et al. stating that in a multilayer wall, centrally located PCM better reduces heat fluxes [209]. Future releases of the platform could add also the choice of the position of the PCM layer in the multilayer wall.

4.2.3 Electrochromic modelling

The EC windows were modelled in the computational platform using only the standard EnergyPlus components. Firstly, two different windows construction named “Bleached Window” and “Dark Window” – correspondent respectively to the clear and the coloured state – were defined in EnergyPlus. The clear state of the device was considered the default state and hence was assigned directly to all the EC windows in the “Fenestration Surface: Detailed” field. Then, to consider the properties switching, “Dark Window” was assigned in the “Window Shading Control” field as “Construction with Shading Name” selecting “Switchable Glazing” as shading type as shown in figure 34.

Field	Units	Obj1	Obj2	Obj3	Obj4
Name		EC_WIN-Perimeter_	EC_WIN-Perimeter_	EC_WIN-Perimeter_	EC_WIN-Perimeter_
Zone Name		Perimeter_bot_ZN_	Perimeter_bot_ZN_	Perimeter_bot_ZN_	Perimeter_mid_ZN_
Shading Control Sequence Number		1	1	1	1
Shading Type		SwitchableGlazii	SwitchableGlazing	SwitchableGlazing	SwitchableGlazing
Construction with Shading Name		DarkWindow	DarkWindow	DarkWindow	DarkWindow
Shading Control Type		OnIfHighSolarOrnWi	OnIfHighSolarOrnWi	OnIfHighSolarOrnWi	OnIfHighSolarOrnWi
Schedule Name		EC_ON	EC_ON	EC_ON	EC_ON
Setpoint	W/m2, W or deg	100	100	100	100
Shading Control Is Scheduled		Yes	Yes	Yes	Yes
Glare Control Is Active		No	No	No	No
Shading Device Material Name					
Type of Slat Angle Control for Blinds					
Slat Angle Schedule Name					
Setpoint 2	W/m2 or deg C	601	601	601	601
Daylighting Control Object Name		Zone1	Zone2	Zone4	Zone6
Multiple Surface Control Type		Group	Group	Group	Group
Fenestration Surface 1 Name		Perimeter bot ZN	Perimeter bot ZN	Perimeter bot ZN	Perimeter mid ZN

Figure 35. Shading control for EC windows in EnergyPlus.

Considering the large availability of commercial products, the EC windows solar and optical parameters are not set by default but can be easily adjusted by the users. Sibilio et al. [210] reviewed all the available commercial products providing an exhaustive

table which is reported below as reference to model reliable EC windows in the platform.

Table 8. Available commercial EC device. Adapted from [210].

Manufacturer	Product	State	U [W/m²K]	VLT [-]	SF [-]
EControl-Glas GmbH & Co.	ECONTROL Double glazing	Clear	1.1	0.5	0.38
		Tinted	1.1	0.10	0.10
	ECONTROL Triple glazing	Clear	0.5	0.40	0.33
		Tinted	0.5	0.09	0.08
Gesimat GmbH	Double glazing with Low-E	Clear	1.1	0.69	0.49
		Tinted	1.1	0.07	0.13
	Triple glazing with Low-E	Clear	0.6	0.61	0.42
		Tinted	0.6	0.06	0.10
SageGlass	Double glazing	Clear	1.4	0.63	0.47
		State2	1.4	0.21	0.16
		State1	1.4	0.06	0.09
		Tinted	1.4	0.01	0.06
	Double glazing with Low-E	Clear	1.1	0.63	0.47
		State2	1.1	0.21	0.16
		State1	1.1	0.06	0.09
		Tinted	1.1	0.01	0.06
	Triple glazing with Low-E	Clear	0.8	0.60	0.42
		State2	0.8	0.19	0.14
		State1	0.8	0.05	0.07
		Tinted	0.8	0.01	0.05
View Dynamic Glass*	Double pane IGU with clear glass	Clear	1.7	0.58	0.40
		State2	1.7	0.40	0.33
		State1	1.7	0.10	0.13
		Tinted	1.7	0.01	0.09

	Double pane IGU with Low-E glass	Clear	1.4	0.48	0.32
		State2	1.4	0.35	0.24
		State1	1.4	0.09	0.10
		Tinted	1.4	0.01	0.07
	Triple pane IGU with clear glass	Clear	1.3	0.51	0.35
		State2	1.3	0.37	0.26
		State1	1.3	0.09	0.10
		Tinted	1.3	0.01	0.07
	Triple pane IGU with Low-E glass	Clear	0.8	0.43	0.29
		State2	0.8	0.31	0.21
		State1	0.8	0.08	0.08
		Tinted	0.8	0.01	0.05
*The values were calculated using the software LBNL Window 7.3					

The computational platform includes a dropdown list with these commercial products and a component that – based on the product selected – automatically gives the thermal and solar parameters useful to run the analyses (figure 35).

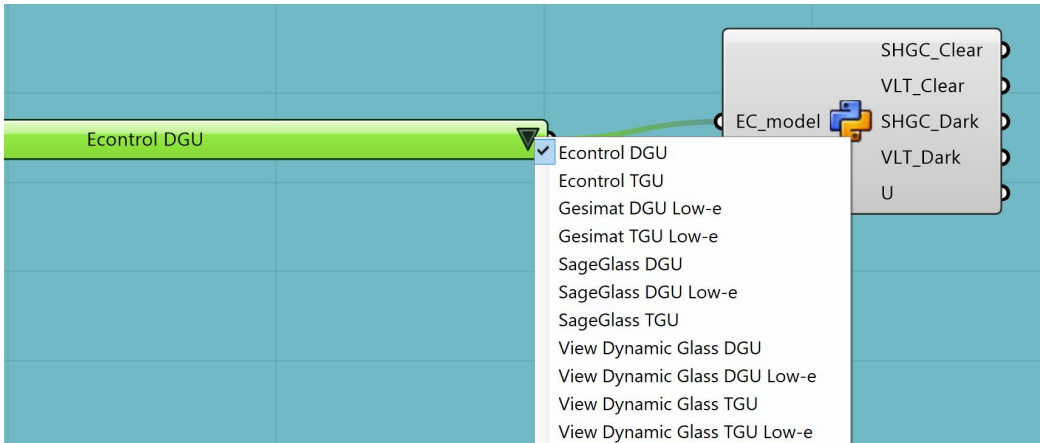


Figure 36. Commercial EC windows provided as viable alternatives in the platform.

Instead, considering the thermal transmittance, values are automatically set in accordance with the location selected for the analysis as described in the previous section. However, the user can freely overwrite these values according to other specific needs. To fully exploit and explore the potential of this technology, the extrinsic control – and its relative thresholds – of the device are not preassigned but can be selected directly by the users in the platform.

In particular, the activation strategy can be set among the following alternatives:

1. Always on
2. Always off
3. On if schedule allows
4. On if high solar on window
5. On if high horizontal solar
6. On if high outdoor air temperature
7. On if high zone air temperature
8. On if high zone cooling
9. On if high glare
10. Meet daylight illuminance setpoint
11. On night if low outdoor temperature and off day
12. On night if low indoor temperature and off day
13. On night if heating and off day
14. On night if low outdoor temperature and on day if cooling
15. On night if heating and on day if cooling
16. Off night and on day if cooling and high solar on window
17. On night and on day if cooling and high solar on window
18. On if high outdoor air temperature and high solar on window
19. On if high outdoor air temperature and high horizontal solar

For each control strategy selected the Grasshopper component requires one or two inputs and, depending on the control strategy selected, a panel is automatically updated to describe the required inputs as shown in figure 36.

Then, the EC component allows to select an activation schedule through four dropdown menus for selecting the start and end months and days. Finally, the user can select the accuracy and the length of the simulation and the frequency of the output report (timestep, hourly, daily, monthly).

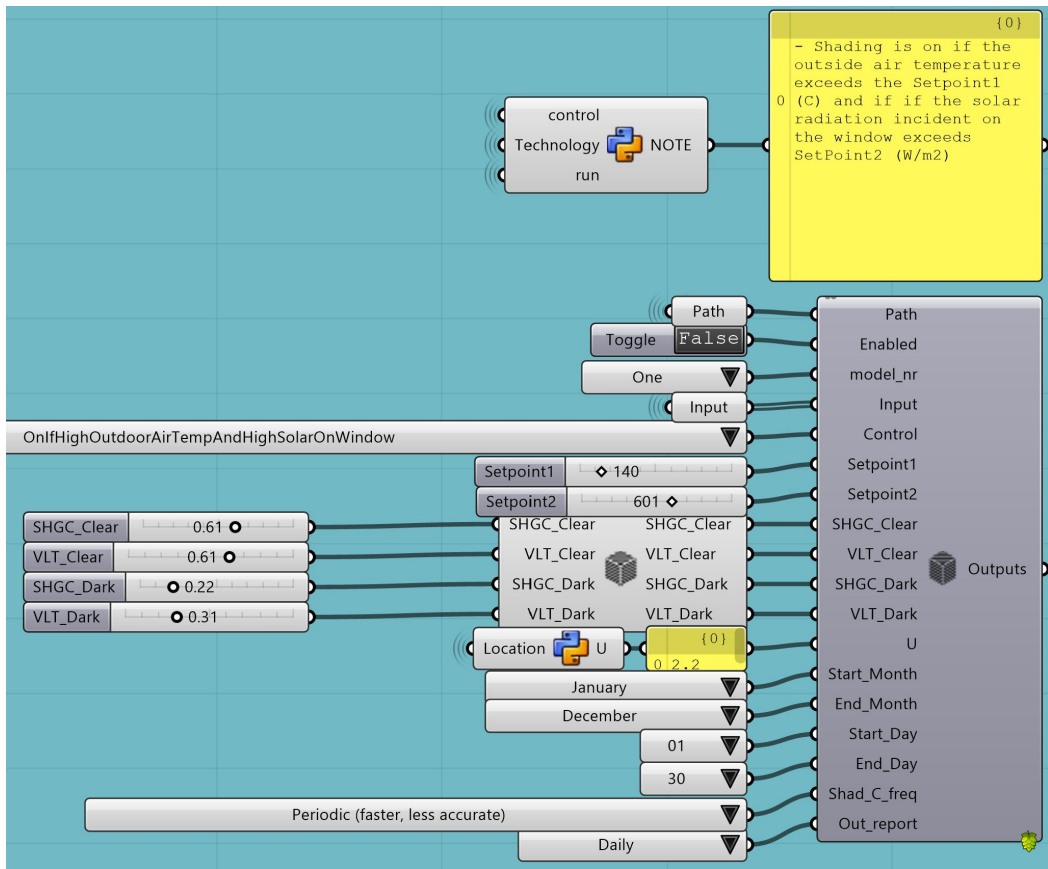


Figure 37. Shading control for EC windows in EnergyPlus.

4.3 Testing the platform: case studies

After the definition of this tool, the platform was tested and pushed to its limits to check its functioning and to identify other eventual limitations that are not predictable simply from a theoretical point of view. To that end, different case studies were considered to test each module starting from extreme and opposite sets of inputs.

Each configuration studied was tested in the warmest and coldest locations and in an intermediate one with a high variation of the environmental parameters; in particular, Larnaca ($CDD_{18^\circ}=1259$, $HDD_{18^\circ}=759$), Helsinki ($CDD_{18^\circ}=33$, $HDD_{18^\circ}=4712$), and Rome ($CDD_{18^\circ}=649$, $HDD_{18^\circ}=1444$) were considered for the testing phase. Moreover, all the simulations were run in both the current climate scenario and 2080 future projection. Finally, regarding the thermal zones considered, the southern and western exposures were chosen to test the algorithm that automatically creates the responsive technology in the IDF according to the zone selected in Grasshopper.

Starting from these general inputs, specific inputs for each technology were selected to consider extreme cases and an intermediate more realistic case. Hence, three different activation criteria were considered for the extrinsically controlled technologies (electrochromic and dynamic shadings) and two different materials were adopted for the intrinsically controlled systems (PCMs). Specifically, extrinsic control was based on a combined outdoor temperature and solar radiation thresholds in order to have an activation criterion that can be considered somehow proportional and connected to the one used in the intrinsically controlled systems. Indeed, the activation of the PCMs depends directly on the envelope temperature which is strictly related to both air temperature and incident solar radiation. Therefore, the extrinsic systems are controlled according to the following strategies:

- “Always on” control: it represents the envelope always in its shaded configuration. This control is created forcing the temperature and the solar radiation thresholds to very low values as described in equation 10 where t is the analysis timestep and the values 0 and 1 of the shading state means respectively unshaded and shaded.

$$\text{Shading state } (t) = \begin{cases} 0 \rightarrow G_f(t) < 0 \text{ W/m}^2 \wedge T_o(t) < -30^\circ\text{C} \\ 1 \rightarrow G_f(t) \geq 0 \text{ W/m}^2 \wedge T_o(t) \geq -30^\circ\text{C} \end{cases} \quad (10)$$

- “Always off” control: it represents the envelope always in its unshaded configuration. This control is created forcing the temperature and the solar radiation thresholds to very high values as described in equation 11.

$$\text{Shading state } (t) = \begin{cases} 0 \rightarrow G_f(t) < 2000 \text{ W/m}^2 \wedge T_o(t) < 50^\circ\text{C} \\ 1 \rightarrow G_f(t) \geq 2000 \text{ W/m}^2 \wedge T_o(t) \geq 50^\circ\text{C} \end{cases} \quad (11)$$

- “Standard” control: it represents the envelope can change its properties switching between the shaded and unshaded configuration according to realistic thresholds as described in equation 12. The specific values of the thresholds (120 W/m² and 15°C) are derived from other studies [40,211] and are not directly optimized in each specific model because, in this testing phase, they are only used to check the envelope responsiveness rather than to minimize the energy demand. In this case, the outdoor temperature threshold (15°C) allows to take advantages in both summer and winter period and an intermediate solar radiation value of 120 W/m² allows to find a balance between lighting and cooling consumption during summer.

$$\text{Shading state } (t) = \begin{cases} 0 \rightarrow G_f(t) < 120 \text{ W/m}^2 \wedge T_o(t) < 15^\circ\text{C} \\ 1 \rightarrow G_f(t) \geq 120 \text{ W/m}^2 \wedge T_o(t) \geq 15^\circ\text{C} \end{cases} \quad (12)$$

In order to have similar control between dynamic shading systems and EC windows, the dynamic shading considered can switch only between two states – rather than three – as the functioning of the three states algorithm was already tested in previous studies [39,40]. Clearly, the aim of these control strategies is to explore and study the envelope behaviour to understand if the results are reliable and, hence, if the platform is modelling properly the responsive technologies. To achieve this goal, the clearest way is to consider two extreme settings and a reliable intermediate one despite these are not the best control strategies from an energy point of view.

Table 9 reports all the main properties of the materials and devices considered in these analyses. The EC parameters are referred to a commercial product – the SageGlass DGU – with a thermal transmittance coherent with the location selected as described in section 3.2. With regard to the intrinsically controlled technologies, a commercial PCM-enhanced plaster panel – the Alba Balance by Saint-Gobain Rigips described in the 4.2.2 subsection – with a melting temperature of 23°C and 26°C were considered to test this module. Finally, the dynamic shading (DS) selected is constituted by a façade pattern of 61 origami-shaped foldable elements (figure 37) on the southern façade and 41 elements on the shorter eastern and western façades inspired by those adopted in the Al Bahr Towers described in section 2.1.3. The shading can be opened and folded according to the activation criterion changing the horizontally projected shading area on the façade from 0.3 m² for the state 1 (ST1) configuration to 1.3 m² for the state 2 (ST2).

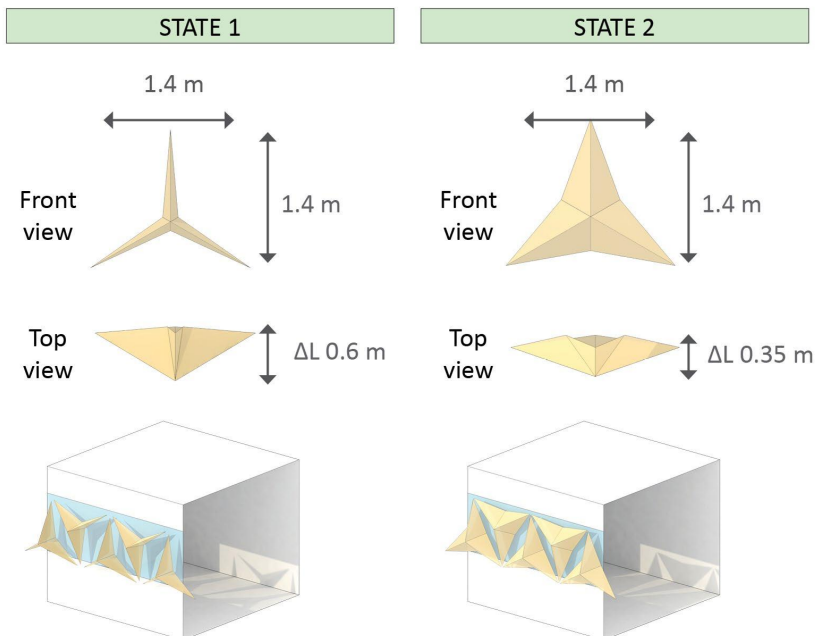


Figure 38. Geometrical details of the dynamic shading system considered. Adapted from [39]

Table 9. Simulations conducted during the testing phase and relative inputs considered.

EC windows					
Code	SHGC _b [-]	SHGC _c [-]	VLT _b [-]	VLT _c [-]	Thresholds [°C] & [W/m ²]
EC_1	0.47	0.06	0.63	0.01	-30°C & 0 W/m ²
EC_2					50°C & 2000 W/m ²
EC_3					15°C & 120 W/m ²
PCM plasterboard					
Code	s [m]	ρ [kg/m ³]	Q _{mel} [kJ/m ²]	c [kJ/m ² K]	Thresholds (T _{mel}) [°C]
PCM_1	0.05	1000	300	28.3	23
PCM_2			330		26
Dynamic Shading					
Code	Area ST1* [m ²]	Area ST2* [m ²]	Number [-]	Type	Thresholds** [°C] & [W/m ²]
DS_1	0.3	1.3	61	Pattern	-30°C & 0 W/m ²
DS_2			(South)		50°C & 2000 W/m ²
DS_3			41 (West)		15°C & 120 W/m ²
All the simulations were run for the three selected locations, for two exposures, and for two climate contexts.					
* To work with a double states shading, model State2 and State3 are geometrically the same.					
**To work with solar radiation and single outdoor temperature threshold the T _{o,max1} is very high (50°C) while T _{o,max2} and G _{f,max} are those reported in this table.					

Each simulation input reported in table 9 was run 6 times to account for all the permutations related to the different locations and climate scenarios. To clearly identify all the simulations conducted, a simulation code was assigned to each input set and “TMY”, and “2080” were used to identify respectively the current scenario – intended as the Typical Meteorological Year – and the 2080 future projection. Therefore, a total number

of 96 simulations were run to test the functioning of the platform and results obtained are described in following figures and tables. The results are divided according to different technologies (different figures), climate scenarios (different subplots), and to control strategies (different columns in each subplot). All the graphs show the total energy variation by source (Eq. 7) to describe the variation of each source and its impact on the total energy demand while further data and elaborations are provided in the tables.

4.3.1 *Electrochromic windows: results*

Starting from the EC models (fig.38), the results obtained shows reasonable values and expected trends confirming the proper modelling of the responsive technology. In particular, the first control strategy (EC_1) corresponds to EC windows “always on” strategy, thus the glazing is always in its dark state. This behaviour can be easily read in the graph as all the locations, all the exposures, and both climate scenarios show a significant reduction of the cooling consumption counterbalanced by an increase of the heating consumption and a strong increase of the lighting demand. This control strategy performs better in hot climates rather than in colder ones and this is perfectly described by the variation of the total energy demand that ranges from a minimum of -4.3% for the western exposure in Larnaca in the future scenario up to a maximum of nearly +24.7% for the western façade in Helsinki in the current climate scenario. Another confirmation can be found in the average energy variation for each location that grows from +0.5% in Larnaca, to +6.7% in Rome, up to +17.4% in Helsinki. The increase in energy consumption in many of the simulations run with this control strategy is related to the non-optimized control; the aim of this analysis is indeed checking the functioning of the platform in both extreme and realistic intermediate cases while the minimization of the energy consumption is currently out of the scope of this testing phase. Changing the climate scenarios increases the overall benefits of the EC windows implementation as this specific control strategy performs better in hot climates, hence the temperature increase due to the climate change improves the overall energy

consumptions. Indeed, the overall average for the current scenario is +14% while for the 2080 scenarios the increase is lower (+3%).

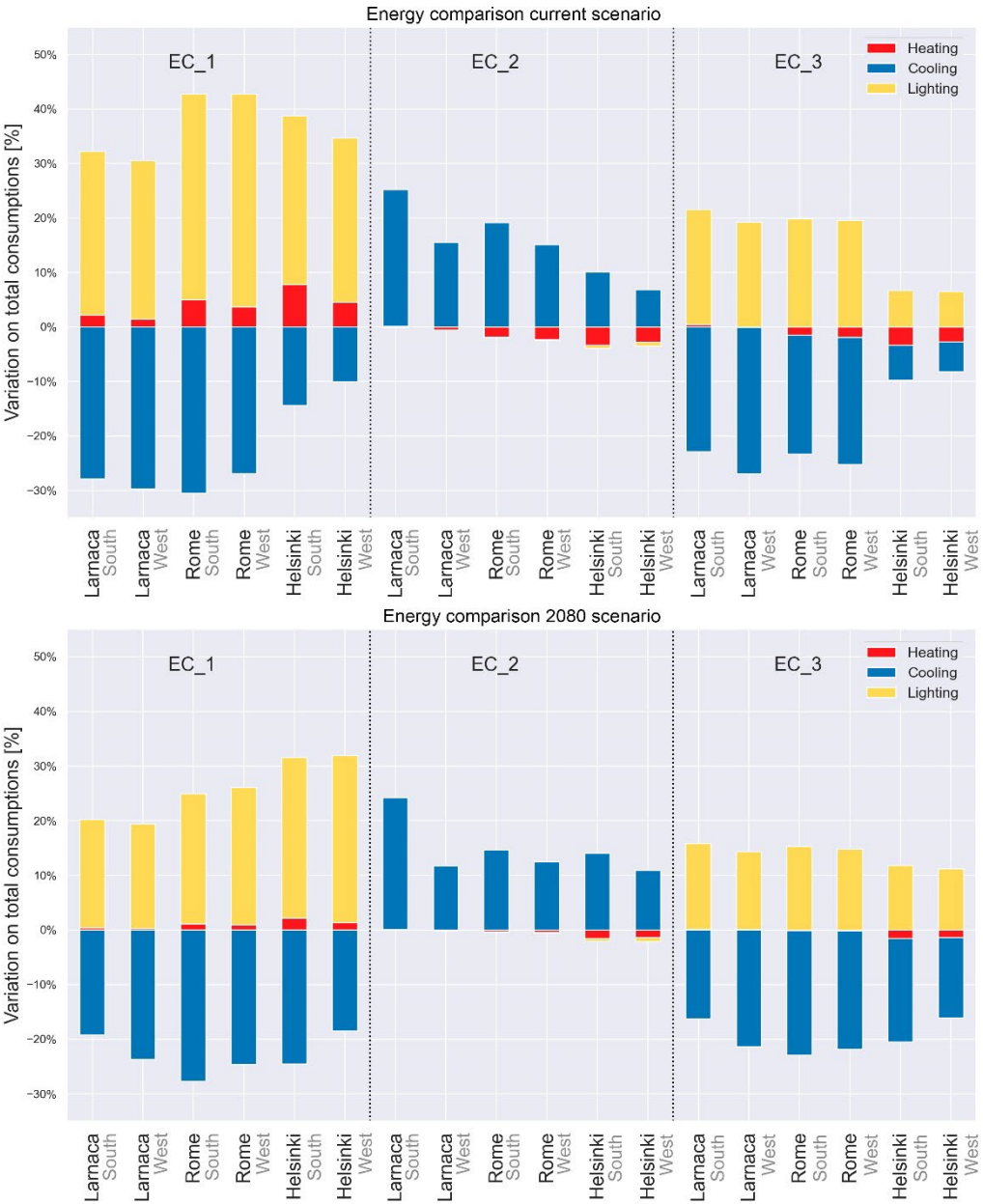


Figure 39. Total energy variation by source for the EC test case study in the current weather scenario (above) and 2080 scenario (below).

Table 10. Results obtained for the EC models.

Code	Total energy variation [%]	Exposure	City	Weather	Weather average	City Average
EC_1	4.3%	South	Larnaca	TMY	+3%	+0.5%
	0.8%	West	Larnaca	TMY		
	1.0%	South	Larnaca	2080	-2%	
	-4.3%	West	Larnaca	2080		
	12.2%	South	Rome	TMY	+14%	+6.7%
	15.8%	West	Rome	TMY		
	-2.8%	South	Rome	2080	-1%	
	1.5%	West	Rome	2080		
	24.3%	South	Helsinki	TMY	+24%	+17.4
	24.7%	West	Helsinki	TMY		
	7.0%	South	Helsinki	2080	+10%	
	13.4%	West	Helsinki	2080		
EC_2	25.1%	South	Larnaca	TMY	+20%	+19%
	14.9%	West	Larnaca	TMY		
	24.1%	South	Larnaca	2080	+18%	
	11.7%	West	Larnaca	2080		
	17.2%	South	Rome	TMY	+15%	+14%
	12.7%	West	Rome	TMY		
	14.2%	South	Rome	2080	13%	
	11.9%	West	Rome	2080		
	6.2%	South	Helsinki	TMY	+5%	+7.6%
	3.3%	West	Helsinki	TMY		
	12.0%	South	Helsinki	2080	+10%	
	8.8%	West	Helsinki	2080		
EC_3	-1.3%	South	Larnaca	TMY	-4%	-4.1%
	-7.7%	West	Larnaca	TMY		
	-0.5%	South	Larnaca	2080	-4%	
	-7.1%	West	Larnaca	2080		
	-3.5%	South	Rome	TMY	-5%	-5.9%
	-5.7%	West	Rome	TMY		
	-7.6%	South	Rome	2080	-7%	
	-7.0%	West	Rome	2080		
	-3.0%	South	Helsinki	TMY	-2%	-4.6%
	-1.8%	West	Helsinki	TMY		

-8.7%	South	Helsinki	2080	-7%
-4.9%	West	Helsinki	2080	

With regards to the “always off” control strategy (EC_2), the EC windows with this control strategy is always in its clear configuration, therefore the expected results should be diametrically opposed to the ones already described. As the window is always in the clear configuration – with a SHGC and VLT higher than those adopted in the reference model – the solar gains are higher in the responsive model rather than in the reference one during both summer and winter. It follows that the cooling consumptions are always higher in the responsive model while heating and lighting are lower. Clearly, this control strategy performs better in cold climates as it increases the cooling consumptions while reduces the heating and lighting demands. The results confirm this expected trend – opposite to the one described in the previous paragraphs – as the city average decreases from +19% in Larnaca, to +14% in Rome, up to +7.6% in Helsinki. Considering the weather scenarios, the expected trend in this case is an increase of the overall consumptions in the future scenario due to the overall increase in outdoor temperature. Nevertheless – with the exception of Helsinki where the variations grow from +5% in current scenario to +10% in 2080 – the average values are very similar in Larnaca (+20% and +18%) and Rome (+15% and +13%). This behaviour can be easily explained considering the different reference models used for these variations. As each weather scenario is compared to the reference model in the same scenario, the strong increase in cooling consumption in hot climates in future scenarios reduces the weight of the effect of the variation of the windows parameters resulting in a lower overall average. To confirm this hypothesis, both current and future results of the responsive model were compared to the reference model in the same scenario (current scenario). In this case, the results obtained confirmed the expected trend where the future scenarios are characterized by higher energy consumptions (+78% Larnaca, +77% Rome).

Finally, considering the EC_3 control strategy, a realistic behaviour of EC windows can be checked in these results. The graph clearly shows that in this case the envelope can

improve both heating and cooling consumptions while the lighting increase is an expected consequence of the dark state in summer mode. Reducing the consumptions in both summer and winter allows to reduce the overall consumptions in all the locations selected; therefore, this is the only control strategy that shows average negative energy variations in all the locations (-4.1% in Larnaca, -5.9% in Rome, -4.6% in Helsinki). Moreover, all the simulations conducted with this control strategy, leads to a reduction of the energy consumptions in the responsive models regardless of the exposure, locations, and climate scenario. This outcome confirms, on the one hand, the right modelling of the electrochromic system through the platform and, on the other hand, a proper choice of the activation threshold. Clearly, as already stated, the optimization of the activation thresholds is out of the scope of this testing activities and further analysis could probably improve these behaviours. However, regardless of the magnitude of the energy variations, the reduction of the energy consumptions in both current and future scenarios confirms that the responsiveness of this technology could be used to improve the resilience of buildings in future climate scenarios.

4.3.2 Phase Change Material: results

The PCMs are characterized by a different behaviour as they act mainly on the thermal inertia of the envelope rather than on the control of the solar radiation. Moreover, these materials can be classified among the intrinsically controlled technologies; hence, the platform cannot be stressed with extreme control strategies but can be tested considering the two available transition temperatures of the same commercial product. Therefore, the comparison is focused on products with similar properties but with transition temperature slightly different (23°C and 26°C) and different melting latent heat (300 kJ/m² and 330 kJ/m²). On the one hand, this choice leads to results pretty similar but, on the other hand, adding other commercial products with different properties (density, conductivity, specific heat) would have introduced too many variables that would have confused the results. Instead, this choice simplifies the comparison between the expected behaviour and the results obtained – which are described in figure 39 and table 11 – making the evaluation of the reliability of the platform more accurate.

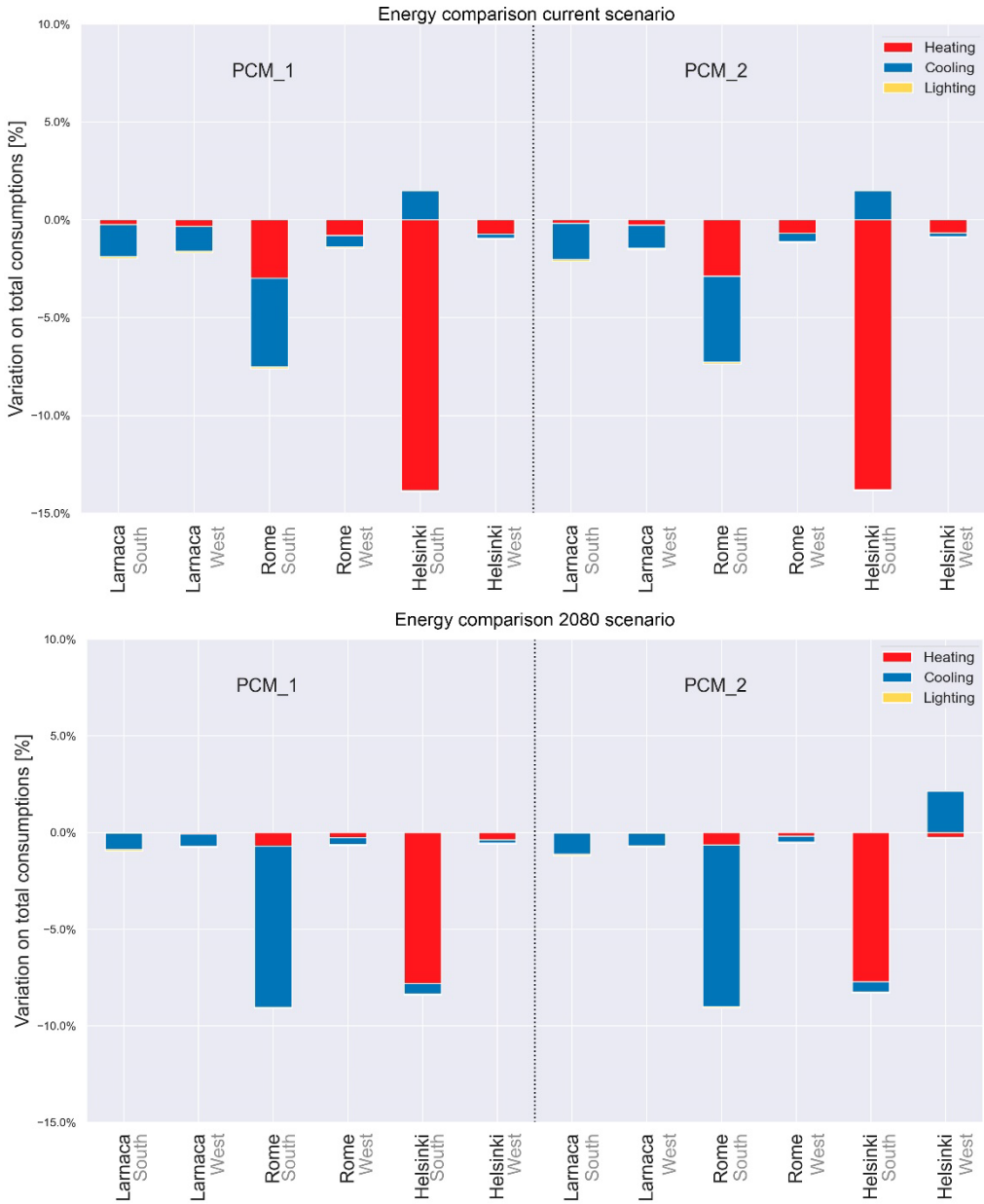


Figure 40. Total energy variation by source for the PCM test case study in the current weather scenario (above) and 2080 scenario (below).

Table 11. Results obtained for the PCM models.

Code	Total energy variation [%]	Exposure	City	Weather	Weather average	City Average	
PCM_1	-2.0%	South	Larnaca	TMY	-1.8%	-1.4%	
	-1.7%	West	Larnaca	TMY			
	-1.0%	South	Larnaca	2080	-0.9%		
	-0.8%	West	Larnaca	2080			
	-7.6%	South	Rome	TMY	-4.5%		-4.7%
	-1.5%	West	Rome	TMY			
	-9.1%	South	Rome	2080	-4.9%		
	-0.7%	West	Rome	2080			
	-12.4%	South	Helsinki	TMY	-6.7	-5.6%	
	-1%	West	Helsinki	TMY			
	-8.4%	South	Helsinki	2080	-4.5%		
	-0.6%	West	Helsinki	2080			
PCM_2	-2.1%	South	Larnaca	TMY	-1.8%		-1.4%
	-1.5%	West	Larnaca	TMY			
	-1.2%	South	Larnaca	2080	-1%		
	-0.8%	West	Larnaca	2080			
	-7.4%	South	Rome	TMY	-4.3%	-4.5%	
	-1.2%	West	Rome	TMY			
	-9.1%	South	Rome	2080	-4.8%		
	-0.6%	West	Rome	2080			
	-12.4%	South	Helsinki	TMY	-6.6%		-5.5%
	-0.9%	West	Helsinki	TMY			
	-8.3%	South	Helsinki	2080	-4.3%		
	+1.8%	West	Helsinki	2080			

The analysis of the results highlights a strong increase of the benefits mainly related to the heating consumptions. This result can be easily read looking at the total energy city average that increases from warmer to colder cities (-1.4% Larnaca, -4.7% Rome, -5.6% Helsinki for PCM_1 and -1.4%, -4.5%, and -5.5% for PCM_2) thanks to a strong rising reduction of the heating consumption. Despite the PCMs can help to reduce also the heating consumptions, the increase of the thermal inertia is mainly adopted as strategy to reduce the cooling consumption. This unexpected trend can be explained considering that the PCMs implementation in the responsive model is considered as an

additional layer to the original envelope of the reference model. Therefore, considering the low conductivity of the PCM plasterboards, the strong reduction of the heating consumption is partly due to the reduced thermal transmittance. To verify this hypothesis, additional simulations were run on the same model increasing the melting temperature to the unreal value of 100°C; in this way, the benefits of the phase change were excluded, and the remaining benefits were only related to the reduced thermal transmittance. The results obtained confirm the hypothesis that part of the benefits is related only to the additional insulation and not to the responsiveness of the envelope. For example, considering the simulation with the highest variation (Helsinki, South, TMY), the heating consumptions are: 2998 kWh for the responsive model, 3998 kWh for the reference model, and 3002 kWh for the fictitious static model. Similarly, in Rome the values obtained are 337 kWh for the responsive model, 545 kWh for the reference model, and 346 kWh for the fictitious static model. Cooling consumptions are also affected by this positive contribution of the low thermal transmittance of the additional layer, but in this case the contribution of the phase change is slightly more effective than in heating mode. For example, for southern exposure in Rome, the cooling consumptions ranges from 4835 kWh for the responsive model, to 5151 kWh for the reference model, to 4847 for the fictitious static model. Clearly, no differences can be found on lighting consumption as this technology acts only on thermal, rather than optical and solar, properties.

The differences between the two considered PCMs are limited as the materials are quite similar. However, the PCM_2 simulations show higher benefits in warmer climates (Larnaca) thanks to its higher melting temperature and latent heat while PCM_1 simulations show better results in colder climates (Rome and Helsinki) as it is easier to reach the lower melting temperature. The comparison between different climate scenarios is difficult due to the low variation percentage (lower than 4% on average), indeed the limited benefits of the PCMs implementation difficultly overcomes the strong consumption variation related to change of weather scenario. Hence, no specific trend can be highlighted with regards to this aspect. Finally, the last trend that can be highlighted from the simulations results regards the lower benefits of PCMs in western exposures.

In particular, the western façades reach lower surface temperatures that do not allow to reach of the PCM transition temperature reducing the thermal storage benefits.

4.3.3 *Dynamic shading: results*

The description of the results of dynamic shading simulations is slightly different from the previous ones as the platform provides three possible output comparisons. In particular, the energy consumptions of the responsive model are compared with the reference model without any shading, with the same model with a static shading corresponding to the dynamic system fixed in its ST1 configuration, and a static shading corresponding to the ST2 configuration. Hence, all the results are plotted and reported in tables according to this breakdown.

Comparison with reference model without shadings

The results obtained from the comparison with the unshaded model are summed up in figure 40. The expected trends should be similar to those described in the EC section as the activation criterion and the concept behind the systems – the solar radiation control – are the same. The main difference between EC and DS – in the comparison with an unshaded reference model – regards the “off” state. Indeed while the EC windows in its clear (off) state has SHGC and VLT higher than the reference model, in this case the folded origami (off) state can however shade the windows due to the presence of the folded surfaces of the shading.

The DS_1 control strategy, which corresponds to the shading system always in its closed (ST2) configuration, clearly shows always a reduction of the cooling consumption related to the reduced summer solar gains. On the other hand, this configuration increases the heating and lighting consumptions. As expected, the advantages (cooling reduction) of this strategy are lower moving from warmer to colder cities while the disadvantages (heating and lighting increases) are higher. This is perfectly described by the variation of the total energy demand that ranges from a minimum of -21.6% for the southern exposure in Larnaca in the current scenario up to a maximum of nearly +15.5% for the western façade in Helsinki in the same climate scenario. It follows that

the overall city average increases according to the location (-12.4% for Larnaca, -4.9% for Rome, +3.7% for Helsinki).

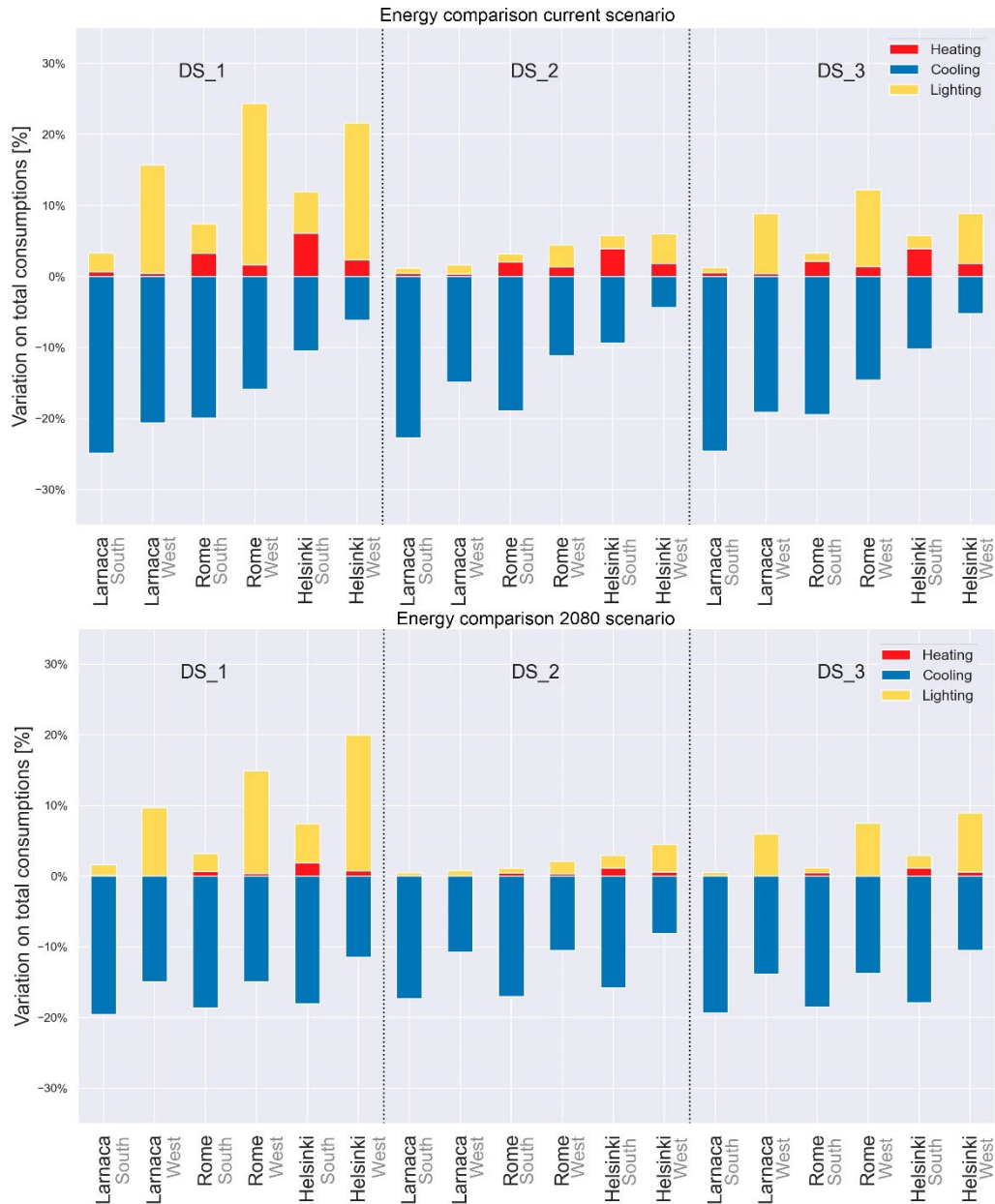


Figure 41. Total energy variation by source for the DS test case study in the current weather scenario (above) and 2080 scenario (below) compared with the reference model without any shading.

Table 12. Results obtained for the DS models compared with the unshaded reference model.

Code	Total energy variation [%]	Exposure	City	Weather	Weather average	City Average
DS_1	-21.6%	South	Larnaca	TMY	-13%	-12.4%
	-4.9%	West	Larnaca	TMY		
	-17.9%	South	Larnaca	2080	-12%	
	-5.3%	West	Larnaca	2080		
	-12.6%	South	Rome	TMY	-2%	-4.9%
	8.5%	West	Rome	TMY		
	-15.5%	South	Rome	2080	-8%	
	0.0%	West	Rome	2080		
	1.4%	South	Helsinki	TMY	8%	3.7%
	15.5%	West	Helsinki	TMY		
	-10.7%	South	Helsinki	2080	-1%	
	8.5%	West	Helsinki	2080		
DS_2	-21.5%	South	Larnaca	TMY	-17%	-15.4%
	-13.2%	West	Larnaca	TMY		
	-16.8%	South	Larnaca	2080	-13%	
	-10.0%	West	Larnaca	2080		
	-15.7%	South	Rome	TMY	-11%	-11.7%
	-6.7%	West	Rome	TMY		
	-15.9%	South	Rome	2080	-12%	
	-8.4%	West	Rome	2080		
	-3.6%	South	Helsinki	TMY	-1%	-4.6%
	1.7%	West	Helsinki	TMY		
	-12.9%	South	Helsinki	2080	-8%	
	-3.6%	West	Helsinki	2080		
DS_3	-23.3%	South	Larnaca	TMY	-17%	-15.1%
	-10.3%	West	Larnaca	TMY		
	-18.8%	South	Larnaca	2080	-13%	
	-7.9%	West	Larnaca	2080		
	-16.5%	South	Rome	TMY	-9%	-10.5%
	-2.4%	West	Rome	TMY		
	-17.3%	South	Rome	2080	-12%	
	-5.9%	West	Rome	2080		
	-4.4%	South	Helsinki	TMY	0%	-4.3%
	3.7%	West	Helsinki	TMY		

-14.9%	South	Helsinki	2080	-13%
-1.5%	West	Helsinki	2080	

Moreover, the graph clearly shows significant differences between western and southern exposures. These differences are greater than those reported in the EC models, because in the DS models the different solar beam angle changes significantly the shades casted on the windows while when EC windows are on their dark state all the windows are “shaded” homogeneously.

As already explained, this control strategy performs better in hot climates rather than in colder ones. Therefore, with regards to the weather scenario, the expected result is a reduction of the energy consumption in the 2080 projection which is overall warmer than the current weather scenario. This trend is confirmed by the results reported in table 11 where the 2080 projection shows total average consumptions lower than those obtained in the current scenario. The only exception is represented by Larnaca where the average differences between current and future averages are very similar (-13% and -12%). The explanation is the same described in the EC subsection and it is due to a different weight of the effect of the responsive technology on the overall energy consumption of the reference model.

Moving to the second activation criterion analysed, the results obtained are in line with those expected for an “always off” control strategy. In particular, according to the extreme activation thresholds selected, the shading system is always folded and hence it is always in its ST1 configuration. As already mentioned, despite the ST1 configuration minimizes the shadows on the windows, it casts however more shadows than the reference model without any shading. It follows that also in this case the trends are similar to those described for the DS_1 control strategy while in the EC models they were diametrically opposed. Moreover, the reduced shading area allows to minimize heating and lighting consumptions with respect to the DS_1 strategy. Hence, the average total energy variation is lower in this case and is gradually lower in colder climates ranging from -15.4% for Larnaca, to -11.7% for Rome, up to -4.6% for Helsinki. This result is reasonable as this control strategy applied to this specific shading system and

compared to an unshaded reference model tends to prioritise the cooling behaviour, as opposed to the same strategy applied to an EC window.

Finally, looking at the third control strategy, the trends are something in between the DS_2 and DS_1 control strategies. The only difference regards the magnitude of the total energy variation which is, on average, slightly higher than the DS_2 case but significantly lower than the DS_1. Comparing DS_2 and DS_3, the lighting consumption in the western zones – which are in between the DS_1 and DS_2 consumptions – reduces the overall benefits of this technology while the southern zones show the lowest energy consumption thanks to a reduced cooling demand. The results obtained are reliable and highlights only a non-optimized activation threshold for the western exposure. The best way to minimize the energy consumption in this case could be changing the control strategy on the western façade moving to an “always off” activation criterion similar to the one adopted in the DS_2. However, as already explained, the focus of this simulations is only to check the reliability of the results and not to minimize the energy consumption. Also in this case, the city average is higher in warmer locations (-15.1% for Larnaca, -10.5% for Rome, -4.3% for Helsinki) thanks to the strong impact of this technology on the control of the solar radiation. Finally, all the considerations done for the DS_2 control strategy can be considered right also for the DS_3 as both trend and magnitude are extremely similar.

Comparison with reference model with static ST1 shading

Changing the reference model used as comparison term can clearly change the results and its interpretation. Providing the comparison with the static shading corresponding to the intermediate state of the dynamic system allows to better interpret the responsiveness modelled and simulated by the platform.

For example, looking at the DS_1 results shown in figure 41, the cooling consumption in the dynamic model – which is always in the ST2 configuration with this control strategy – are lower than their respective in the ST1 reference model even if the magnitude of the reduction is lower than the one obtained comparing the dynamic and the unshaded model.

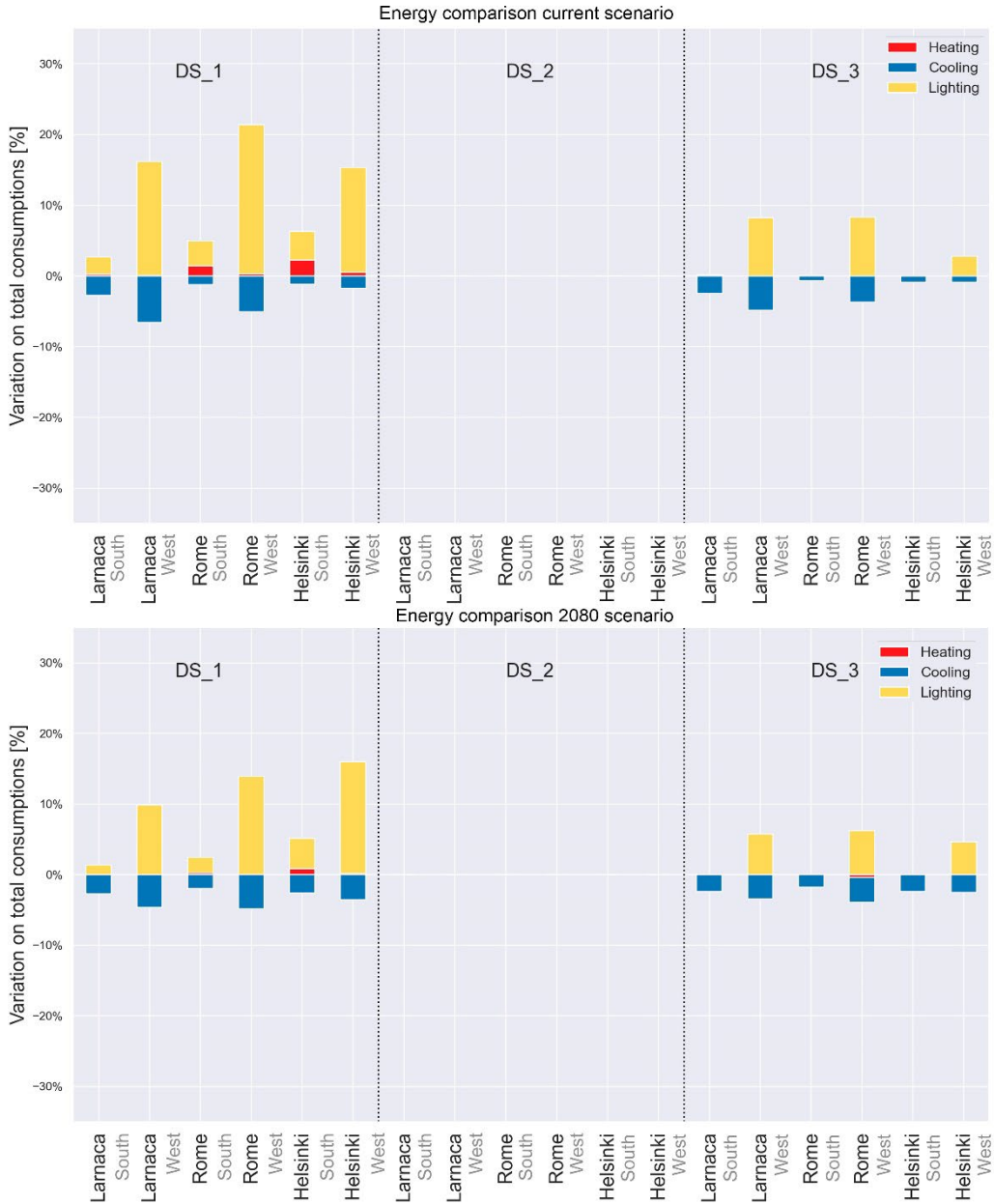


Figure 42. Total energy variation by source for the DS test case study in the current weather scenario (above) and 2080 scenario (below) compared with the reference model with a static ST1 shading.

Table 13. Results obtained for the DS models compared with the static ST1 shading.

Code	Total energy variation [%]	Exposure	City	Weather	Weather average	City Average
DS_1	0.0%	South	Larnaca	TMY	+4.8%	+3.4%
	9.6%	West	Larnaca	TMY		
	-1.3%	South	Larnaca	2080	+2%	
	5.2%	West	Larnaca	2080		
	3.8%	South	Rome	TMY	+10%	+7.4%
	16.3%	West	Rome	TMY		
	0.5%	South	Rome	2080	+4.8%	
	9.1%	West	Rome	2080		
	5.2%	South	Helsinki	TMY	+9.4%	+8.5%
	13.6%	West	Helsinki	TMY		
	2.5%	South	Helsinki	2080	+7.5%	
	12.5%	West	Helsinki	2080		
DS_2	0.0%	South	Larnaca	TMY	0.0%	0.0%
	0.0%	West	Larnaca	TMY		
	0.0%	South	Larnaca	2080	0.0%	
	0.0%	West	Larnaca	2080		
	0.0%	South	Rome	TMY	0.0%	0.0%
	0.0%	West	Rome	TMY		
	0.0%	South	Rome	2080	0.0%	
	0.0%	West	Rome	2080		
	0.0%	South	Helsinki	TMY	0.0%	0.0%
	0.0%	West	Helsinki	TMY		
	0.0%	South	Helsinki	2080	0.0%	
	0.0%	West	Helsinki	2080		
DS_3	-2.3%	South	Larnaca	TMY	+0.6%	+0.3%
	3.4%	West	Larnaca	TMY		
	-2.4%	South	Larnaca	2080	0%	
	2.3%	West	Larnaca	2080		
	-1.0%	South	Rome	TMY	+1.8%	+1.2%
	4.7%	West	Rome	TMY		
	-1.7%	South	Rome	2080	+0.5%	
	2.7%	West	Rome	2080		
-0.8%	South	Helsinki	TMY	+0.6%	+0.2%	
2.0%	West	Helsinki	TMY			

-2.4%	South	Helsinki	2080	-0.1%
2.1%	West	Helsinki	2080	

This result is reasonable because both the static ST1 reference model and the dynamic model reduce the incoming solar radiation compared to the unshaded model. Nevertheless, the dynamic model can furtherly reduce the solar radiation adopting the ST2 shading configuration (which is always on in the DS_1 control strategy). Clearly, having a highly shaded configuration during the whole year leads to increases in heating and lighting consumptions that largely overcome the cooling benefits. In this cooling-oriented control strategy colder locations are penalised as described in table 13; in particular, the average energy variation increases from +3.4% in Larnaca, to +7.4% in Rome, to +8.5% in Helsinki. For the same reason, the effect of the climate change combined with this control strategy reduces the energy variation which is always lower in the 2080 projection compared to the current scenario.

As already explained, the DS_2 is an “always off” control strategy; hence, the responsive model is always in its less shading configuration (ST1). It follows that the reference model and the responsive model should be exactly the same. The results obtained confirms this hypothesis as all the differences obtained comparing the two models are 0. Moving to the DS_3 control strategy, the results obtained confirms the proper modelling of the responsiveness of the façade, similarly to what already described in the previous subsection for the unshaded model. Indeed, all the southern exposures show a reduction of the overall energy consumption if compared con both DS_1 and DS_2 strategies; on the contrary, the western exposures show values lower than the DS_1 but higher than the DS_2. As already stated, this is simply an effect of the non-optimized thresholds as the shading effect on a western façade is higher due to the lower position of the sun. Therefore, simply increasing the activation threshold for the western façade in the DS_3 strategy would improve the energy behaviour making this strategy the most performing.

Comparison with reference model with static ST2 shading

Finally, the results obtained for the dynamic model were compared with the static ST2 reference model and figure 42 and table 14 describe the comparison outcomes. Contrary to the comparison with the ST1 reference model, in this case the dynamic model can take on less-shaded configurations, increasing the incoming solar radiation. It follows that the expected behaviour is opposite to the one described in the previous subsection as, compared to the ST2 reference model, the dynamic model should reduce the lighting and heating consumptions increasing the cooling consumption.

Clearly, the DS_1 control strategy forces the shading always in its “on” configuration, hence it is always in the ST2 state. Therefore, similarly to what described for the DS_2 in the previous ST1 reference model, the DS_1 control strategy does not show any difference with the reference model as both are always in the ST2 configuration. In reality, very slight differences (lower than 0.1%) can be found but are simply related to the approximations adopted during the data elaboration rather than to real energy differences.

The DS_2 control forces the shading in its “off” configuration during the whole simulation; therefore, the comparison with the reference model corresponds to a comparison between a ST1 model (the responsive model) and the ST2 model (the reference model). It follows that the comparison is the same conducted in the previous subsection – with inverted terms – for the DS_1 control strategy (in this case the ST1 was the reference and the ST2 was the responsive model) hence the results should be equal in magnitude and opposite in sign. The results obtained confirm the expectations with very small differences which are related to data approximation and to minor differences (singularly lower than 2% and lower than 0.6% on average) regarding mainly the western exposures. Clearly, all the simulations and comparison can be affected by minor errors which can be due to slight geometric differences between the models or to data approximations; these errors are higher in the western exposure because – as already stated – the shading effect is higher on these façades due to the lower solar height that increases the casted shadow on the windows.

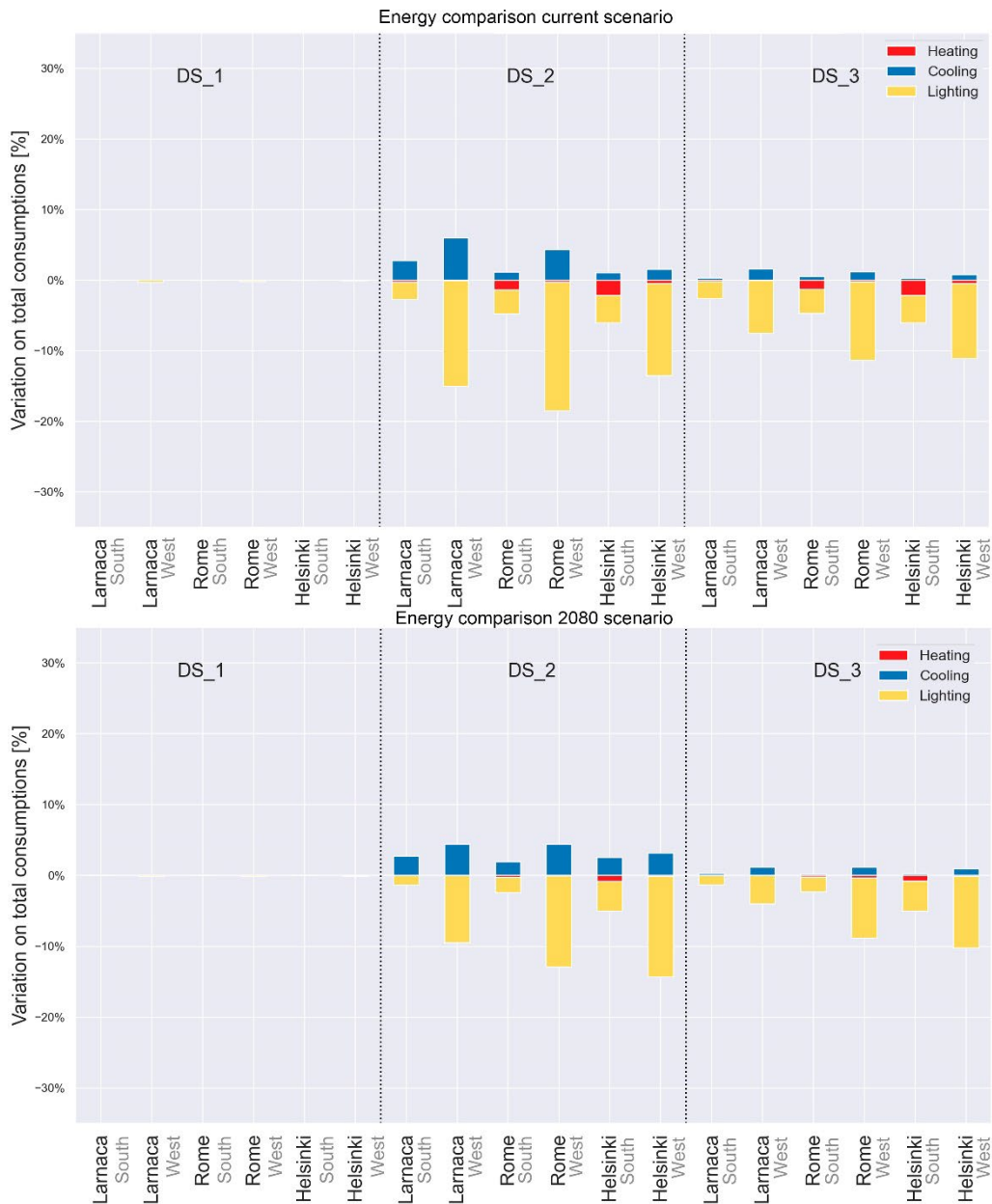


Figure 43. Total energy variation by source for the DS test case study in the current weather scenario (above) and 2080 scenario (below) compared with the reference model with a static ST2 shading.

Table 14. Results obtained for the DS models compared with the static ST2 shading.

Code	Total energy variation [%]	Exposure	City	Weather	Weather average	City Average
DS_1	0.0%	South	Larnaca	TMY	-0.1%	-0.1%
	-0.3%	West	Larnaca	TMY		
	0.0%	South	Larnaca	2080		
	-0.1%	West	Larnaca	2080		
	0.0%	South	Rome	TMY	-0.1%	-0.1%
	-0.1%	West	Rome	TMY		
	0.0%	South	Rome	2080		
	-0.2%	West	Rome	2080		
	0.0%	South	Helsinki	TMY	0.0%	0.0%
	-0.1%	West	Helsinki	TMY		
	0.0%	South	Helsinki	2080		
	-0.1%	West	Helsinki	2080		
DS_2	0.0%	South	Larnaca	TMY	-4.5%	-3.2%
	-9.0%	West	Larnaca	TMY		
	1.3%	South	Larnaca	2080		
	-5.1%	West	Larnaca	2080		
	-3.6%	South	Rome	TMY	-8.9%	-6.7%
	-14.2%	West	Rome	TMY		
	-0.5%	South	Rome	2080		
	-8.5%	West	Rome	2080		
	-5.0%	South	Helsinki	TMY	-8.5%	-7.7%
	-12.0%	West	Helsinki	TMY		
	-2.5%	South	Helsinki	2080		
	-11.2%	West	Helsinki	2080		
DS_3	-2.3%	South	Larnaca	TMY	-4.1%	-3.0%
	-5.9%	West	Larnaca	TMY		
	-1.1%	South	Larnaca	2080		
	-2.9%	West	Larnaca	2080		
	-4.6%	South	Rome	TMY	-7.4%	-5.7%
	-10.2%	West	Rome	TMY		
	-2.2%	South	Rome	2080		
	-6.0%	West	Rome	2080		
	-5.7%	South	Helsinki	TMY	-8.0%	-7.5%
	-10.3%	West	Helsinki	TMY		

-4.8%	South	Helsinki	2080	-0.1%
-9.3%	West	Helsinki	2080	

However, also the results obtained for the DS_2 control strategy can be considered reliable and in line with the responsive behaviour of the shading system.

Finally, the DS_3 control strategy compares a realistic responsive shading system with a fixed shading system in the ST2 configuration. The responsive model can switch to a less shading configuration when the outdoor temperature and the solar radiation are below the thresholds. Hence, the expected results are a decrease of the lighting and heating consumptions during winter and a slight increase of the cooling consumption during summer, the latter mainly due to non-optimized thresholds. Figure 42 confirms this reliable trend as the responsive model requires less energy compared to the reference mainly thanks to a strong reduction of the lighting demand. The advantage of this control strategy compared to the ST2 reference model grows in colder climates ranging from -3% for Larnaca, to -5.7% for Rome, up to -7.5% for Helsinki. In colder climates, the number of activation timesteps is clearly lower hence the shading stays longer in its ST1 configuration that allows higher natural lighting; moreover, in this case colder climates means also higher latitude hence the benefits on the artificial lighting demand are amplified by the lower solar height and its higher lighting penetration.

Looking at the different climate scenarios, the increase in outdoor temperature related to the climate change increases the activation timesteps reducing the differences between the responsive and reference model. Indeed, the benefits of the responsive systems in the current scenarios are always higher than the corresponding ones in future scenarios. Finally, considering the different exposures, as already stated, the western exposures amplify the shading effects; hence, in this case the benefits are higher thanks to a stronger lighting reduction that leads to an average total energy variation of -3.5% for southern zones and -7.4% for western zones.

To sum up, all the results obtained can be considered consistent with the expected energy behaviour. Specifically, only 3 simulations were affected by slight differences in energy reduction magnitude (however lower than 2%) while all the expected energy

trends were confirmed. Moreover, the responsiveness of the technology proposed can nearly always improve the energy behaviour of the building and the only exceptions are related to the choice of the activation thresholds. Indeed, optimizing the thresholds and using different values for different exposures could have furtherly increased the benefits of these systems. However, as already stated, the aim of this phase was to stress and test the platform under extreme and realistic conditions rather than optimizing the energy behaviour; hence, according to the results shown, the primary goal of this section can be considered achieved.

4.4 Limitations and future developments

The testing phase showed the reliability and usefulness of the platform, that allowed – in few hours – to run and compare nearly 100 simulations of different complex responsive systems in different contexts in a standardized and comparable way. The main strength of this tool is clearly the simplification of the modelling and simulation phases and the above-described applications confirmed the achievement of the set goals. Nevertheless, the platform in its current form is characterized by some limitations that should be considered before adopting this tool. It is worth highlighting that the main aim of this first version was to develop and test the structure of the platform rather than providing already a complete tool. Indeed, the nature of the platform allows continuous and easy implementations that create an always evolving tool. Therefore, most of the following reported limitations are not structural limitations but are simply referred to the current state of the platform and it follows that most of them can be easily implemented in the future versions.

Firstly, at the moment, the users can run only energy analyses through the platform and the improvement and the analyses of the comfort can be conducted only indirectly through the selection of few activation strategies – e.g., glare control, illuminance control, indoor air temperature control, etc – in the electrochromic module. The comfort analysis is another broad and complex theme to discuss and develop, therefore it is not included in this platform. Probably, the best way to study this topic in the future development is to create another specific Grasshopper script – based on the same concepts – where all the inputs and outputs are optimized for the comfort analyses otherwise merging everything in a single script would lead to a confusing input/output manager that could reduce the user-friendliness and the speed of the modelling phase.

Furthermore, at the moment, the platform includes only one office reference model. Undoubtedly, despite the office models are the most widely used in this kind of analyses, adding further models in the future developments of the tool can increase the usefulness and the number of users.

Another interesting and easy to implement module, can be the modelling of the urban context which is currently not considered in this first version. The development of this

module can be easily done through the Rhinoceros modelling interface, similarly to the already explained geometrical modelling of the dynamic shadings. Hence, the code should simply read the coordinates of the modelled geometries and write them in the idf file as already explained.

With regards to the dynamic shadings, as already described in the validation study [40], with the current Python workaround the activation criteria must be based on variables that are not influenced by the simulation history (e.g., illuminance, outdoor temperature, solar radiation etc.). Currently, it is not possible to link the activation of the shading system with endogenous variables such as the indoor temperature, but future studies can implement this feature considering the convergence of predicted and measured indoor temperature profiles in an iterative simulation loop as proposed in the validation study [40].

The only limitation that could be considered “structural” regards the modelling of specific buildings. This limitation can be considered partially out of the scope of this study as the main concept of the platform is to provide a tool to compare different technologies in a standardized environment. Therefore, changing the reference model means losing part of this comparability which is not suggested for the technologies’ comparison. Nevertheless, changing part of the code behind the platform, external models could be implemented inside the platform. In the author’s opinion this should be another kind of tool, which can be clearly inspired by this platform as the functioning of the interface and data management is the same. For example, in this new platform, the user could provide an idf where thermal zones and envelope properties are codified in a standardized way; hence, the platform can easily and automatically create the set of models for the different locations changing the envelope properties according to the locations. Then the simulation and output management codes of the original platform can be used in this new tool. Clearly, this is simply one of the possible alternatives to this platform which has been designed – as already explained in previous sections – for both non-expert and expert users; the latter can start from this tool to develop their own platform according to their specific need.

Finally, the testing phase highlighted few repeated simulations when multiple analyses are conducted. Despite this is not considered a limitation but simply an optimization, a future development could include the use of a list of simulations as input to avoid the repetition of the same simulations in complex studies reducing the overall simulation time. Furthermore, the analysis of the PCM simulations highlighted a kind of “interference” of the insulation effect of the additional PCMs layers. This choice can be considered proper if the platform is used to assess the benefits of a retrofit intervention using PCMs, instead could make difficult the comparison in case of evaluation on new buildings. However, as stated and demonstrated in the previous section, the current platform can analyse the differences related to this extra insulation effect simply changing the melting temperature of the PCM with a fictitious very high melting temperature to consider only the insulation excluding the effect of the phase change. To ease the use of the platform, future developments could allow to choose between two different reference models. The first one – already implemented in the platform – could be used for retrofitting evaluation and consider the PCM as an additional layer, the second one could be used to compare the PCM model with a reference model equipped with an additional traditional plasterboard with the same thickness of the additional PCM layers. Clearly, if the user adopts this second reference model, it cannot be compared with other technologies due to differences in the envelope stratigraphy.

Finally, as already described in the previous sections, the DOE reference model are still updated to September 2012 and despite the internal loads update conducted in this study, the creation and the use of a new specific reference model could be an interesting future development to increase the reliability of the results and the spread of this tool. Furthermore, regarding the future scenarios, the use of CCWorldWeatherGenerator to develop the future weather files lead to the adoption of a single GCM output and the use of an outdated emission scenario which could be considered a limitation for this study. Nevertheless, as already mentioned, this tool is still the most used in the building research field and the differences with other more sophisticated or up to dated software are still negligible.

To sum up, the current version of the platform can be considered a complete methodological basis for future developments. Despite the platform is already complete and functioning, additional modules or extra features could be easily implemented – thanks to its modular and open-source structure – to broaden the scope of the tool.

5. CONCLUSIONS

The main concept behind this thesis is strictly related to the current awareness that the human induced climate change has increased and is still increasing frequency and magnitude of temperature anomalies and extreme adverse weather events. The strong impact of the building sector on the global climate-altering emissions makes this research field particularly significant and interesting to mitigate the negative effects of the human activities on climate and ecosystems. Despite the recent commitments of the main world Countries to improve the buildings energy efficiency, currently we can only mitigate the effects and reduce the damages of the climate change, but we cannot completely avoid them in the near future. These assumptions increase the importance to furtherly improve the energy efficiency evaluating new design strategies.

Among these possible strategies, this research is focused on responsive technologies for envelope design. Responsive technologies can react to external stimuli changing their properties – thermal, geometric, solar, etc. – managing the transfer and storage of heat, light, water, and/or air. Originally the responsiveness of these technologies was adopted to accommodate the short/mid-term environmental variations (sub hourly, hourly, daily, seasonally). Nevertheless, considering the buildings lifespans and the climate change effects, the operational boundary conditions of an envelope designed today – usually referred to historical weather data – will be probably different from the ones we considered in the designing phase. Therefore, the responsiveness of these systems could be also useful to improve the energy behaviour of buildings during their whole lifespans implementing a reactivity to long-term (decades) climate variations. The introduction of these innovative technologies adds a new complexity layer to the building physics phenomena because the envelope is no longer conceived simply as a shield between the interior and exterior environment, but it is an interface that can change and adapt itself according to specific boundary conditions. Shifting from a static traditional envelope to a dynamic system multiplies the complexities also in the building performance simulation field. In the traditional approach the main variable was the variation of the external environment – already defined in the weather file – and the simulation was simply the continuous energy balance of the thermal zones according to the

static envelope properties. On the contrary, responsive technologies continuously change the envelope properties according to certain internal or external variables – e.g., indoor/outdoor temperature, solar radiation, surface temperature, etc. – and this behaviour requires specific modelling approaches or workarounds. These approaches can be more or less achievable depending on the users' background as many of them require programming codes – internal or external to the simulation software, depending on the complexity of the systems – to properly model the responsive systems.

The main aim of this research is to provide the right tools to study and understand the behaviour of responsive technologies in different locations and different climate scenarios to improve the energy resilience of buildings. The tool developed is an interactive computational platform that allows, on the one hand, to simulate the behaviour of responsive envelopes and compare them with traditional static systems and, on the other hand, allows to understand the potentials of these systems also in the long-term adaptation to the climate change effects. The core of the platform is constituted by EnergyPlus, used as simulation engine, and Python used for input/output management and for launching the simulations while the user interface is realized in Grasshopper. Thanks to this structure, the users can simply download the platform on their computer and open the Grasshopper script to access to all the features of the platform. Hence the users can simply manage the general inputs from four main drop-down lists: locations (25 European cities), weather files (current, 2050, 2080), and responsive technologies (electrochromic, dynamic shading, phase change materials). Then, specific inputs such as control strategies, activation thresholds can be set simply using sliders and drop-down lists in the specific Grasshopper technology module. Once all the required inputs are provided, the simulations can be run simply activating a Boolean toggle and the platform directly provides a standardized comparison sheet where the selected responsive technology is compared with a traditional static one. Moreover, the main energy consumption outputs are provided as float numerical panels to allow further analyses, optimizations, and comparisons directly in Grasshopper. Similarly, in the platform folder all the complete simulation outputs, based on more detailed reporting frequencies, can be easily accessed for further analyses.

This structure allows the use of the platform for both expert and non-expert users in different ways. For example, non-expert users have limited access to the core modules of the platform to avoid modelling mistakes. Indeed, the platform provides different modules – validated through specific studies published in last years – which are considered as a black box for non-expert users. Nevertheless, expert users can easily access to the source code and modify them according to their specific needs or can expand the platform with additional modules for new technologies. Therefore, the structure of the platform itself allows further developments and collaborative approaches to consider new technologies or further customization of the energy models for more detailed analyses.

The testing phase conducted highlighted that all the results are compatible with the expected trends. Therefore, the developed platform allows – with few limitations described in the dedicated section – to easily model and run a huge number of simulations in limited time with reliable results. Moreover, using the platform during the testing phase confirmed that the main advantage relies undoubtedly in its easiness and speed. Furthermore, it allows to model and manage also complex algorithms – such as the one for the dynamic shadings – without any specific programming knowledge. This latter advantage can undoubtedly widen the catchment area of this platform improving the spread of this research field.

Moreover, despite the testing phase was mainly a validation tool, it can also provide the first indications regarding the evaluation of the selected technologies. Firstly, the main result is the definition of the central role of the control strategy in extrinsically controlled systems. For example, the energy variation of the model equipped with EC systems can vary from +24% to -7% depending on the control strategy. Secondly, the PCMs seems to be little affected by the variation of the melting temperature in the considered range (23-26°C). Further specific comparisons on these technologies have been voluntarily avoided in this research as the case studies were considered mainly as a validation of the platform and, hence, no detailed optimization on the control strategies were conducted.

To sum up, starting from the analyses of the current status of the responsive envelope design and from the current awareness of climate change and future resilience of buildings, this research developed a new tool for researchers and practitioners for a first preliminary analysis of the responsive technologies in different locations and in different climate scenarios. The aim of this tool is to ease and speed up the energy modelling of complex energy phenomena to facilitate the analyses and the comparisons of these technologies in different contexts. While from a technological point of view many studies are analysing these systems, their energy analyses are getting behind. Without having reliable energy tools for studying these devices, they are too often not considered as viable alternatives. The evolution and the spread of this tool can hopefully bridge this gap improving the spread of the responsive technologies in the envelope design field which are currently still not widespread and this is a missed opportunity to innovate and improve our buildings' resilience, energy efficiency, and design strategies.

6. ACKNOWLEDGEMENTS

I would like to gratefully acknowledge my supervisors Prof. Francesco Fiorito and Prof. Guido Raffaele Dell'Osso for the advices and for the opportunity to develop this challenging research always in a stimulating environment despite all the difficulties related to the Covid pandemic.

Many of the topic of this research were developed in collaboration with other important Universities that I gratefully acknowledge for the opportunity of visiting new Countries, new institutions, and for the new perspectives that they gave to my research. In particular, I would like to thank Prof. Roel Loonen and Prof. Jan Hensen for the fruitful period spent at the Eindhoven University of Technology (TU/e). Thanks to their contributions, we developed a fundamental module to simulate the dynamic shading devices within the computational platform. I would like to thank also Prof. Kristoffer Negendahl from the Technical University of Denmark (DTU) and Jakob Strømmand-Andersen from Henning Larsen for the inspiring period spent in Copenhagen to analyse and define future scenarios to evaluate energy flexibility of buildings.

I would also like to reserve special thanks to all my colleagues and in particular to Stelladriana Volpe, Ludovica Maria Campagna, and Valentino Sangiorgio for the support, chats, and collaborations we had together.

Finally, I would like to acknowledge Rossella who supported all my choices during these three years.

7. LIST OF ABBREVIATIONS

AKE	Acclimated Kinetic Envelope	DSF	Dynamic Shading File
AR	Assessment Report	DSF	Dynamic Shading
ASHRAE	American Society of Heating, Refrigerating and Air-Conditioning Engineers	EC	Electrochromic
c	Specific Heat	ECBCS	- Energy Conservation in Buildings and Community Systems Programme
CABS	Climate Adaptive Building Shells	EDSM	Equivalent Dynamic Shading
CDD18°	Cooling Degree Days referred to 18°C	EER	Energy Efficiency Ratio
CEC	Conventional Electrochromic	EMS	Energy Management System
cL	Specific Heat in liquid state	EPW	Energy Plus Weather
ConFD	Conduction Finite Difference	ESSM	Equivalent Static Shading Models
COP	Coefficient of Performance	fm	Fraction melted
cS	specific Heat in the solid state	GC	Gasochromic
CTF	Conduction Transfer Function	GCM	Global Climate Models
CVRMSE	Cumulative Variation of Root Mean Squared Error	Gf	incident facade irradiance
DOE	Department of Energy	GHG	GreenHouse Gas
DGU	Double Glazing Unit	H	Total Enthalpy

h	Enthalpy per unit mass	PTFE	Polytetrafluoroethylene
HDD_{18°}	Heating Degree Days referred to 18°C	PV	Photovoltaic
HS	Harmonized scenario	PVC	PhotoVoltaChromic
HVAC	Heating Ventilation and Air Conditioning	Q	Heat
IDF	Input Data File	Q_{mel}	Melting latent heat
IEA	International Energy Agency	RBE	Responsive Building Element
IEQ	Indoor Environmental Quality	RCM	Regional Climate Model
ITO	tin doped indium oxide	RCP	Representative Concentration Pathways
LHS	latent heat storage	s	Thickness
LSPR	localized surface plasmon resonance	SHGC	Solar Heat Gain Coefficient
m	Mass	SHS	sensible heat storage
MBE	Mean Bias Error	SMA	Shape Memory Alloy
Mtoe	Million tonnes of oil equivalent	SMH	Shape Memory Hybrids
NEC	Near Infrared Radiation switching electrochromic	SMP	Shape Memory Polymers
NIR	Near Infrared Radiation	SSF	Static Shading Files
OS	Overshoot Scenario	SSM	Static Shading Model
PC	Photochromic	SSP	Shared Socio-Economic Pathways
PCM	Phase Change Material	ST	State 1/2/3
PEC	PhotoElectroChromic	1/2/3	
PIP	Pip Installs Packages	T	Temperature
		t	time

TC	Thermochromic
T_m	Melting temperature
TMY	Typical Meteorological Year
T_o	Outdoor Temperature
VAV	Variable Air Volume
VL	Visible Light
VLT	Visible Light Transmittance
λ	Conductivity
ρ	Density

8. REFERENCES/BIBLIOGRAFIA

1. IPCC *Climate Change 2014: Final Report - Chapter 9. Mitigation of Climate Change Working Group III Contribution to the Fifth Assessment Report of the Intergovernmental Panel on Climate Change*; 2014;
2. IEA *World Energy Outlook 2016*; 2016;
3. Rousselot Marie; Pollier, K. *Energy Efficiency Trend in Buildings*; 2018;
4. Progress on Energy Efficiency in Europe — European Environment Agency Available online: <https://www.eea.europa.eu/data-and-maps/indicators/progress-on-energy-efficiency-in-europe-3/assessment> (accessed on 9 January 2023).
5. U.S. Energy Information Administration *August 2020 Monthly Energy Review*; 2020;
6. U.S. Department of Energy 2011 Buildings Energy Data Book. *Office of Energy Efficiency and Renewable Energy 2012*.
7. Cao, X.; Dai, X.; Liu, J. Building Energy-Consumption Status Worldwide and the State-of-the-Art Technologies for Zero-Energy Buildings during the Past Decade. *Energy Build* **2016**, *128*, 198–213, doi:10.1016/j.enbuild.2016.06.089.
8. United Nations General Assembly *Transforming Our World: The 2030 Agenda for Sustainable Development*; 2015;
9. United Nations *The Paris Agreement*; 2015;
10. United Nations *COP26 The Glasgow Climate Pact*; 2021;
11. EU Parliament *Directive (EU) 2018/844 of the European Parliament and of the Council of 30 May 2018 Amending Directive 2010/31/EU on the Energy Performance of Buildings and Directive 2012/27/EU on Energy Efficiency*; 2018;
12. Council of the European Union Directive 2010/31/EU of the European Parliament and of the Council of 19 May 2010 on the Energy Performance of Buildings. *Official Journal of the European Union*.
13. European Commission Proposal for a Directive of the European Parliament and of the Council on the Energy Performance of Buildings. **2021**.
14. Buildings – Analysis - IEA Available online: <https://www.iea.org/reports/buildings> (accessed on 11 January 2023).
15. Tracking Buildings 2021 – Analysis - IEA Available online: <https://www.iea.org/reports/tracking-buildings-2021> (accessed on 7 March 2022).

16. H.-O. Pörtner, D.C. Roberts, E.S. Poloczanska, K. Mintenbeck, M.T.; A. Alegría, M. Craig, S. Langsdorf, S. Löschke, V. Möller, A.O. *IPCC, 2022: Summary for Policymakers*; 2022;
17. Portner, H.-O.; Roberts, D.C. *Climate Change 2022: Impacts, Adaptation and Vulnerability Working Group II Contribution to the Sixth Assessment Report of the Intergovernmental Panel on Climate Change*; Cambridge, 2022;
18. Eight Warmest Years on Record Witness Upsurge in Climate Change Impacts | World Meteorological Organization Available online: <https://public.wmo.int/en/media/press-release/eight-warmest-years-record-witness-upsurge-climate-change-impacts> (accessed on 11 January 2023).
19. Campagna, L.M.; Fiorito, F. On the Impact of Climate Change on Building Energy Consumptions: A Meta-Analysis. *Energies* 2022, *Vol. 15*, Page 354 **2022**, *15*, 354, doi:10.3390/EN15010354.
20. Energy Agency, I. Review 2021 Assessing the Effects of Economic Recoveries on Global Energy Demand and CO 2 Emissions in 2021 Global Energy. **2021**.
21. Building Envelopes – Analysis - IEA Available online: <https://www.iea.org/reports/building-envelopes> (accessed on 7 March 2022).
22. Global CCS Global Status Report 2021. **2021**.
23. Chua, K.J.; Chou, S.K.; Yang, W.M.; Yan, J. Achieving Better Energy-Efficient Air Conditioning - A Review of Technologies and Strategies. *Appl Energy* 2013.
24. Ng, L.C.; Persily, A.K.; Emmerich, S.J. Consideration of Envelope Airtightness in Modelling Commercial Building Energy Consumption. *International Journal of Ventilation* **2014**, doi:10.1080/14733315.2014.11684030.
25. Elsland, R.; Peksen, I.; Wietschel, M. Are Internal Heat Gains Underestimated in Thermal Performance Evaluation of Buildings? In Proceedings of the Energy Procedia; 2014.
26. Feng, W.; Zhang, Q.; Ji, H.; Wang, R.; Zhou, N.; Ye, Q.; Hao, B.; Li, Y.; Luo, D.; Lau, S.S.Y. A Review of Net Zero Energy Buildings in Hot and Humid Climates: Experience Learned from 34 Case Study Buildings. *Renewable and Sustainable Energy Reviews* **2019**, doi:10.1016/j.rser.2019.109303.
27. United Nations Environment Programme (2021). *2021 Global Status Report for Buildings and Construction: Towards a Zero-emission, Efficient and Resilient Buildings and Construction Sector*; 2021;

28. Loonen, R.C.G.M. Approaches for Computational Performance Optimization of Innovative Adaptive Façade Concepts, Technische Universiteit Eindhoven, 2018.
29. Perino, M.; Serra, V. Switching from Static to Adaptable and Dynamic Building Envelopes: A Paradigm Shift for the Energy Efficiency in Buildings. *Journal of Façade Design and Engineering* **2015**, doi:10.3233/fde-150039.
30. McLeod, R.S.; Hopfe, C.J.; Kwan, A. An Investigation into Future Performance and Overheating Risks in Passivhaus Dwellings. *Build Environ* **2013**, doi:10.1016/j.buildenv.2013.08.024.
31. Fasi, M.A.; Budaiwi, I.M. Energy Performance of Windows in Office Buildings Considering Daylight Integration and Visual Comfort in Hot Climates. *Energy Build* **2015**, doi:10.1016/j.enbuild.2015.09.024.
32. Aflaki, A.; Mahyuddin, N.; Al-Cheikh Mahmoud, Z.; Baharum, M.R. A Review on Natural Ventilation Applications through Building Façade Components and Ventilation Openings in Tropical Climates. *Energy Build* 2015.
33. Cannavale, A.; Fiorito, F.; Resta, D.; Gigli, G. Visual Comfort Assessment of Smart Photovoltachromic Windows. *Energy Build* **2013**, doi:10.1016/j.enbuild.2013.06.019.
34. Hosseini, S.M.; Mohammadi, M.; Rosemann, A.; Schröder, T.; Lichtenberg, J. A Morphological Approach for Kinetic Façade Design Process to Improve Visual and Thermal Comfort: Review. *Build Environ* 2019.
35. Al Horr, Y.; Arif, M.; Katafygiotou, M.; Mazroei, A.; Kaushik, A.; Elsarrag, E. Impact of Indoor Environmental Quality on Occupant Well-Being and Comfort: A Review of the Literature. *International Journal of Sustainable Built Environment* 2016.
36. Carlucci, F. A Review of Smart and Responsive Building Technologies and Their Classifications. *Future Cities and Environment* **2021**, 7, doi:10.5334/FCE.123/METRICS/.
37. Carlucci, F.; Cannavale, A.; Triggiano, A.A.; Squicciarini, A.; Fiorito, F. Phase Change Material Integration in Building Envelopes in Different Building Types and Climates: Modeling the Benefits of Active and Passive Strategies. *Applied Sciences* 2021, Vol. 11, Page 4680 **2021**, 11, 4680, doi:10.3390/APP11104680.
38. Carlucci, F.; Fiorito, F. Implementation of Smart Technologies in Building Envelopes: Methodological Approach and Comparative Analyses in a Hot-Summer Mediterranean Climate. In Proceedings of the Colloqui.AT.e 2021 Design and construction Tradition and innovation in the practice of

- architecture; Sicignano, E., Ed.; EdicomEdizioni - ISBN 978-88-96386-62-0, 2021.
39. Carlucci, F.; Campagna, L.M.; Fiorito, F. Technological and Energy Assessment of an Origami-Based Kinetic Shading System in Typical and Future Climate Scenarios. In Proceedings of the ColloquiATe 2022 ; 2022.
 40. Carlucci, F.; Loonen, R.C.G.M.; Fiorito, F.; Hensen, J.L.M. A Novel Approach to Account for Shape-Morphing and Kinetic Shading Systems in Building Energy Performance Simulations. <https://doi.org/10.1080/19401493.2022.2142294> **2022**, 1–20, doi:10.1080/19401493.2022.2142294.
 41. Energy Flexibility of Building Systems in Future Scenarios: Optimization of the Control Strategy of a Dynamic Shading System and Definition of a New Energy Flexibility Metric. *Energy Build* **2023**, 113056, doi:10.1016/J.ENBUILD.2023.113056.
 42. Loonen, R.C.G.M.; Trčka, M.; Cóstola, D.; Hensen, J.L.M. Climate Adaptive Building Shells: State-of-the-Art and Future Challenges. *Renewable and Sustainable Energy Reviews* **2013**, *25*, 483–493, doi:10.1016/j.rser.2013.04.016.
 43. Aelenei, D.; Aelenei, L.; Vieira, C.P. Adaptive Façade: Concept, Applications, Research Questions. *Energy Procedia* **2016**, *91*, 269–275, doi:10.1016/j.egypro.2016.06.218.
 44. Negroponte, N. Soft Architecture Machines. *The New Media Reader* 1975.
 45. Davies, M. A Wall for All Seasons. *RIBA Journal* **1981**, *88*, 55–57.
 46. Favoino, F.; Goia, F.; Perino, M.; Serra, V. Experimental Assessment of the Energy Performance of an Advanced Responsive Multifunctional Façade Module. *Energy Build* **2014**, doi:10.1016/j.enbuild.2013.08.066.
 47. Attia, S.; Bilir, S.; Safy, T.; Struck, C.; Loonen, R.; Goia, F. Current Trends and Future Challenges in the Performance Assessment of Adaptive Façade Systems. *Energy Build* **2018**, *179*, 165–182, doi:10.1016/j.enbuild.2018.09.017.
 48. Moloney, J. A Framework for the Design of Kinetic Façades. In Proceedings of the Computer-Aided Architectural Design Futures, CAADFutures 2007 - Proceedings of the 12th International CAADFutures Conference; 2007.
 49. Konstantoglou, M.; Tsangrassoulis, A. Dynamic Operation of Daylighting and Shading Systems: A Literature Review. *Renewable and Sustainable Energy Reviews* 2016.
 50. Wigginton, M. *Intelligent Skins*; 2013;

51. Favoino, F.; Giovannini, L.; Loonen, R. Smart Glazing in Intelligent Buildings: What Can We Simulate? *GPD 2017 - Glass Performance Days 2017* **2017**, 8–15.
52. Ghosh, A.; Norton, B. Advances in Switchable and Highly Insulating Autonomous (Self-Powered) Glazing Systems for Adaptive Low Energy Buildings. *Renew Energy* **2018**.
53. Heiselberg, P. IEA ECBCS Annex 44 Integrating Environmentally Responsive Elements in Buildings - Expert Guide Part 1: Responsive Building Concepts. *Foundations* **2009**.
54. Aa, A. van der; Heiselberg, P.; Perino, M. Designing with Responsive Building Elements. *IEA-ECBCS Annex 44 Integrating Environmentally Responsive Elements in Buildings* **2011**.
55. Wang, J.; Beltrán, L.O.; Kim, J. From Static to Kinetic: A Review of Acclimated Kinetic Building Envelopes. In Proceedings of the World Renewable Energy Forum, WREF 2012, Including World Renewable Energy Congress XII and Colorado Renewable Energy Society (CRES) Annual Conferen; 2012.
56. Hayes-Roth, B. An Architecture for Adaptive Intelligent Systems. *Artif Intell* **1995**, doi:10.1016/0004-3702(94)00004-K.
57. Romano, R.; Aelenei, L.; Aelenei, D.; Mazzucchelli, E.S. What Is an Adaptive Façade? Analysis of Recent Terms and Definitions from an International Perspective. *Journal of Facade Design and Engineering* **2018**, 6, 065–076, doi:10.7480/jfde.2018.3.2478.
58. Addington, d. M.; L.shock, D. Smart Materials and New Technologies For the Architecture and Design Professions. *Elsevier* **2005**.
59. Lawrence, T.M.; Boudreau, M.C.; Helsen, L.; Henze, G.; Mohammadpour, J.; Noonan, D.; Patteeuw, D.; Pless, S.; Watson, R.T. Ten Questions Concerning Integrating Smart Buildings into the Smart Grid. *Build Environ* **2016**, doi:10.1016/j.buildenv.2016.08.022.
60. Hasselaar, B.L.H. Climate Adaptive Skins: Towards the New Energy-Efficient Façade. *WIT Transactions on Ecology and the Environment* **2006**, 99, 351–360, doi:10.2495/RAV060351.
61. Attia, S.; Lioure, R.; Declaude, Q. Future Trends and Main Concepts of Adaptive Facade Systems. *Energy Sci Eng* **2020**, doi:10.1002/ese3.725.
62. Loonen, R.; Rico-Martinez, J.; Favoino, F.; Brzezicki, M.; Menezo, C.; La Ferla, G.; Aelenei, L. Design for Façade Adaptability: Towards a Unified and Systematic Characterization. *10th Conference on Advanced Building Skins* **2015**.
63. Wang, J.; Beltrán, L.O.; Kim, J. From Static to Kinetic: A Review of Acclimated Kinetic Building Envelopes. In Proceedings of the World

- Renewable Energy Forum, WREF 2012, Including World Renewable Energy Congress XII and Colorado Renewable Energy Society (CRES) Annual Conferen; 2012.
64. Ramzy, N.; Fayed, H. Kinetic Systems in Architecture: New Approach for Environmental Control Systems and Context-Sensitive Buildings. *Sustain Cities Soc* **2011**, doi:10.1016/j.scs.2011.07.004.
 65. Ochoa, C.E.; Capeluto, I.G. Strategic Decision-Making for Intelligent Buildings: Comparative Impact of Passive Design Strategies and Active Features in a Hot Climate. *Build Environ* **2008**, doi:10.1016/j.build-env.2007.10.018.
 66. Kuznik, F.; David, D.; Johannes, K.; Roux, J.J. A Review on Phase Change Materials Integrated in Building Walls. *Renewable and Sustainable Energy Reviews* 2011.
 67. Elias, C.N.; Stathopoulos, V.N. A Comprehensive Review of Recent Advances in Materials Aspects of Phase Change Materials in Thermal Energy Storage. *Energy Procedia* **2019**, *161*, 385–394, doi:10.1016/j.egypro.2019.02.101.
 68. Soares, N.; Costa, J.J.; Gaspar, A.R.; Santos, P. Review of Passive PCM Latent Heat Thermal Energy Storage Systems towards Buildings' Energy Efficiency. *Energy Build* 2013.
 69. Akeiber, H.; Nejat, P.; Majid, M.Z.A.; Wahid, M.A.; Jomehzadeh, F.; Zeynali Famileh, I.; Calautit, J.K.; Hughes, B.R.; Zaki, S.A. A Review on Phase Change Material (PCM) for Sustainable Passive Cooling in Building Envelopes. *Renewable and Sustainable Energy Reviews* **2016**, *60*, 1470–1497, doi:10.1016/j.rser.2016.03.036.
 70. Farzanehnia, A.; Khatibi, M.; Sardarabadi, M.; Passandideh-Fard, M. Experimental Investigation of Multiwall Carbon Nanotube/Paraffin Based Heat Sink for Electronic Device Thermal Management. *Energy Convers Manag* **2019**, doi:10.1016/j.enconman.2018.10.037.
 71. Neri, G.; Koehler, A.; De Parolis, M.N.; Zolesi, V. ESA Conditioned Container: A System for Passive Temperature Controlled Transportation of Experiments for the International Space Station. In Proceedings of the Proceedings of the International Astronautical Congress, IAC; Naples, Italy.
 72. De Gracia, A.; Cabeza, L.F. Phase Change Materials and Thermal Energy Storage for Buildings. *Energy Build* 2015.
 73. Berardi, U.; Soudian, S. Benefits of Latent Thermal Energy Storage in the Retrofit of Canadian High-Rise Residential Buildings. *Build Simul* **2018**, doi:10.1007/s12273-018-0436-x.

74. Fiorito, F. Phase-Change Materials for Indoor Comfort Improvement in Lightweight Buildings. A Parametric Analysis for Australian Climates. *Energy Procedia* **2014**, *57*, 2014–2022, doi:10.1016/j.egypro.2014.10.066.
75. De Matteis, V.; Cannavale, A.; Martellotta, F.; Rinaldi, R.; Calcagnile, P.; Ferrari, F.; Ayr, U.; Fiorito, F. Nano-Encapsulation of Phase Change Materials: From Design to Thermal Performance, Simulations and Toxicological Assessment. *Energy Build* **2019**, *188–189*, 1–11, doi:10.1016/j.enbuild.2019.02.004.
76. Kośny, J. *PCM-Enhanced Building Components - An Application of Phase Change Materials in Building Envelopes and Internal Structures*; Springer, 2015; ISBN 9783319142852.
77. Cabeza, L.F.; Castell, A.; Barreneche, C.; De Gracia, A.; Fernández, A.I. Materials Used as PCM in Thermal Energy Storage in Buildings: A Review. *Renewable and Sustainable Energy Reviews* **2011**, *15*, 1675–1695, doi:10.1016/j.rser.2010.11.018.
78. Kenisarin, M.M. Thermophysical Properties of Some Organic Phase Change Materials for Latent Heat Storage. A Review. *Solar Energy* **2014**, doi:10.1016/j.solener.2014.05.001.
79. Yuan, Y.; Zhang, N.; Tao, W.; Cao, X.; He, Y. Fatty Acids as Phase Change Materials: A Review. *Renewable and Sustainable Energy Reviews* **2014**.
80. Su, W.; Darkwa, J.; Kokogiannakis, G. Review of Solid-Liquid Phase Change Materials and Their Encapsulation Technologies. *Renewable and Sustainable Energy Reviews* **2015**.
81. Milián, Y.E.; Gutiérrez, A.; Grágeda, M.; Ushak, S. A Review on Encapsulation Techniques for Inorganic Phase Change Materials and the Influence on Their Thermophysical Properties. *Renewable and Sustainable Energy Reviews* **2017**, *73*, 983–999, doi:10.1016/j.rser.2017.01.159.
82. Salunkhe, P.B.; Shembekar, P.S. A Review on Effect of Phase Change Material Encapsulation on the Thermal Performance of a System. *Renewable and Sustainable Energy Reviews* **2012**, *16*, 5603–5616, doi:10.1016/j.rser.2012.05.037.
83. Gil, A.; Medrano, M.; Martorell, I.; Lázaro, A.; Dolado, P.; Zalba, B.; Cabeza, L.F. State of the Art on High Temperature Thermal Energy Storage for Power Generation. Part 1-Concepts, Materials and Modellization. *Renewable and Sustainable Energy Reviews* **2010**.
84. Navarro, L.; de Gracia, A.; Colclough, S.; Browne, M.; McCormack, S.J.; Griffiths, P.; Cabeza, L.F. Thermal Energy Storage in Building Integrated

- Thermal Systems: A Review. Part 1. Active Storage Systems. *Renew Energy* **2016**, 88, 526–547, doi:10.1016/j.renene.2015.11.040.
85. Weinläder, H.; Körner, W.; Strieder, B. A Ventilated Cooling Ceiling with Integrated Latent Heat Storage - Monitoring Results. *Energy Build* **2014**, doi:10.1016/j.enbuild.2014.07.013.
 86. Lizana, J.; de-Borja-Torrejon, M.; Barrios-Padura, A.; Auer, T.; Chacartegui, R. Passive Cooling through Phase Change Materials in Buildings. A Critical Study of Implementation Alternatives. *Appl Energy* **2019**, doi:10.1016/j.apenergy.2019.113658.
 87. Fiorentini, M.; Cooper, P.; Ma, Z. Development and Optimization of an Innovative HVAC System with Integrated PVT and PCM Thermal Storage for a Net-Zero Energy Retrofitted House. *Energy Build* **2015**, doi:10.1016/j.enbuild.2015.02.018.
 88. Real, A.; García, V.; Domenech, L.; Renau, J.; Montés, N.; Sánchez, F. Improvement of a Heat Pump Based HVAC System with PCM Thermal Storage for Cold Accumulation and Heat Dissipation. *Energy Build* **2014**, doi:10.1016/j.enbuild.2014.04.029.
 89. de Gracia, A.; Navarro, L.; Castell, A.; Cabeza, L.F. Energy Performance of a Ventilated Double Skin Facade with PCM under Different Climates. *Energy Build* **2015**, doi:10.1016/j.enbuild.2015.01.011.
 90. Sharif, M.K.A.; Al-Abidi, A.A.; Mat, S.; Sopian, K.; Ruslan, M.H.; Sulaiman, M.Y.; Rosli, M.A.M. Review of the Application of Phase Change Material for Heating and Domestic Hot Water Systems. *Renewable and Sustainable Energy Reviews* 2015.
 91. Khan, M.M.A.; Ibrahim, N.I.; Mahbubul, I.M.; Muhammad, Ali, H.; Saidur, R.; Al-Sulaiman, F.A. Evaluation of Solar Collector Designs with Integrated Latent Heat Thermal Energy Storage: A Review. *Solar Energy* 2018.
 92. Navarro, L.; Barreneche, C.; Castell, A.; Redpath, D.A.G.; Griffiths, P.W.; Cabeza, L.F. High Density Polyethylene Spheres with PCM for Domestic Hot Water Applications: Water Tank and Laboratory Scale Study. *J Energy Storage* **2017**, doi:10.1016/j.est.2017.07.025.
 93. Najafian, A.; Haghghat, F.; Moreau, A. Integration of PCM in Domestic Hot Water Tanks: Optimization for Shifting Peak Demand. *Energy Build* **2015**, doi:10.1016/j.enbuild.2015.05.036.
 94. Hasan, A.; McCormack, S.J.; Huang, M.J.; Norton, B. Energy and Cost Saving of a Photovoltaic-Phase Change Materials (PV-PCM) System through Temperature Regulation and Performance Enhancement of Photovoltaics. *Energies (Basel)* **2014**, doi:10.3390/en7031318.

95. Lu, W.; Liu, Z.; Flor, J.F.; Wu, Y.; Yang, M. Investigation on Designed Fins-Enhanced Phase Change Materials System for Thermal Management of a Novel Building Integrated Concentrating PV. *Appl Energy* **2018**, doi:10.1016/j.apenergy.2018.05.030.
96. Faheem, A.; Ranzi, G.; Fiorito, F.; Lei, C. A Numerical Study on the Thermal Performance of Night Ventilated Hollow Core Slabs Cast with Micro-Encapsulated PCM Concrete. *Energy Build* **2016**, doi:10.1016/j.enbuild.2016.06.014.
97. Navarro, L.; de Gracia, A.; Niall, D.; Castell, A.; Browne, M.; McCormack, S.J.; Griffiths, P.; Cabeza, L.F. Thermal Energy Storage in Building Integrated Thermal Systems: A Review. Part 2. Integration as Passive System. *Renew Energy* **2016**, *85*, 1334–1356, doi:10.1016/j.renene.2015.06.064.
98. Cabeza, L.F.; Castellón, C.; Nogués, M.; Medrano, M.; Leppers, R.; Zubillaga, O. Use of Microencapsulated PCM in Concrete Walls for Energy Savings. *Energy Build* **2007**, doi:10.1016/j.enbuild.2006.03.030.
99. Ramakrishnan, S.; Wang, X.; Sanjayan, J.; Wilson, J. Thermal Performance Assessment of Phase Change Material Integrated Cementitious Composites in Buildings: Experimental and Numerical Approach. *Appl Energy* **2017**, doi:10.1016/j.apenergy.2017.05.144.
100. Kosny, J.; Kossecka, E.; Brzezinski, A.; Tleoubaev, A.; Yarbrough, D. Dynamic Thermal Performance Analysis of Fiber Insulations Containing Bio-Based Phase Change Materials (PCMs). *Energy Build* **2012**, doi:10.1016/j.enbuild.2012.05.021.
101. Castellón, C.; Medrano, M.; Roca, J.; Cabeza, L.F.; Navarro, M.E.; Fernández, A.I.; Lázaro, A.; Zalba, B. Effect of Microencapsulated Phase Change Material in Sandwich Panels. *Renew Energy* **2010**, doi:10.1016/j.renene.2010.03.030.
102. Weinlaeder, H.; Koerner, W.; Heidenfelder, M. Monitoring Results of an Interior Sun Protection System with Integrated Latent Heat Storage. *Energy Build* **2011**, doi:10.1016/j.enbuild.2011.06.007.
103. Weinläder, H.; Beck, A.; Fricke, J. PCM-Facade-Panel for Daylighting and Room Heating. In Proceedings of the Solar Energy; Pergamon, February 1 2005; Vol. 78, pp. 177–186.
104. Barrenechea, C.; Navarro, H.; Serrano, S.; Cabeza, L.F.; Fernández, A.I. New Database on Phase Change Materials for Thermal Energy Storage in Buildings to Help PCM Selection. In Proceedings of the Energy Procedia; 2014.

105. Heim, D.; Clarke, J.A. Numerical Modelling and Thermal Simulation of PCM-Gypsum Composites with ESP-r. In Proceedings of the Energy and Buildings; Elsevier, August 1 2004; Vol. 36, pp. 795–805.
106. Zhang, Y.; Zhou, G.; Lin, K.; Zhang, Q.; Di, H. Application of Latent Heat Thermal Energy Storage in Buildings: State-of-the-Art and Outlook. *Build Environ* **2007**, *42*, 2197–2209, doi:10.1016/j.buildenv.2006.07.023.
107. Baetens, R.; Jelle, B.P.; Gustavsen, A. Properties, Requirements and Possibilities of Smart Windows for Dynamic Daylight and Solar Energy Control in Buildings: A State-of-the-Art Review. *Solar Energy Materials and Solar Cells* 2010.
108. Granqvist, C.G.; Bayrak Pehlivan, İ.; Niklasson, G.A. Electrochromics on a Roll: Web-Coating and Lamination for Smart Windows. *Surf Coat Technol* **2018**, doi:10.1016/j.surfcoat.2017.08.006.
109. Cannavale, A. Chromogenic Technologies for Energy Saving. *Clean Technologies* **2020**, *2*, 462–475, doi:10.3390/cleantechnol2040029.
110. Carlucci, F. A Review of Smart and Responsive Building Technologies and Their Classifications. *Future Cities and Environment* **2021**, *7*, doi:10.5334/FCE.123.
111. DeForest, N.; Shehabi, A.; Selkowitz, S.; Milliron, D.J. A Comparative Energy Analysis of Three Electrochromic Glazing Technologies in Commercial and Residential Buildings. *Appl Energy* **2017**, *192*, 95–109, doi:10.1016/j.apenergy.2017.02.007.
112. DeForest, N.; Shehabi, A.; O'Donnell, J.; Garcia, G.; Greenblatt, J.; Lee, E.S.; Selkowitz, S.; Milliron, D.J. United States Energy and CO₂ Savings Potential from Deployment of Near-Infrared Electrochromic Window Glazings. *Build Environ* **2015**, doi:10.1016/j.buildenv.2015.02.021.
113. Garcia, G.; Buonsanti, R.; Llordés, A.; Runnerstrom, E.L.; Bergerud, A.; Milliron, D.J. Near-Infrared Spectrally Selective Plasmonic Electrochromic Thin Films. *Adv Opt Mater* **2013**, doi:10.1002/adom.201200051.
114. Llordés, A.; Garcia, G.; Gazquez, J.; Milliron, D.J. Tunable Near-Infrared and Visible-Light Transmittance in Nanocrystal-in-Glass Composites. *Nature* **2013**, doi:10.1038/nature12398.
115. Hee, W.J.; Alghoul, M.A.; Bakhtyar, B.; Elayeb, O.; Shameri, M.A.; Al-rubaih, M.S.; Sopian, K. The Role of Window Glazing on Daylighting and Energy Saving in Buildings. *Renewable and Sustainable Energy Reviews* **2015**, *42*, 323–343, doi:10.1016/j.rser.2014.09.020.
116. Martin, P.M. Optical Materials: Smart Optical Materials. In *Encyclopedia of Modern Optics, Five-Volume Set*; Elsevier Inc., 2004; pp. 9–16 ISBN 9780123693952.

117. Mukherjee, S.; Hsieh, W.L.; Smith, N.; Goulding, M.; Heikenfeld, J. Electrokinetic Pixels with Biprimary Inks for Color Displays and Color-Temperature-Tunable Smart Windows. *Appl Opt* **2015**, doi:10.1364/ao.54.005603.
118. Casini, M. Active Dynamic Windows for Buildings: A Review. *Renew Energy* **2018**, *119*, 923–934, doi:10.1016/j.renene.2017.12.049.
119. Delalat, F.; Ranjbar, M.; Salamati, H. Blue Colloidal Nanoparticles of Molybdenum Oxide by Simple Anodizing Method: Decolorization by PdCl₂ and Observation of in-Liquid Gasochromic Coloration. *Solar Energy Materials and Solar Cells* **2016**, doi:10.1016/j.solmat.2015.08.038.
120. Lampert, C.M. Chromogenic Smart Materials. *Materials Today* 2004.
121. Lee, S.G.; Lee, D.Y.; Lim, H.S.; Lee, D.H.; Lee, S.; Cho, K. Switchable Transparency and Wetting of Elastomeric Smart Windows. *Advanced Materials* **2010**, *22*, 5013–5017, doi:10.1002/adma.201002320.
122. Shian, S.; Clarke, D.R. Electrically Tunable Window Device. *Opt Lett* **2016**, doi:10.1364/ol.41.001289.
123. Kim, H.N.; Ge, D.; Lee, E.; Yang, S. Multistate and On-Demand Smart Windows. *Advanced Materials* **2018**, *30*, 1–7, doi:10.1002/adma.201803847.
124. Koenders, S.J.M.; Loonen, R.C.G.M.; Hensen, J.L.M. Investigating the Potential of a Closed-Loop Dynamic Insulation System for Opaque Building Elements. *Energy Build* **2018**, *173*, 409–427, doi:10.1016/j.enbuild.2018.05.051.
125. Pflug, T.; Nestle, N.; E. Kuhn, T.; Siroux, M.; Maurer, C. Modeling of Façade Elements with Switchable U-Value. *Energy Build* **2018**, doi:10.1016/j.enbuild.2017.12.044.
126. Pflug, T.; Bueno, B.; Siroux, M.; Kuhn, T.E. Potential Analysis of a New Removable Insulation System. *Energy Build* **2017**, *154*, 391–403, doi:10.1016/j.enbuild.2017.08.033.
127. Kamalifarvestani, M.; Saidur, R.; Mekhilef, S.; Javadi, F.S. Performance, Materials and Coating Technologies of Thermochromic Thin Films on Smart Windows. *Renewable and Sustainable Energy Reviews* 2013.
128. Warwick, M.E.A.; Binions, R. Advances in Thermochromic Vanadium Dioxide Films. *J Mater Chem A Mater* **2014**, doi:10.1039/c3ta14124a.
129. Ke, Y.; Zhou, C.; Zhou, Y.; Wang, S.; Chan, S.H.; Long, Y. Emerging Thermal-Responsive Materials and Integrated Techniques Targeting the Energy-Efficient Smart Window Application. *Adv Funct Mater* **2018**, doi:10.1002/adfm.201800113.
130. Zhang, Y.; Tso, C.Y.; Iñigo, J.S.; Liu, S.; Miyazaki, H.; Chao, C.Y.H.; Yu, K.M. Perovskite Thermochromic Smart Window: Advanced Optical

- Properties and Low Transition Temperature. *Appl Energy* **2019**, doi:10.1016/j.apenergy.2019.113690.
131. Ke, Y.; Chen, J.; Lin, G.; Wang, S.; Zhou, Y.; Yin, J.; Lee, P.S.; Long, Y. Smart Windows: Electro-, Thermo-, Mechano-, Photochromics, and Beyond. *Adv Energy Mater* **2019**, *9*, 1–38, doi:10.1002/aenm.201902066.
 132. Timmermans, G.H.; Saes, B.W.H.; Debije, M.G. Dual-Responsive “Smart” Window and Visually Attractive Coating Based on a Diarylethene Photochromic Dye. *Appl Opt* **2019**, doi:10.1364/ao.58.009823.
 133. Miluski, P.; Kochanowicz, M.; Zmojda, J.; Dorosz, D. Optical Properties of Spirooxazine-Doped PMMA Fiber for New Functional Applications. *Optical Engineering* **2017**, *56*, 047105, doi:10.1117/1.oe.56.4.047105.
 134. Wang, S.; Fan, W.; Liu, Z.; Yu, A.; Jiang, X. Advances on Tungsten Oxide Based Photochromic Materials: Strategies to Improve Their Photochromic Properties. *J Mater Chem C Mater* **2018**.
 135. Cannavale, A.; Cossari, P.; Eperon, G.E.; Colella, S.; Fiorito, F.; Gigli, G.; Snaith, H.J.; Listorti, A. Forthcoming Perspectives of Photoelectrochromic Devices: A Critical Review. *Energy Environ Sci* **2016**.
 136. Cannavale, A.; Martellotta, F.; Fiorito, F.; Ayr, U. The Challenge for Building Integration of Highly Transparent Photovoltaics and Photoelectrochromic Devices. *Energies (Basel)* **2020**, *13*, doi:10.3390/en13081929.
 137. Wu, J.J.; Hsieh, M. Da; Liao, W.P.; Wu, W.T.; Chen, J.S. Fast-Switching Photovoltachromic Cells with Tunable Transmittance. *ACS Nano* **2009**, doi:10.1021/nn900428s.
 138. Fiorito, F.; Cannavale, A.; Santamouris, M. Development, Testing and Evaluation of Energy Savings Potentials of Photovoltachromic Windows in Office Buildings. A Perspective Study for Australian Climates. *Solar Energy* **2020**, *205*, 358–371, doi:10.1016/j.solener.2020.05.080.
 139. Fazel, A.; Izadi, A.; Azizi, M. Low-Cost Solar Thermal Based Adaptive Window: Combination of Energy-Saving and Self-Adjustment in Buildings. *Solar Energy* **2016**, doi:10.1016/j.solener.2016.04.008.
 140. Goia, F.; Perino, M.; Serra, V. Experimental Analysis of the Energy Performance of a Full-Scale PCM Glazing Prototype. *Solar Energy* **2014**, *100*, 217–233, doi:10.1016/j.solener.2013.12.002.
 141. Giovannini, L.; Goia, F.; Lo Verso, V.R.M.; Serra, V. Phase Change Materials in Glazing: Implications on Light Distribution and Visual Comfort. Preliminary Results. *Energy Procedia* **2017**, *111*, 357–366, doi:10.1016/j.egypro.2017.03.197.
 142. Vigna, I.; Bianco, L.; Goia, F.; Serra, V. Phase Change Materials in Transparent Building Envelopes: A Strengths, Weakness, Opportunities and

- Threats (SWOT) Analysis. *Energies (Basel)* **2018**, *11*, doi:10.3390/en11010111.
143. Al Dakheel, J.; Aoul, K.T. Building Applications, Opportunities and Challenges of Active Shading Systems: A State-of-the-Art Review. *Energies (Basel)* **2017**, *10*, doi:10.3390/en10101672.
 144. Badarnah, L. Form Follows Environment: Biomimetic Approaches to Building Envelope Design for Environmental Adaptation. *Buildings 2017*, *Vol. 7, Page 40* **2017**, *7*, 40, doi:10.3390/BUILDINGS7020040.
 145. Doumpiotti, C.; Greenberg, E.L.; Karatzas, K. Embedded Intelligence: Material Responsiveness in Façade Systems. *Life In:formation: On Responsive Information and Variations in Architecture - Proceedings of the 30th Annual Conference of the Association for Computer Aided Design in Architecture, ACADIA 2010* **2010**, 258–262.
 146. Alberto, S.; Lorenzo, V.; Andrea Giovanni, M.; Tiziana, P. An Innovative Sun Shading System for Facade Application That Involves Smart Materials and Novel Geometry Morphing. In *Proceedings of the Facade Tectonics 2020 World Congress*; 2020.
 147. Khoo, C.K.; Salim, F.; Burry, J. Designing Architectural Morphing Skins with Elastic Modular Systems. *International Journal of Architectural Computing* **2011**, doi:10.1260/1478-0771.9.4.397.
 148. Denz, P.R.; Sauer, C.; Waldhör, E.F.; Schneider, M.; Vongsingha, P. Smart Textile Sun-Shading. *Journal of Facade Design and Engineering* **2021**, *9*, 101–116, doi:10.7480/JFDE.2021.1.5539.
 149. Lienhard, J.; Schleicher, S.; Poppinga, S.; Masselter, T.; Milwich, M.; Speck, T.; Knippers, J. Flectofin: A Hingeless Flapping Mechanism Inspired by Nature. *Bioinspir Biomim* **2011**, doi:10.1088/1748-3182/6/4/045001.
 150. Wei, Z.; Yiqun, W.; Menghui, S. Modeling and Simulation of Electric-Hydraulic Control System for Bending Roll System. *2008 IEEE International Conference on Robotics, Automation and Mechatronics, RAM 2008* **2008**, 661–664, doi:10.1109/RAMECH.2008.4681470.
 151. Fiorito, F.; Sauchelli, M.; Arroyo, D.; Pesenti, M.; Imperadori, M.; Maserà, G.; Ranzi, G. Shape Morphing Solar Shadings: A Review. *Renewable and Sustainable Energy Reviews* **2016**, *55*, 863–884, doi:10.1016/j.rser.2015.10.086.
 152. Zawidzki, M. Dynamic Shading of a Building Envelope Based on Rotating Polarized Film System Controlled by One-Dimensional Cellular Automata in Regular Tessellations (Triangular, Square and Hexagonal). *Advanced Engineering Informatics* **2015**, *29*, 87–100, doi:10.1016/J.AEI.2014.09.008.

153. Attia, S. Evaluation of Adaptive Facades: The Case Study of Al Bahr Towers in the UAE. **2016**, *2016*, 8, doi:10.5339/QPROC.2016.QGBC.8.
154. Andy, A.; Giorgio, B.; David, E.; Roy, J.; Leonora, L.; John, L.; Konrad, X. The Al Bahar Towers: Multidisciplinary Design for Middle East High-Rise. *Arup Journal* **2013**, 90–95.
155. Babilio, E.; Miranda, R.; Fraternali, F. On the Kinematics and Actuation of Dynamic Sunscreens with Tensegrity Architecture. *Front Mater* **2019**, 6, 7, doi:10.3389/FMATS.2019.00007/BIBTEX.
156. Martone, P.T.; Boiler, M.; Burgert, I.; Dumais, J.; Edwards, J.; MacH, K.; Rowe, N.; Rueggeberg, M.; Seidel, R.; Speck, T. Mechanics without Muscle: Biomechanical Inspiration from the Plant World. *Integr Comp Biol* **2010**, 50, 888–907, doi:10.1093/icb/icq122.
157. Al-Masrani, S.M.; Al-Obaidi, K.M. Dynamic Shading Systems: A Review of Design Parameters, Platforms and Evaluation Strategies. *Autom Constr* **2019**, 102, 195–216, doi:10.1016/j.autcon.2019.01.014.
158. Welcome | TRNSYS : Transient System Simulation Tool Available online: <https://www.trnsys.com/> (accessed on 22 September 2022).
159. IDA ICE - Simulation Software | EQUA Available online: <https://www.equa.se/en/ida-ice> (accessed on 22 September 2022).
160. Corrado, V.; Fabrizio, E. Steady-State and Dynamic Codes, Critical Review, Advantages and Disadvantages, Accuracy, and Reliability. *Handbook of Energy Efficiency in Buildings: A Life Cycle Approach* **2019**, 263–294, doi:10.1016/B978-0-12-812817-6.00011-5.
161. Carlucci, F.; Cannavale, A.; Triggiano, A.A.; Squicciarini, A.; Fiorito, F. Phase Change Material Integration in Building Envelopes in Different Building Types and Climates: Modeling the Benefits of Active and Passive Strategies. *Applied Sciences* **2021**, 11, 4680, doi:10.3390/app11104680.
162. Aburas, M.; Ebendorff-Heidepriem, H.; Lei, L.; Li, M.; Zhao, J.; Williamson, T.; Wu, Y.; Soebarto, V. Smart Windows – Transmittance Tuned Thermochromic Coatings for Dynamic Control of Building Performance. *Energy Build* **2021**, 235, doi:10.1016/j.enbuild.2021.110717.
163. Carlucci, F.; Cannavale, A.; Fiorito, F. Electrochromic Window Integration in Adaptive Building Envelopes in Different Climates: A Genetic Optimization of Switchable Glazing Parameters to Reduce Energy Consumptions in Office Buildings. *J Phys Conf Ser* **2021**, 2069, doi:10.1088/1742-6596/2069/1/012131.
164. Cannavale, A.; Zampini, G.; Carlucci, F.; Pugliese, M.; Martellotta, F.; Ayr, U.; Maiorano, V.; Ortica, F.; Fiorito, F.; Latterini, L. Energy and Daylighting Performance of Building Integrated Spirooxazine

- Photochromic Films. *Solar Energy* **2022**, *242*, 424–434, doi:10.1016/J.SOLENER.2021.10.058.
165. Hu, J.; Yu, X.B. Adaptive Thermochromic Roof System: Assessment of Performance under Different Climates. *Energy Build* **2019**, *192*, 1–14, doi:10.1016/J.ENBUILD.2019.02.040.
 166. US Department of Energy *Input Output Reference*. *EnergyPlus*; 2021;
 167. Marion, W. New Typical Meteorological Years and Solar Radiation Data Manual. **1978**, doi:10.2172/134988.
 168. Marion, W.; Urban, K. User's Manual for Derived from the 1961-1990 National Solar Radiation Data Base. **1995**.
 169. Wilcox, S.; Marion, W. Innovation for Our Energy Future Users Manual for TMY3 Data Sets. **2008**.
 170. World Meteorological Organization; United Nations Environment Programme Climate Change 1992 The Supplementary Report to the IPCC Scientific Assessment. **1992**.
 171. IPCC Climate Change 2001: Synthesis Report. A Contribution of Working Groups I, II, and III to the Third Assessment Report of the Intergovernmental Panel on Climate Change. **2001**.
 172. IPCC *Climate Change 2007: Synthesis Report. Contribution of Working Groups I, II and III to the Fourth Assessment Report of the Intergovernmental Panel on Climate Change*; Geneva, 2007;
 173. Organization, W.M.; United Nations Environment Programme IPCC Special Report: Emissions Scenarios. Summary for Policymakers. **2000**.
 174. Contribution of Working Groups I, I. and I. to the F.A.R. of the I.P. on C.C. *IPCC 2014 Climate Change 2014: Synthesis Report.*; 2014; ISBN 9781139177245.
 175. IPCC Annex II: Glossary. In *Climate Change 2014: Synthesis Report. Contribution of Working Groups I, II and III to the Fifth Assessment Report of the Intergovernmental Panel on Climate Change*; 2014.
 176. IPCC *Climate Change 2022: Impacts, Adaptation and Vulnerability. Contribution of Working Group II to the Sixth Assessment Report of the Intergovernmental Panel on Climate Change*; 2022;
 177. IPCC Annex I: Glossary. In *Global Warming of 1.5°C. An IPCC Special Report on the impacts of global warming of 1.5°C above pre-industrial levels and related global greenhouse gas emission pathways, in the context of strengthening the global response to the threat of climate change.*; Cambridge University Press, 2022; pp. 541–562.
 178. Uppala, S.M.; Kallberg, P.W.; Simmons, A.J.; Andrae, U.; Bechtold, V.D.; Fiorino, M.; Gibson, J.K.; Haseler, J.; Hernandez, A.; Kelly, G.A.;

- et al. The ERA-40 Re-Analysis. *Quarterly Journal of the Royal Meteorological Society* **2005**, *131*, 2961–3012.
179. Guan, L. Preparation of Future Weather Data to Study the Impact of Climate Change on Buildings. *Build Environ* **2009**, *44*, 793–800, doi:10.1016/j.buildenv.2008.05.021.
 180. Trzaska, S.; Schnarr, E. A Review of Downscaling Methods for Climate Change Projections 2014.
 181. Berardi, U.; Jafarpur, P. Assessing the Impact of Climate Change on Building Heating and Cooling Energy Demand in Canada. *Renewable and Sustainable Energy Reviews* **2020**, *121*, 109681, doi:10.1016/j.rser.2019.109681.
 182. Belcher, S.E.; Hacker, J.N.; Powell, D.S. Constructing Design Weather Data for Future Climates. *Building Services Engineering Research and Technology* **2005**, *26* (1), 49–61.
 183. P.Tootkaboni, M.; Ballarini, I.; Zinzi, M.; Corrado, V. A Comparative Analysis of Different Future Weather Data for Building Energy Performance Simulation. *Climate* **2021**, *9*, 1–16, doi:10.3390/cli9020037.
 184. U.S. Department of Energy *EnergyPlus™ Version 9.6 Documentation: Getting Started*; 2022;
 185. Loonen, R.C.G.M.; Favoino, F.; Hensen, J.L.M.; Overend, M. Review of Current Status, Requirements and Opportunities for Building Performance Simulation of Adaptive Facades†. *J Build Perform Simul* **2017**, *10*, 205–223, doi:10.1080/19401493.2016.1152303.
 186. Field, K.; Deru, M.; Studer, D. Using Doe Commercial Reference Buildings for Simulation Studies. *Proceedings of the SimBuild 2010 Fourth National Conference of IBPSA-USA* **2010**.
 187. Deru, M.; Field, K.; Studer, D.; Benne, K.; Griffith, B.; Torcellini, P.; Liu, B.; Halverson, M.; Winiarski, D.; Rosenberg, M.; et al. U.S. Department of Energy Commercial Reference Building Models of the National Building Stock. *Publications (E)* **2011**, doi:NREL Report No. TP-5500-46861.
 188. US Department of Energy EnergyPlus Engineering Reference: The Reference to EnergyPlus Calculations. *US Department of Energy* 2021, Available online: <https://energyplus.net/documenta>.
 189. ANSI/ASHRAE *ASHRAE Guideline 14-2002 Measurement of Energy and Demand Savings*; 2002;
 190. *ASHRAE Guideline 14 -2014: Measurement of Energy, Demand, and Water Savings*; 2014;
 191. Ministry of Economic Development *Ministerial Decree 26/06/2015, Applicazione Delle Metodologie Di Calcolo Delle Prestazioni Energetiche e*

- Definizione Delle Prescrizioni e Dei Requisiti Minimi Degli Edifici*; 2015; pp. 1–8;
192. Gagarin, V.G. Thermal Performance as the Main Factor of Energy Saving of Buildings in Russia. *Procedia Eng* **2016**, 112–119.
 193. Schettler-Kohler, H.-P.; Ahlke, I. EPBD Implementation in Germany. *Concerted action Energy performance of buildings* **2018**.
 194. Danish Knowledge Centre for Energy Savings in Buildings *Energy Requirements of BR18 A Quick Guide for the Construction Industry on the Danish Building Regulations 2018*; 2018;
 195. Brekke, T.; Isachsen, O.K.; Strand, M. EPBD Implementation in Norway. *Concerted action Energy performance of buildings* **2018**.
 196. Kim, H.; Park, K.S.; Kim, H.Y.; Song, Y.H. Study on Variation of Internal Heat Gain in Office Buildings by Chronology. *Energies* **2018**, Vol. 11, Page 1013 **2018**, 11, 1013, doi:10.3390/EN11041013.
 197. Berger, T.; Amann, C.; Formayer, H.; Korjenic, A.; Pospichal, B.; Neurrer, C.; Smutny, R. Impacts of External Insulation and Reduced Internal Heat Loads upon Energy Demand of Offices in the Context of Climate Change in Vienna, Austria. *Journal of Building Engineering* **2016**, 5, 86–95, doi:10.1016/J.JOBE.2015.11.005.
 198. Bitkom, V. Vendor-Neutral Tendering of Multi-Function Devices.
 199. International Code Council *2021 International Energy Conservation Code*; 2021; ISBN 978-1-60983-961-1.
 200. Samani, S.A.; Alavi, S.M.S.Z. Are Open-Plan Office Designs Still Popular After Coronavirus Pandemic? *Performance Improvement* **2020**, 59, 24, doi:10.1002/PFI.21931.
 201. UNI 10339:1995 - UNI Ente Italiano Di Normazione Available online: <https://store.uni.com/uni-10339-1995> (accessed on 16 January 2023).
 202. Jentsch, M.F.; James, P.A.B.; Bourikas, L.; Bahaj, A.B.S. Transforming Existing Weather Data for Worldwide Locations to Enable Energy and Building Performance Simulation under Future Climates. *Renew Energy* **2013**, 55, 514–524, doi:10.1016/j.renene.2012.12.049.
 203. Yang, Y.; Javanroodi, K.; Nik, V.M. Climate Change and Energy Performance of European Residential Building Stocks – A Comprehensive Impact Assessment Using Climate Big Data from the Coordinated Regional Climate Downscaling Experiment. *Appl Energy* **2021**, 298, 117246, doi:10.1016/j.apenergy.2021.117246.
 204. P.Tootkaboni, M.; Ballarini, I.; Zinzi, M.; Corrado, V. A Comparative Analysis of Different Future Weather Data for Building Energy Performance Simulation. *Climate* **2021**, 9, 1–16, doi:10.3390/cli9020037.

205. Rutten, D.; Robert McNeel & Associates Grasshopper Available online: <https://www.grasshopper3d.com/> (accessed on 12 January 2022).
206. Rhino - The Hops Component Available online: <https://developer.rhino3d.com/guides/compute/hops-component/> (accessed on 17 November 2022).
207. Tabares-Velasco, P.C.; Christensen, C.; Bianchi, M. Verification and Validation of EnergyPlus Phase Change Material Model for Opaque Wall Assemblies. *Build Environ* **2012**, doi:10.1016/j.buildenv.2012.02.019.
208. Zastawna-Rumin, A.; Kisilewicz, T.; Berardi, U. Novel Simulation Algorithm for Modeling the Hysteresis of Phase Change Materials. *Energies (Basel)* **2020**, *13*, 1200, doi:10.3390/en13051200.
209. Zwanzig, S.D.; Lian, Y.; Brehob, E.G. Numerical Simulation of Phase Change Material Composite Wallboard in a Multi-Layered Building Envelope. *Energy Convers Manag* **2013**, *69*, 27–40, doi:10.1016/j.enconman.2013.02.003.
210. Sibilio, S.; Rosato, A.; Scorpio, M.; Iuliano, G.; Ciampi, G.; Vanoli, G.P.; De Rossi, F. A Review of Electrochromic Windows for Residential Applications. *International Journal of Heat and Technology* **2016**, doi:10.18280/ijht.34S241.
211. Carlucci, F.; Fiorito, F. Methodological Approach and Comparative Analyses for Smart Envelopes Assessment in Three Different Temperate Climates. *Rivista Tema* **2022**, *8*, doi:10.30682/TEMA0801M.

CURRICULUM



Francesco Carlucci is a chartered Engineer and PhD candidate at the Polytechnic University of Bari (Italy). After his master's degree in Architectural Engineering at the Polytechnic of Bari and the II level postgraduate course in "Energy management of buildings and infrastructure" at Polytechnic University of Milan, he has continued to deepen building envelopes and energy modelling topics.

CURRENT POSITION

November 2019 – Ongoing

PhD candidate, Course: Risk and environmental, territorial and building development
Polytechnic University of Bari, DICATECh department, XXXV Cycle

“Responsive envelopes performance analysis in current and future climate scenarios: development of an interactive computational platform”

Supervisors: Prof. Francesco Fiorito, Prof. Guido Raffaele Dell’Osso

Co-supervisors: Roel Loonen, Kristoffer Negendahl

RESEARCH ACTIVITY

November 2019 – Ongoing

JOURNAL PAPERS

- **Carlucci F**, K. Negendahl, F. Fiorito, *Energy flexibility of building systems in future scenarios: optimization of the control strategy of a dynamic shading system and definition of a new energy flexibility metric*, *Energy and Buildings* 2023. DOI: <https://doi.org/10.1016/j.enbuild.2023.113056>
- **Carlucci F**, Loonen R.L.C.G.M, Fiorito F, Hensen J.L.M. *A novel approach to account for shape-morphing and kinetic shading systems in building energy performance simulations*. *Journal of Building Performance Simulation* 2022. DOI: <https://doi.org/10.1080/19401493.2022.2142294>
- Fiorito F, Vurro G, **Carlucci F**, Campagna L.M, De Fino M, Carlucci S, Fatiguso F. *Adaptation of Users to Future Climate Conditions in Naturally Ventilated Historic Buildings: Effects on Indoor Comfort*. *Energies* 2022. DOI: <https://doi.org/10.3390/en15144984>
- **Carlucci F**, Fiorito F. *Methodological approach and comparative analyses for smart envelopes assessment in three different temperate climates*. *TEMA Technologies Engineering Materials Architecture* 2022. DOI: <https://doi.org/10.30682/tema0801m>

- **Carlucci, F.**; Cannavale, A.; Triggiano, A.A.; Squicciarini, A.; Fiorito, F. *Phase Change Material Integration in Building Envelopes in Different Building Types and Climates: Modelling the Benefits of Active and Passive Strategies*. *Applied Sciences* 2021. DOI: <https://doi.org/10.3390/app11104680>
- Cannavale, A, Zampini G, **Carlucci F**, Pugliese M, Martellotta F, Ayr U, Maiorano V, Ortica F, Fiorito F, Latterini L. *Energy and daylighting performance of building integrated spirooxazine photochromic*. *Solar Energy* 2021. DOI: <https://doi.org/10.1016/j.solener.2021.10.058>
- **Carlucci, F.** *A Review of Smart and Responsive Building Technologies and their Classifications*. *Future Cities and Environment* 2021, 7(1), p.10. DOI: <http://doi.org/10.5334/fce.123>
- **Carlucci F**, Cannavale A, Fiorito F. *Electrochromic window integration in adaptive building envelopes in different climates: a genetic optimization of switchable glazing parameters to reduce energy consumptions in office buildings*. *Journal of Physics: Conference Series*. DOI: 10.1088/1742-6596/2069/1/012131
- Campagna L. M., **Carlucci F**, Russo P, Fiorito F. *Energy performance assessment of passive buildings in future climatic scenarios: the case of study of the childcare centre in Putignano (Bari, Italy)*. *Journal of Physics: Conference Series*. DOI: 10.1088/1742-6596/2069/1/012146
- **Carlucci F**, Tiano W. *Acoustic design and optimization of an organic architecture, a cross disciplinary design of an open-space airport case study*. *Journal of Physic: Conference Series*. DOI: 10.1088/1742-6596/2069/1/012160

CONFERENCE PAPERS

- **Carlucci F**, Campagna L.M, Fiorito F. *Technological and energy assessment of an origami-based kinetic shading system in typical and future climate scenarios*. *ColloquiAte Conference "Memory and Innovation" 2022*, ISBN: 978-88-945937-4-7
- **Carlucci F**, Fiorito F. *Implementation of smart technologies in building envelopes: methodological approach and comparative analyses in a hot-summer Mediterranean climate*. *ColloquiAte Conference 2021*, ISBN: 978-88-96386-62-0
- Cannavale, **Carlucci F**, Fiorito F, Martellotta F, Ayr U, Berardi U. *Thermal enhancement of windows performance by means of innovative technologies*. *ATI Conference 2021*. DOI: <https://doi.org/10.1051/e3sconf/202131202015>
- **Carlucci F**, Merla M. *Cross-disciplinary design optimization: parametric façade design for an educational facility in the Middle East*. *PLEA 2020 Conference*, ISBN:978-84-9749-794-7.

WORKING EXPERIENCE

2014 - Ongoing

Deerns Italia SPA, Via Guglielmo Silva 36, Milano (MI)

2018 - Ongoing

Integrated design and engineering consultancy

Facade and building physics consultant, Sustainability group

Representative works:

- **Il Sole24Ore Headquarter**, Office building, Milano, ITALIA | Arch. Renzo Piano
- **Gelendzhik Airport**, Gelendzhik, RUSSIA | Arch. FUKSAS
- **Transportation Education Center**, Museo, Doha, QATAR | Arch. OneWorks

Esse Ingegneria s.r.l., Corso Vittorio Emanuele II n.171, Bari (BA)

2015 - 2017

Engineering firm, role: employee

Alvisi Kirimoto + Partners., Viale Parioli n.40, Roma (RM)

2014 - 2015

Architectural firm, role: intern

EDUCATION

2008 - Ongoing

PhD candidate, Course Risk and environmental, territorial and building development 2019 - Ongoing
Polytechnic University of Bari, DICATECh department, XXXV Cycle

“Responsive envelopes performance analysis in current and future climate scenarios: development of an interactive computational platform”

Supervisor: Prof. Francesco Fiorito, Prof. Guido Raffaele Dell’Osso

II Level postgraduate course “Energy management of buildings and infrastructures” 2017 - 2019
Polytechnic of Milan – Prof. Giuliano Dall’O’ | **mark 110/110**

Thesis:

“Parametric optimization of a vertical shading to balance energy efficiency and daylighting comfort”

MSc in Building Engineering-Architecture

2008 - 2014

5 years single cycle | **110/110 cum Laude**

Thesis:

“Concert halls with variable acoustic using coupled volumes: from mathematical models to built form”